**ORIGINAL PAPER**

# Energy consumption reduction in OFDMA wireless sensor networks in existence of interference hazards

Osama H. Elgazzar[1] · Imbaby I. Mahmoud[2]

## Abstract

Energy consumption reduces Wireless Sensor Network's (WSN's) lifetime. Hence, this paper addresses energy saving problematic in cooperative Orthogonal Frequency Division Multiplexing Access (OFDMA) systems for WSNs (COFDMA-WSN). Analytical handlings are implemented. The performance improvement of COFDMA-WSNs is executed by considering two different COFDMA-WSNs schemes. These schemes represent classical COFDMA-WSNs and Relay Supported (R-S) COFDMA-WSNs. Additionally, there are different pondered configurations due to these schemes. These configurations denote classical OFDMA network with classical WSN, R-S OFDMA network with classical WSN, classical OFDMA network with R-S WSN, and R-S OFDMA network with R-S WSN. Moreover, each configuration is applied with four different fractional frequency reuse (FrFR) techniques. These techniques represent strict (St) FrFR technique with Frequency Reuse Factor (FReF) = 3, St FrFR technique with FReF = 4, sectored (Sc) FrFR technique and soft frequency reuse (SoFR) technique. Consequently, there are sixteen different patterns of COFDMA-WSNs are considered. Moreover, closed-form terms (CFTs) for cluster-head's (C-H's) signal to interference ratio (SIR) and sensor node's (SN's) SIR are presented. Additionally, different metrics are evaluated to contrast the performance of altered patterns using the obtained CFTs. The outcomes demonstrate, that St FrRF4 system outperforms other systems in prime and ensuing links. The cause of this outcome can be credited, to the frequency reuse process decrement due to FReF increment. As a result, the interference sources decrease. Hence, the interfering signals drop. Consequently, St FrRF4 system achieves the highest values of SIR. Moreover, St FrRF3 technique has the second usage priority in the prime link. But, it loses this preference in the ensuing link and SoFR technique that applied in the fourth configuration takes this significance. The work outcomes attain much higher C-H's and SN's SIR improvements. Accordingly, the packet transmission and protocol behaviour are enhanced. So, the energy consumption is reduced. Consequently, WSN's lifetime is maximized.

**Keywords** Wireless sensor networks · COFDMA-WSN · Relay supported COFDMA-WSN systems · FrFR techniques · Performance valuation metrics · Energy saving · OFDMA networks

✉ Osama H. Elgazzar
  osamah.elgazzar@gmail.com

  Imbaby I. Mahmoud
  imbabyisma@yahoo.com

[1] Engineering Department, Nuclear Research Centre, Atomic Energy Authority, Inshas, Egypt

[2] Radiation Engineering Department, National Centre for Radiation Research and Technology, Atomic Energy Authority, Cairo, Egypt

## 1 Introduction

Wireless Sensor Networks (WSNs) consist of large number of tiny devices called sensor nodes (SNs) [1]. These SNs can be employed in WSN surroundings through three ways. These ways represent regular, mobile SNs, and random deployment [2]. These connections variety helped WSNs to speedily gaining attractiveness in many critical areas [3]. Unfortunately, energy consumption issue represents a vast challenge in WSN. This is due to the impossibility of replacing or recharging the SNs' batteries in most hostile environments [4]. So, a method to reduce the energy consumption and increase the overall WSN life [4] is

investigated. Furthermore, an approach to harvest and store energy in a machine to machine network through radio frequency signals adopting the wireless powered communication paradigm is proposed [5]. Additionally, a proposed way to reduce power consumption in wireless sensors is studied [6]. Although, these approaches reduce energy consumption problem to some extent it can't completely eliminate this problem under interference condition. The hazard of interference is that it causes packet loss and so additional energy are consumed for the retransmission process [8]. Thus, some studies tended to use the cooperative Orthogonal Frequency Division Multiplexing Access (OFDMA) networks for WSNs (COFDMA-WSN) to reduce the interference impact [7]. In these networks, OFDMA network represents the backhaul of the WSN. Consequently, the secure resource distribution problematic is addressed for an OFDMA two-way relay WSN [10]. Additionally, joint neighbour discovery and coarse time-of-arrival estimation in WSNs via OFDMA [8] is introduced. Regrettably, it is noticed, that co-channel interference (CoCI) is originated in COFDMA-WSN due to frequency reuse technique deployment [9]. So, reducing CoCI is a necessity in order to improve the system performance. Thus, transmission performance enhancement is addressed by adjusting the transmission rate and the payload size in response to the change of CoCI [10]. Additionally, fractional frequency reuse (FrFR) scheme is assumed [11] to reduce CoCI and achieve high energy conservation. However, these papers have not considered the energy consumption reduction through incorporating FrFR technique and relaying technique together with the hierarchical protocol deployment. Therefore, based on this complex combination, there are sixteen patterns are studied in this paper.

This paper aims to offer an effective method for improving WSN performance through lessening the energy consumption. So, theoretical performance analysis of COFDMA-WSN is conducted via considering two different COFDMA-WSN schemes. These schemes represent classical COFDMA-WSN and relay supported (R-S) COFDMA-WSN. Furthermore, different configurations are considered due to these schemes. These configurations denote classical OFDMA network with classical WSN, R-S OFDMA network with classical WSN, classical OFDMA network with R-S WSN, and R-S OFDMA network with R-S WSN. Moreover, each configuration applies four different FrFR techniques. These techniques represent strict (St) FrFR technique with Frequency Reuse Factor (FReF) = 3 (it will be referred to by the acronym St FrFR3), St FrFR technique with FReF = 4 (it will be referred to by the acronym St FrFR4), sectored (Sc) FrFR technique and soft frequency reuse (SoFR) technique. Consequently, there are sixteen different patterns of COFDMA-WSN are addressed. Additionally, closed-form

terms (CFTs) for cluster-head's (C-H's) signal to interference ratio (SIR) and SN's SIR are presented. Furthermore, several performance metrics are valued to contrast all patterns using the gotten CFTs. The work outcomes contribute to enhancing the packet transmission, link stability and protocol behaviour. So, the WSNs' performance is greatly improved. Accordingly, the WSN life time is maximized.

This paper is systematized as follows: Sect. 2 describes the basic assumptions and model description. Section 3 attentions on the metrics for performance estimation of different patterns. Section 4 offerings the outcomes and discussion. The work conclusion is presented in Sect. 5.

## 2 Basic assumptions and model description

This section presents the analysis of dissimilar configurations of COFDMA-WSN system. In this system, hierarchical protocol is considered due to its efficiency in reducing the required transmitted energy of data packets. Therefore, the communication is accomplished in two phases as revealed in Fig. 1. In first phase, BS transmits the signal to C-H through prime link.

In second phase, C-H communicates with SNs through ensuing link. Moreover, the main parameters of experimentation are shown in Table 1. Also, the reference values of these parameters are taken from [11, 22] and [23]. Furthermore, the considered configurations denote classical OFDMA network with classical WSN, R-S OFDMA network with classical WSN, classical OFDMA network with R-S WSN, and R-S OFDMA network with R-S WSN. Each configuration is deployed with four different FrFR techniques to advance the performance of overall system through dropping the interference impact. These techniques represent strict St FrFR3 technique, St FrFR4 technique, Sc FrFR technique and SoFR technique as shown in Fig. 2.

Additionally, the analytical handling of the pondered configurations yielded CFTs for C-H's SIR and SN's SIR as presented in the following subsections. These CFTs are
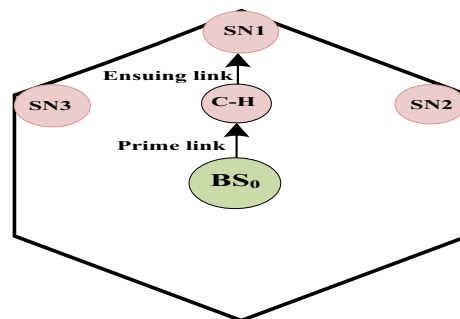


**Fig. 1** Concept illustration of COFDMA-WSN system

**Table 1** Simulation parameters of the proposed COFDMA-WSN configurations

| Parameter | Value | Parameter | Value |
|---|---|---|---|
| Macro cell structure | Hexagonal grid two tier with 19 cell sites | Centre frequency | 2 GHz |
| System bandwidth | 10 MHz | Cell radius | 1000 m |
| Pathloss Exponent | 4 | Noise figure | −147 dBm / Hz |
| Power control factor | 1 | Number of sensors | Four in each cell |
| Transmission power consumption | 97.9 mW | Logarithmic standard deviation under shadowing effect | 8 |
| Consumed power during reception | 112.2 mW | Data packet size | 500 bytes |
| Drain efficiency parameter of the amplifier | 0.35 | Number of retransmission attempts | 10 |

then evaluated to contrast the behaviour of dissimilar configurations by assess several metrics. For simplicity, definition of all notations are shown in Table 2.

## 2.1 Analysis of Classical COFDMA-WSN

The first configuration considers a classical WSN implemented with a classical OFDMA network. Thus, OFDMA network based WSN consisting of two-tier FrFR system is constructed. In this system, there is a centralized BS and a set of N pre-assigned SNs denoted by C-H, $SN_1$, $SN_2$, and $SN_3$ in each cell of radius $R_a$ (m). Each cell is distributed into inner and outer sections due to FrFR deployment. So, the deployed SNs are arranged in a regular arrangement in the outer area. Additionally, all SNs aim to exchange information over an OFDMA channel using clustering concept. Therefore, a C-H is implemented in each cluster to distribute synchronization signals within its cluster, keep the radio resources, and act as a gateway between the cluster and neighbouring clusters. Consequently, the C-H node takes the responsibility of managing the cluster as the cellular BS. In addition, it is assumed, that C-H is placed in front of the cellular BS at a distance equal to $R_{C-H}$ (m) ($R_{C-H}$ = 1/2 of $R_a$). This configuration contains different four patterns due to FrFR technique deployment as revealed in Fig. 3. So, the next subsections provide the analytical treatment for the considered patterns of this configuration.

### 2.1.1 Analysis of St FrFR system

Two- tier St FrFR based WSN structure is pondered as revealed in Fig. 4. This system consists of 19 cells. Every cell is separated in to outer and inner areas. Inner area deploys frequency band (BF) ($BF_0$). Furthermore, the outer region uses BFs ($BF_1$, $BF_2$ and $BF_3$) when FReF = 3 is

applied as shown in Fig. 4(a). Moreover, these BFs is reformed to $BF_1$, $BF_2$, $BF_3$ and $BF_4$ when FReF = 4 is used as shown in Fig. 4(b). Additionally, in order to reduce the interference between the SNs themselves and between the SNs and BS, each outer BF in the outer area is distributed into five sub-band frequencies ($S_Fs$) as revealed in Fig. 4(c, d). Moreover, it is presumed, that SN of interest is positioned at the outermost location with coordinates (0, 1) as demonstrated in Fig. 4(e). Furthermore, signal to interference plus noise ratio (SINR) is used to governor CoCI between co-channel BSs and co-channel C-Hs that use the same frequency in the COFDMA-WSN. Consequently, in order to compute the SINR computation of C-H (X,Y) situated at a distance $s = \sqrt{X^2 + Y^2}$ from the aiding BS ($BS_0$), the following equality is used [12]

$$SINR(X, Y) = \frac{J_{0a}\, E_{0\hbar}\, H_{0a\hbar}}{\zeta_{\hbar}^2 + \sum\limits_{i=1}^{g} (J_{ia}\, E_{i\hbar}\, H_{ia\hbar})} \tag{1}$$

where $J_{0a}$ signifies the channel Propagation Path Gain (PPG) (dB) associated between SN a and $BS_0$. Furthermore, this parameter terms the inverse of Path-Loss (PLo) (dB) between $BS_0$ and SN a ($J_{0a} = 1/PLo_{0a}$), $\zeta_{\hbar}^2$ indicates the Additive White Gaussian Noise (AWGN) channel noise power (watt), $J_{ia}$ represents channel PPG between SN a and interfering BSs (dB), $E_{0\hbar}$ indicates $BS_0$'s transmit power on subcarrier $\hbar$ (watt), $E_{i\hbar}$ designates interfering BSs' transmit power (watt), $H_{0a\hbar}$ represents channel Fast Fading (FaF) power (watt) between SN a and $BS_0$, and $H_{ia\hbar}$ denotes the channel FaF power (watt) between SN a and interfering BSs. In addition, the factor $J_{0a}$ is directly related to $s^{-\eta}$ i.e. ($J_{0u} \propto s^{-\eta}$) where $\eta$ characterizes the PLo Exponent (PLoE) and s denotes the space (m) between the BS and SN a. Consequently, this relative can be expressed as $J_{0a} = J_0\, s^{-\eta}$ where $J_0$ denotes the relational constant that is
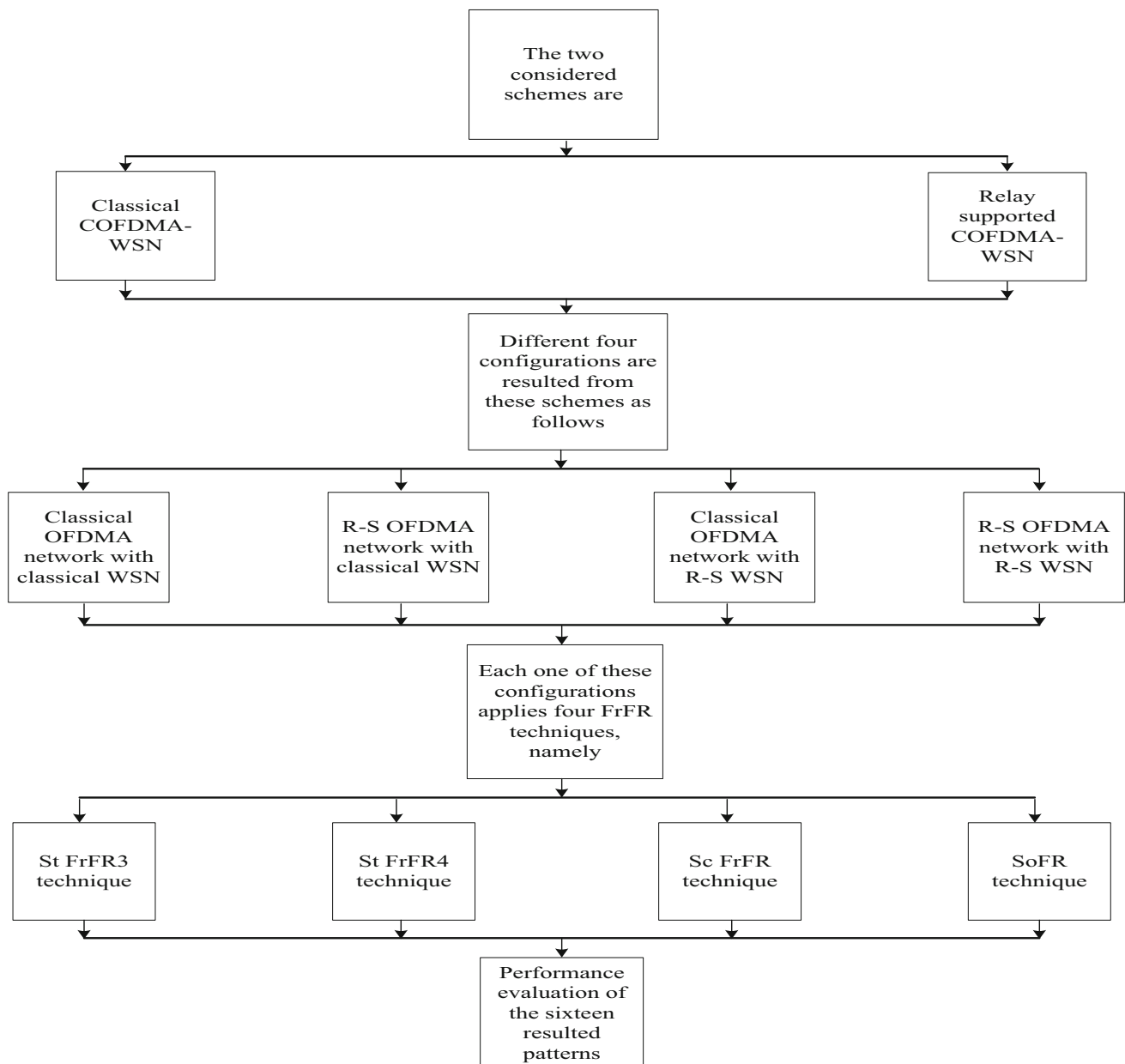
```
                          ┌──────────────┐
                          │  The two     │
                          │  considered  │
                          │  schemes are │
                          └──────┬───────┘
         ┌───────────────────────┼───────────────────────┐
  ┌──────────────┐                                 ┌──────────────┐
  │  Classical   │                                 │    Relay     │
  │  COFDMA-     │                                 │  supported   │
  │  WSN         │                                 │  COFDMA-     │
  └──────┬───────┘                                 │  WSN         │
         │                                          └──────┬───────┘
         └───────────────────────┬───────────────────────┘
                          ┌──────────────┐
                          │ Different four│
                          │ configurations│
                          │ are resulted  │
                          │ from these    │
                          │ schemes as    │
                          │ follows       │
                          └──────┬───────┘
```

Different four configurations are resulted from these schemes as follows

- Classical OFDMA network with classical WSN
- R-S OFDMA network with classical WSN
- Classical OFDMA network with R-S WSN
- R-S OFDMA network with R-S WSN

Each one of these configurations applies four FrFR techniques, namely

- St FrFR3 technique
- St FrFR4 technique
- Sc FrFR technique
- SoFR technique

Performance evaluation of the sixteen resulted patterns

**Fig. 2** Idea diagram of COFDMA-WSN patterns for energy consumption reduction

expressed as $J_0 = (c/4\pi f_o)^2$ where $f_o$ and c indicate the employed BS's centre frequency (Hz) and light speed (m/s), respectively. Additionally, the parameter $J_{ia}$ is defined as $J_{ia} = J_i s_i^{-\eta}$ where $s_i$ represents the separation space (m) between the interfering BSs and SN a and $J_i$ denotes the second relational constant. This relational constant is expressed by $J_i = (c/4\pi f_i)^2$ where $f_i$ is the interfering BSs' centre frequency (Hz). Moreover, symbols i and g represent the group of all interfering BSs (i.e. BSs that employing a similar BF as $BS_0$). Therefore, g signifies the number of co-channel cells and i indicates the co-channel cell index. Besides, the sources of interference are wholly surrounding BSs that deploy identical BF as $BS_0$. Thus, the sources of

interference that affecting C-H are wholly surrounding BSs that employ an identical BF as $BS_0$. Accordingly, C-H suffers from 6 BSs with numbers (8, 10, 12, 14, 16 and 18) which usage same $S_F$ ($S_{F1-1}$) as $BS_0$ in the outer section when St FrFR3 technique is employed. Furthermore, when St FrFR4 technique is deployed, the C-H suffers from 6 BSs with numbers (7, 9, 11, 13, 15 and 17). Furthermore, it is presumed, that fading powers of the channel are distinct with mean equal one, i.e. ($H_{0a\hbar} = 1$), and the key influence arises from interference rather than noise in COFDMA-WSNs. So, noise impact is ignored in this analysis. Accordingly, Eq. (1) is rewritten to calculate C-H's SIR [13] as follows

**Table 2** Notation definition

| Notation | Definition | Notation | Definition | Notation | Definition |
|---|---|---|---|---|---|
| $R_{C-H}$ | Distance between macro cell BS and C-H | $s_i$ | Separation space between the interfering BSs and SN a | $T_{Rsec}$ | Interference parameter because of co-channel RSs that deploy $S_{F1-6}$ in surrounding cells for Sc FrFR in R-S OFDMA network |
| $R_a$ | Cell radius | $J_i$ | Second relational constant | $T_{oR}$ | Outer interference parameters for R-S SoFR system |
| $J_{0a}$ | Channel propagation path gain associated between SN a and $BS_0$ | $f_i$ | Interfering BSs' centre frequency | $SIR_{SRC-H}$ | C-H's SIR of SoFR technique |
| $\zeta_\hbar^2$ | Additive White Gaussian Noise channel noise power | $g$ | Number of co-channel cells | $T_{RW}$ | Interference parameter due to CoCI fom co-channel RSs that use $S_{F1-6}$ as the serving RS in R-S WSN |
| $J_{ia}$ | Channel propagation path gain between SN a and interfering BSs | $i$ | Co-channel cell index | $SIR_{RW3}$ | S'Ns SIR achieved by using FrFR3 technique in R-S WSN |
| $E_{0\hbar}$ | $BS_0$'s transmit power on subcarrier m | $E_0$ | $BS_0$'s transmitted power | $T_{RWsec}$ | Interference parameter because of all co-channel RSs that use $S_{F1-2}$ similar to the aiding RS in R-S WSN |
| $E_{i\hbar}$ | Interfering BSs' transmit power | $j$ | Interfering BSs set due to redeploying same $S_F$ in the outer area | $T_{oRW}$ | Outer interference parameter in R-S WSN |
| $H_{0a\hbar}$ | Channel Fast Fading power between SN a and $BS_0$ | $s_j$ | Distance between 6 interfering BSs which employ $S_{F1-1}$ and C-H | $SIR_{WSFR}$ | SN's SIR of SoFR technique in R-S WSN |
| $H_{ia\hbar}$ | Channel FaF power of the between SN a and interfering BSs | $E_j$ | Interfering BSs' transmitted power that disturb the C-H | $T_{oR4}$ | Outer interference parameters for R-S COFDMA-WSN |
| $\eta$ | PLo Exponent | $J_j$ | Outer relational constant | $SIR_{SRC-H4}$ | C-H's SIR of SoFR technique for R-S COFDMA-WSN |
| $s$ | Space between the BS and SN a | $f_j$ | Interfering BSs' centre frequency | $T_{RF}$ | Interference factor originated form co-channel RSs in surrounding cells |
| $J_0$ | Relational constant | $SIR_{C-H}$ | C-H's SIR | $j_{RS}$ | Interfering RSs group in the outer region that use $S_{F1-2}$ |
| $f_o$ | Employed BS's centre frequency | $T_{FRF}$ | Interference parameter because of using FrFR technique | $SIR_{C-HR4}$ | C-H's SIR from the second TS when FrFR4 technique is deployed |
| $c$ | Light speed | $g_3$ | Interfering BSs group in the outer region that use $S_{F1-1}$ for St FrFR3 | $SIR_{Rsec}$ | C-H's SIR of the second TS using Sc FrFR system in second configuration |
| $SIR_{C-H3}$ | Attained C-H's SIR using St FrFR3 technique in the first configuration | $SIR_{C-H4}$ | Achieved C-H's SIR when St FrFR4 is applied in the first configuration | $T_{iR}$ | Inner interference parameter R-S SoFR system |
| $g_4$ | Interfering BSs set that use $S_{F1-1}$ for St FrFR4 | $SIR_{SN3}$ | Attained SN's SIR when St FrFR3 technique is used in the first configuration | $MRC_{SRC-H}$ | C-H's MRC when SoFR technique is used in the second configuration |
| $SIR_{SN4}$ | SN's SIR when St FrFR4 technique is utilized in the first configuration | $SIR_{Sec}$ | Attained C-H's SIR when Sc FrFR technique is employed in the first configuration | $j_{RW}$ | Interfering RSs group in R-S WSN |
| $T_{Sec}$ | Seven interfering BSs' PLo distances summation | $SIR_{SNSC}$ | Attained SN's SIR when Sc FrFR technique is deployed in the first configuration | $SIR_{RW4}$ | Attained SN's SIR by using FrFR4 technique in R-S WSN |
| $\varepsilon$ | Signifies power control factor | $T_{iF}$ | inner interference factor in OFDMA network | $SIR_{RWsec}$ | SN's SIR of the second TS for Sc FrFR system in R-S WSN |
| $J_{ku}$ | Channel propagation path gain between C-H and its | $J_{ju}$ | Channel propagation path gain between C-H and its | $T_{iRW}$ | Inner interference parameter in R-S WSN |

**Table 2** (continued)

| Notation | Definition interfering $BS_k$ in the inner area | Notation | Definition interfering $BS_j$ in the outer area | Notation | Definition |
|---|---|---|---|---|---|
| $MRC_{WS}$ | MRC of SN of SoFR technique in R-S WSN | $T_{iR4}$ | Inner interference parameters for R-S COFDMA-WNS | $SIR_{WSFR4}$ | SN's SIR of SoFR technique for R-S COFDMA-WSN |
| $SIR_{SFR}$ | C-H's SIR of SoFR technique when first configuration is used | $T_{iSN}$ | Inner interference factor in WSN | $\sigma$ | Negative half of the PLoE ($-\eta/2$) |
| $SIR_{SNSFR}$ | attained SN's SIR using SoFR technique when first configuration is deployed | $SIR_{C\text{-}HR3}$ | C-H's SIR attained through second TS when St FrFR3 technique is deployed | $MRC_{C\text{-}HR3}$ | Obtained C-H's MRC when St FrFR3 system is used in the second configuration |
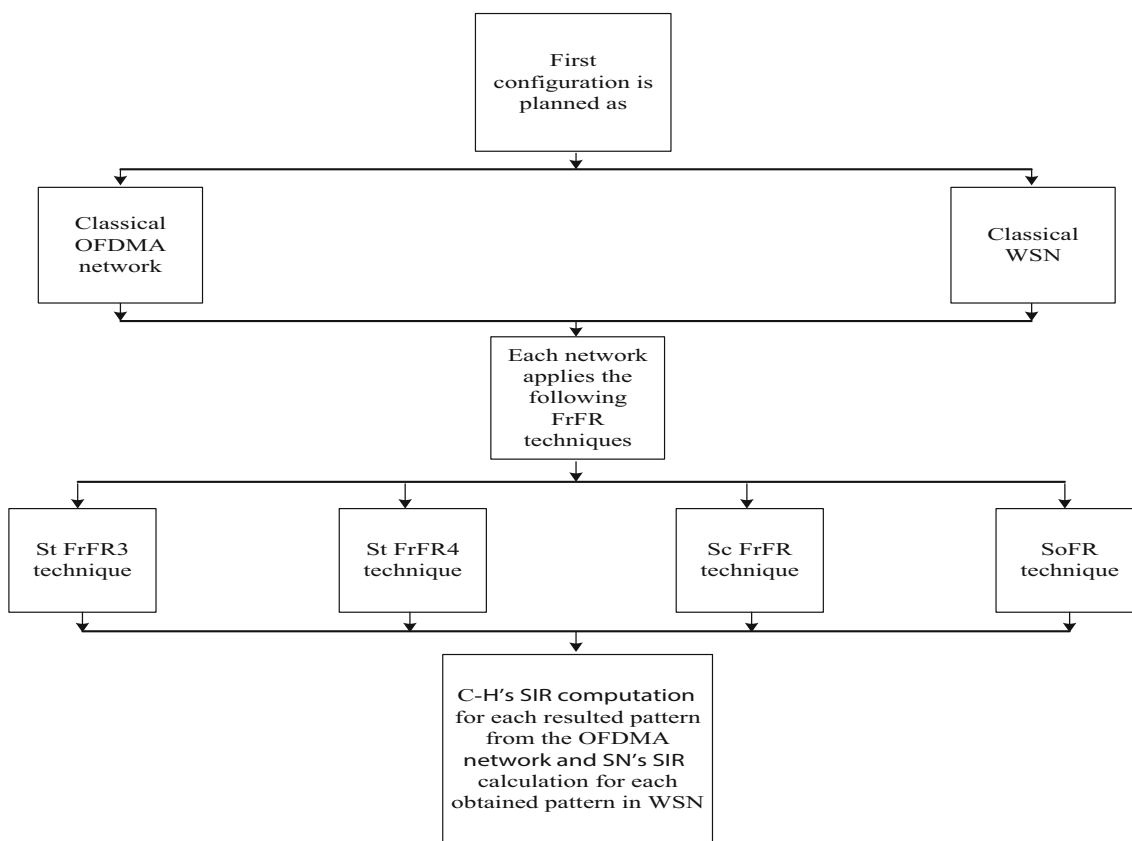


**Fig. 3** Concept illustration of classical COFDMA-WSN patterns for energy consumption reduction

$$SIR(X, Y) = \frac{E_0 J_0 s^{-\eta}}{\sum\limits_{j=1}^{j=6} E_j J_j s_j^{-\eta}} \qquad (2)$$

where $E_0$ denotes $BS_0$'s transmitted power (watt), j refers to interfering BSs set due to redeploying same $S_F$ ($S_{F1\text{-}1}$) in the outer area, $s_j$ is the distance (m) between 6 interfering BSs which employ $S_{F1\text{-}1}$ and C-H, $E_j$ denotes interfering BSs' transmitted power (watt) that disturb the C-H, $J_j$ represents outer relational constant. This constant can be stated as $J_j = (c/4\pi f_j)^2$ where $f_j$ is the interfering BSs'

centre frequency (Hz). In addition, it is postulate that the SNs' interference is negligible and all BSs transmit with identical power. Accordingly, the common SIR calculation for C-H can be formulated as follows

$$SIR_{C-H}(X, Y) = \frac{J_o s^{-\eta}}{\sum\limits_{j=1}^{j=6} J_j s_j^{-\eta}} \qquad (3)$$

where $SIR_{C\text{-}H}$ is the C-H's SIR. Furthermore, values of $J_o$ and $J_j$ are equal because of using same $S_{F1\text{-}1}$ in the outer area by all BSs. Hence, Eq. (3) can be modified as follows
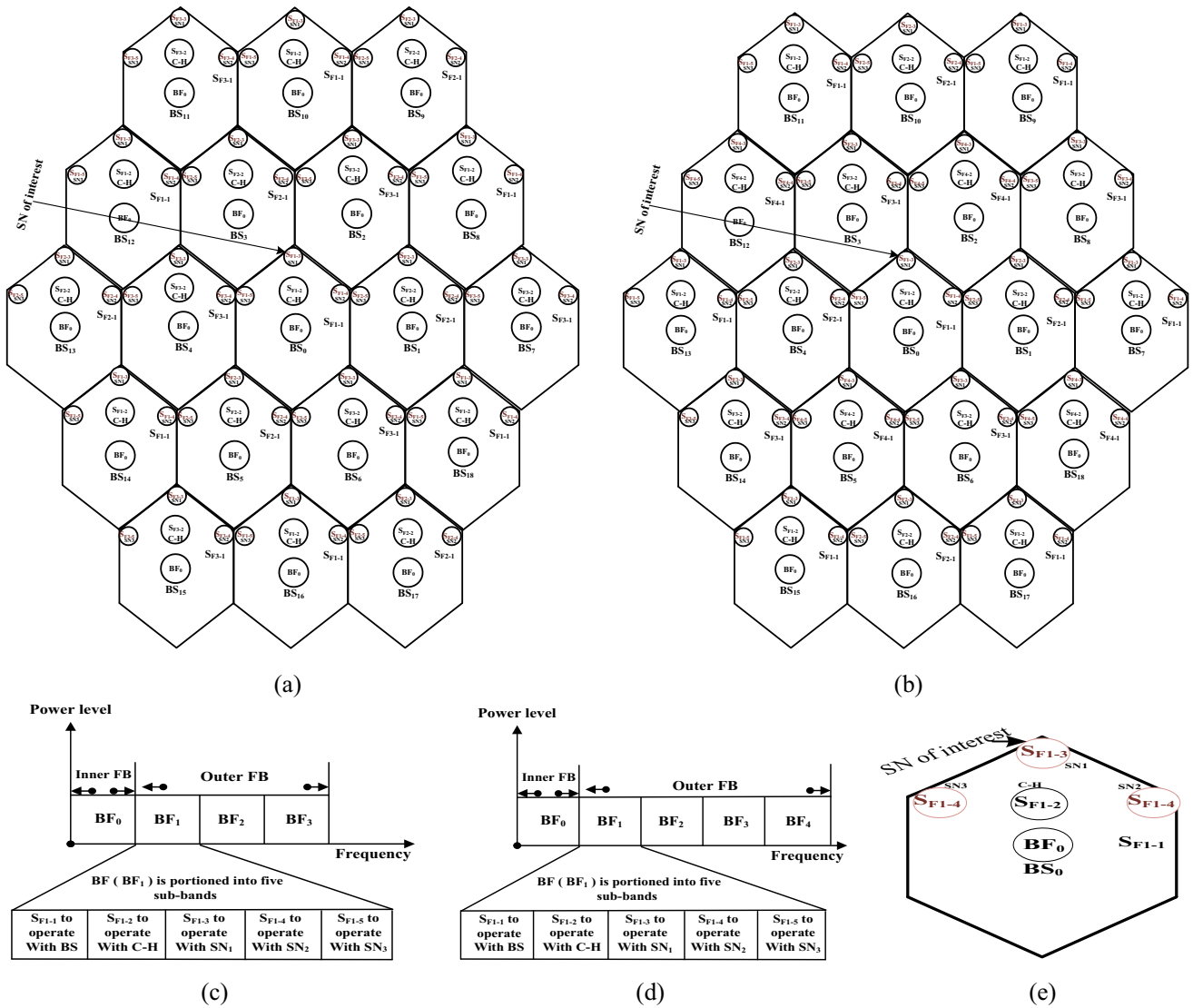
**Fig. 4** Two-tier St FrFR network **a** St FrFR3 pattern **b** St FrFR4 pattern **c** Frequency allocation for St FrFR3 **d** frequency allocation for St FrFR4 (e) Cell layout

$$SIR_{C-H}(X, Y) = \frac{s^{-\eta}}{\sum_{j=1}^{j=6} s_j^{-\eta}} \tag{4}$$

Moreover, it is supposed that (x, y) signifies the normalized coordinates to $R_a$ i.e. $(x, y) = (X/R_a, Y/R_a)$. Therefore, normalized separation space is equivalent to $R_a s = \sqrt{X^2 + Y^2}$. Consequently, Eq. (4) can be modified to denote the C-H's SIR term in normalized coordinates as follows

$$SIR_{C-H}(x, y) = \frac{(x^2 + y^2)^{\sigma}}{T_{FRF}(x, y)} \tag{5}$$

where the factor $T_{FRF}$ represents the interference parameter because of using FrFR technique, and σ designates the negative half of the PLoE (-η/2). Accordingly, this factor is

calculated from the following relative when St FrFR3 technique is employed

$$T_3(x, y) = \sum_{g_3=1}^{g_3=6} \left[ (x + x_{g_3})^2 + (y + y_{g_3})^2 \right]^{\sigma} \tag{6}$$

where $g_3$ represents the interfering BSs group in the outer region that use $S_{F1-1}$. Additionally, Table 3 clarifies the outer area allotted BSs' BFs. Furthermore, the BSs' normalized coordinates are demonstrated in the same table. Hence, the parameter $T_3$ can be expressed as follows

$$T_3(x,y) = \left[ \left( x \pm \frac{3}{2}\sqrt{3} \right)^2 + \left( y - \frac{3}{2} \right)^2 \right]^{\sigma} + \left[ x^2 + (y \pm 3)^2 \right]^{\sigma} + \left[ \left( x \pm \frac{3}{2}\sqrt{3} \right)^2 + \left( y + \frac{3}{2} \right)^2 \right]^{\sigma} \tag{7}$$

**Table 3** Coordinates outer region assigned frequencies of BSs in different FrFR systems

| BS | x | y | FrFR3 | FrFR4 | Sc FrFR | SoFR |
|----|----|----|----|----|----|----|
| 0 | 0 | 0 | $BF_1$ | $BF_1$ | $BF_1, BF_2, BF_3$ | $BF_1$ |
| 1 | $\sqrt{3}$ | 0 | $BF_2$ | $BF_2$ | $BF_1, BF_2, BF_3$ | $BF_2$ |
| 2 | $\sqrt{3}/2$ | 3/2 | $BF_3$ | $BF_3$ | $BF_1, BF_2, BF_3$ | $BF_3$ |
| 3 | $-\sqrt{3}/2$ | 3/2 | $BF_2$ | $BF_4$ | $BF_1, BF_2, BF_3$ | $BF_2$ |
| 4 | $-\sqrt{3}$ | 0 | $BF_3$ | $BF_2$ | $BF_1, BF_2, BF_3$ | $BF_3$ |
| 5 | $-\sqrt{3}/2$ | −3/2 | $BF_2$ | $BF_3$ | $BF_1, BF_2, BF_3$ | $BF_2$ |
| 6 | $\sqrt{3}/2$ | −3/2 | $BF_3$ | $BF_4$ | $BF_1, BF_2, BF_3$ | $BF_3$ |
| 7 | $2\sqrt{3}$ | 0 | $BF_3$ | $BF_1$ | $BF_1, BF_2, BF_3$ | $BF_3$ |
| 8 | $3\sqrt{3}/2$ | 3/2 | $BF_1$ | $BF_4$ | $BF_1, BF_2, BF_3$ | $BF_1$ |
| 9 | $\sqrt{3}$ | 3 | $BF_2$ | $BF_1$ | $BF_1, BF_2, BF_3$ | $BF_2$ |
| 10 | 0 | 3 | $BF_1$ | $BF_2$ | $BF_1, BF_2, BF_3$ | $BF_1$ |
| 11 | $-\sqrt{3}$ | 3 | $BF_3$ | $BF_1$ | $BF_1, BF_2, BF_3$ | $BF_3$ |
| 12 | $-3\sqrt{3}/2$ | 3/2 | $BF_1$ | $BF_3$ | $BF_1, BF_2, BF_3$ | $BF_1$ |
| 13 | $-2\sqrt{3}$ | 0 | $BF_2$ | $BF_1$ | $BF_1, BF_2, BF_3$ | $BF_2$ |
| 14 | $-3\sqrt{3}/2$ | −3/2 | $BF_1$ | $BF_4$ | $BF_1, BF_2, BF_3$ | $BF_1$ |
| 15 | $-\sqrt{3}$ | −3 | $BF_3$ | $BF_1$ | $BF_1, BF_2, BF_3$ | $BF_3$ |
| 16 | 0 | −3 | $BF_2$ | $BF_2$ | $BF_1, BF_2, BF_3$ | $BF_1$ |
| 17 | $\sqrt{3}$ | −3 | $BF_3$ | $BF_1$ | $BF_1, BF_2, BF_3$ | $BF_2$ |
| 18 | $3\sqrt{3}/2$ | −3/2 | $BF_2$ | $BF_3$ | $BF_1, BF_2, BF_3$ | $BF_1$ |

Therefore, by replacing the worth of Eq. (7) into Eq. (5), C-H's SIR when St FrFR3 technique is used can be computed as follows

$$SIR_{C-H3} = \left[ \left(\frac{1}{4}\right)^{-\sigma} \left( \left(\frac{25}{4}\right)^{\sigma} + 2\left(\frac{31}{4}\right)^{\sigma} + 2\left(\frac{43}{4}\right)^{\sigma} + \left(\frac{49}{4}\right)^{\sigma} \right) \right]^{-1} \tag{8}$$

where $SIR_{C-H3}$ denotes the attained C-H's SIR using St FrFR3 technique in the first configuration. Furthermore, the parameter $T_{FRF}$ is calculated for St FrFR4 as follows

$$T_4(x,y) = \sum_{g_4=1}^{g_4=6} \left[ (x+x_{g_4})^2 + (y+y_{g_4})^2 \right]^{\sigma} \tag{9}$$

where $g_4$ represents the interfering BSs set that use $S_{F1-1}$. Hence, this parameter can be expressed as follows

$$T_4(x,y) = \left[ \left(x+\sqrt{3}\right)^2 + (y\pm3)^2 \right]^{\sigma} + \left[ \left(x-\sqrt{3}\right)^2 + (y\pm3)^2 \right]^{\sigma} + \left[ \left(x\pm2\sqrt{3}\right)^2 + y^2 \right]^{\sigma} \tag{10}$$

Consequently, by replacing the worth of Eq. (10) into Eq. (5), C-H's SIR when St FrFR4 is used can be calculated as follows

$$SIR_{C-H4} = \left[ \left(\frac{1}{4}\right)^{-\sigma} 2\left( \left(\frac{37}{4}\right)^{\sigma} + \left(\frac{61}{4}\right)^{\sigma} + \left(\frac{49}{4}\right)^{\sigma} \right) \right]^{-1} \tag{11}$$

where $SIR_{C-H4}$ indicates the achieved C-H's SIR when St FrFR4 is applied in the first configuration. Moreover, it is supposed, that C-H transmits to SN that placed at the second corner with x = 0, y = 1. Accordingly, Eq. (5) is modified to definite the SN's SIR in normalized coordinates as follows

$$SIR_{SN}(x,y) = \frac{\left(x^2 + (y-0.5)^2\right)^{\sigma}}{T_{SN}(x,y)} \tag{12}$$

where $T_{SN}$ represents the interference parameter because of using FrFR technique. Accordingly, this parameter is calculated, when St FrFR3 technique is used, as follows

$$T_{SN3}(x,y) = \sum_{t_3=1}^{t_3=6} \left[ (x+x_{t_3})^2 + (y+y_{t_3})^2 \right]^{\sigma} \tag{13}$$

where $t_3$ symbolizes the interfering C-Hs that redeploy $S_{F1-2}$.

Furthermore, Table 4 shows the six interfering C-Hs coordinates. So, $T_{SN3}$ parameter is assessed as follows

$$T_{SN3}(x,y) = \left[ \left(x\pm\frac{3}{2}\sqrt{3}\right)^2 + (y+1)^2 \right]^{\sigma} + \left[ x^2 + (y-3.5)^2 \right]^{\sigma} + \left[ \left(x\pm\frac{3}{2}\sqrt{3}\right)^2 + (y-2)^2 \right]^{\sigma} + \left[ x^2 + (y+2.5)^2 \right]^{\sigma} \tag{14}$$

Therefore, by exchanging the worth of Eq. (14) into Eq. (5), SN's SIR for St FrFR3 technique can be evaluated as follows

$$SIR_{SN3} = \left[ \left(\frac{1}{4}\right)^{-\sigma} \left( \left(\frac{25}{4}\right)^{\sigma} + 2\left(\frac{31}{4}\right)^{\sigma} + 2\left(\frac{43}{4}\right)^{\sigma} + \left(\frac{49}{4}\right)^{\sigma} \right) \right]^{-1} \tag{15}$$

where $SIR_{SN3}$ denotes the attained SN's SIR when St FrFR3 technique is used in the first configuration. Moreover, the factor $T_{SN}$ is valued when St FrFR4 technique is used as follows

$$T_{SN4}(x,y) = \sum_{t_4=1}^{t_4=6} \left[ (x+x_{t_4})^2 + (y+y_{t_4})^2 \right]^{\sigma} \tag{16}$$

where $t_4$ denotes the interfering C-Hs set in the outer area that employ $S_{F1-2}$. Hence, this factor is represented as follows

**Table 4** Interfering C-Hs' Coordinates for St FrFR technique

| | Interfering C-Hs' coordinates in FrFR3 | | | Interfering C-Hs' coordinates in FrFR4 | | |
|---|---|---|---|---|---|---|
| Cell no | X | Y | | Cell no | X | Y |
| 8 | $3\sqrt{3}/2$ | 2 | | 7 | $2\sqrt{3}$ | 1/2 |
| 10 | 0 | 3.5 | | 9 | $\sqrt{3}$ | 3.5 |
| 12 | $-3\sqrt{3}/2$ | 2 | | 11 | $-\sqrt{3}$ | 3.5 |
| 14 | $-3\sqrt{3}/2$ | $-1$ | | 13 | $-2\sqrt{3}$ | 1/2 |
| 16 | 0 | $-2.5$ | | 15 | $-\sqrt{3}$ | $-2.5$ |
| 18 | $3\sqrt{3}/2$ | $-1$ | | 17 | $\sqrt{3}$ | $-2.5$ |

$$T_4(x,y)=\left[\left(x\pm\sqrt{3}\right)^2+(y-3.5)^2\right]^\sigma+\left[\left(x\pm2\sqrt{3}\right)^2+(y-0.5)^2\right]^\sigma$$
$$+\left[\left(x\pm\sqrt{3}\right)^2+(y+2.5)^2\right]^\sigma \tag{17}$$

Consequently, by replacing the worth of Eq. (17) into Eq. (5), SN's SIR when St FrFR4 technique is used, can be estimated as follows

$$SIR_{SN4}=\left[\left(\frac{1}{4}\right)^{-\sigma}\left(2\left(\frac{37}{4}\right)^\sigma+\left(\frac{13}{4}\right)^\sigma+\left(\frac{-47}{4}\right)^\sigma\right.\right.$$
$$\left.\left.+\left(\frac{49}{4}\right)^\sigma+\left(\frac{61}{4}\right)^\sigma\right)\right]^{-1} \tag{18}$$

where $SIR_{SN4}$ indicates SN's SIR when St FrFR4 technique is utilized in the first configuration.

### 2.1.2 Analysis of Sc FrFR system

Two tier Sc FrFR based WSN arrangement is considered as revealed in Fig. 5(a). Here, the outer area is separated into three parts. Consequently, the whole Bandwidth (BW) is distributed equally between each part in the outer and the inner areas. Thus, inner region employs $BF_0$ to cover cell centre users (CCUs). Additionally, outer region uses BFs ($BF_1$, $BF_2$ and $BF_3$) to serve cell edge users (CEUs) as shown in Fig. 5(b). Each outer region BF is more distributed into two dissimilar sets of $S_F$s. The first set denotes $S_{F1-1}$, $S_{F2-1}$, and $S_{F3-1}$, which are assigned to BS. Additionally, the second group represents $S_{F1-2}$, $S_{F2-2}$, and $S_{F3-2}$, which are allocated to C-Hs as depicted in Fig. 5(c). In this system, the sector that deploys $S_{F1-1}$ covers the C-H. Consequently, the C-H hurts from 7 interfering cells (coloured cells) which employ similar BF as demonstrated in Fig. 5(a). So, Eq. (5) can be modernized to definite the C-H's SIR formula as follows

$$SIR_{Sec}(x,y)=\frac{(x^2+y^2)^\sigma}{T_{Sec}(x,y)} \tag{19}$$

where $T_{Sec}$ is the seven interfering BSs' PLo distances summation. Accordingly, the factor $T_{Sec}$ can be computed as follows

$$T_{Sec}(x,y)=\sum_{g_s=1}^{g_s=7}\left[\left(x+x_{g_s}\right)^2+\left(y+y_{g_s}\right)^2\right]^\sigma \tag{20}$$

where $g_S$ indicates set of outer region interfering BSs that use $S_{F1-1}$. Hence, the interference parameter in Sc FrFR system is calculated using Table 3 as follows

$$T_{Sec}(x,y)=\left[\left(x\pm\frac{\sqrt{3}}{2}\right)^2+\left(y+\frac{3}{2}\right)^2\right]^\sigma+\left[\left(x\pm\frac{3\sqrt{3}}{2}\right)^2+\left(y+\frac{3}{2}\right)^2\right]^\sigma$$
$$+\left[x^2+(y+3)^2\right]^\sigma+\left[\left(x\pm\sqrt{3}\right)^2+(y+3)^2\right]^\sigma \tag{21}$$

Consequently, by replacing the worth of Eq. (21) into Eq. (19), C-H's SIR can be formulated as follows

$$SIR_{Sec}=\left[\left(\frac{1}{4}\right)^{-\sigma}\left(2\left(\frac{19}{4}\right)^\sigma+2\left(\frac{43}{4}\right)^\sigma+2\left(\frac{61}{4}\right)^\sigma+\left(\frac{49}{4}\right)^\sigma\right)\right]^{-1} \tag{22}$$

where $SIR_{Sec}$ denotes the attained C-H's SIR when Sc FrFR technique is employed in the first configuration. On the other hand, when C-H transmits to SN through ensuing link, Eq. (19) can be adjusted to represent SN's SIR as follows

$$SIR_{SCSN}(x,y)=\frac{\left(x^2+(y-0.5)^2\right)^\sigma}{T_{SCSN}(x,y)} \tag{23}$$

where $T_{SCSN}$ represents the interference factor. Accordingly, this parameter is assessed as follows

$$T_{SNSC}(x,y)=\sum_{t_{SC}=1}^{t_{SC}=7}\left[\left(x+x_{t_{SC}}\right)^2+\left(y+y_{t_{SC}}\right)^2\right]^\sigma \tag{24}$$

where $t_{SC}$ signifies the interfering set of C-Hs. Moreover, Table 5 shows the seven interfering C-Hs coordinates. Hence, this interference factor is valued as follows
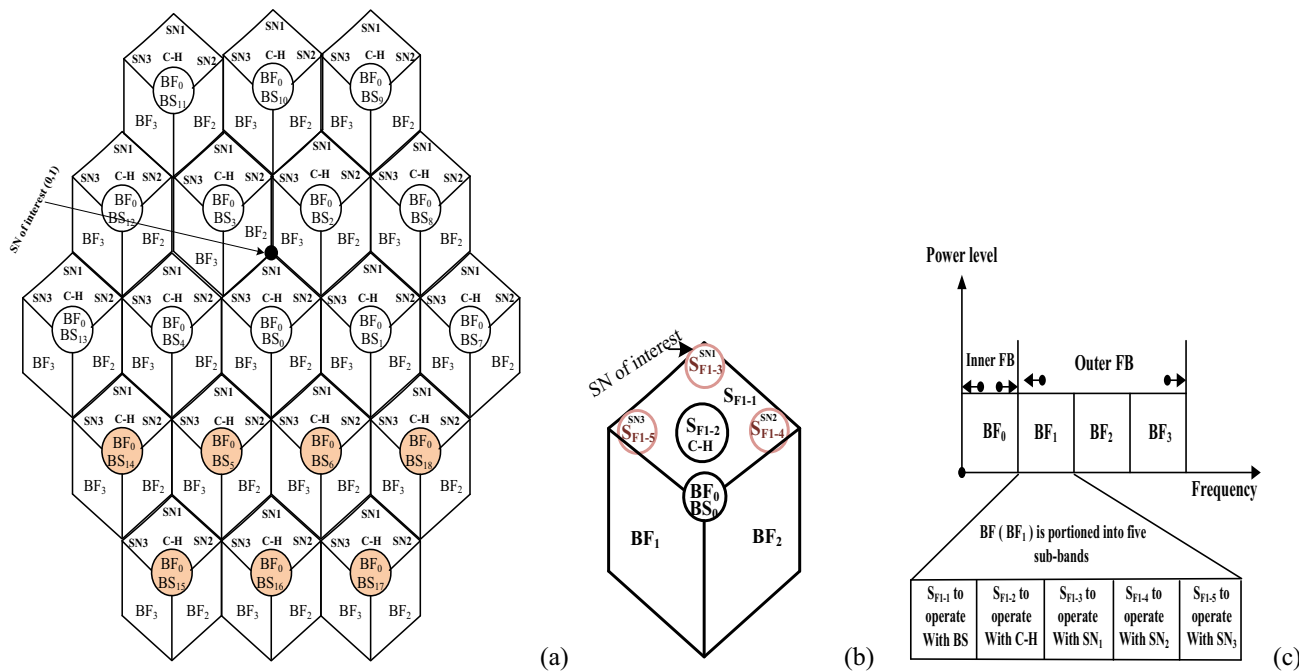
Fig. 5 Sectored FrFR network a System design, b Cell arrangement, c Frequency allocation partition

**Table 5** Interfering C-Hs' Coordinates for Sc FrFR and SoFR techniques

| | Interfering C-Hs' coordinates in Sc FrFR | | | Interfering C-Hs' coordinates in SoFR | | |
|---|---|---|---|---|---|---|
| | Cell no | X | Y | Cell no | X | Y |
| | 5 | $-\sqrt{3}/2$ | $-1$ | 8 | $3\sqrt{3}/2$ | 2 |
| | 6 | $\sqrt{3}/2$ | $-1$ | 10 | 0 | 3.5 |
| | 14 | $-3\sqrt{3}/2$ | $-1$ | 12 | $-3\sqrt{3}/2$ | 2 |
| | 15 | $-\sqrt{3}$ | $-2.5$ | 14 | $-3\sqrt{3}/2$ | $-1$ |
| | 16 | 0 | $-2.5$ | 16 | 0 | $-2.5$ |
| | 17 | $\sqrt{3}$ | $-2.5$ | 18 | $3\sqrt{3}/2$ | $-1$ |
| | 18 | $3\sqrt{3}/2$ | $-1$ | | | |

$$T_{SNSC}(x,y)=\left[\left(x\pm\frac{3}{2}\sqrt{3}\right)^2+(y+1)^2\right]^\sigma+\left[\left(x\pm\frac{\sqrt{3}}{2}\right)^2+(y+1)^2\right]^\sigma$$
$$+\left[x^2+(y+2.5)^2\right]^\sigma+\left[\left(x\pm\sqrt{3}\right)^2+(y+2.5)^2\right]^\sigma \tag{25}$$

Accordingly, by exchanging the worth of Eq. (25) into Eq. (23), SN's SIR equation can be evaluated as follows

$$SIR_{SNSC}=\left[\left(\frac{1}{4}\right)^{-\sigma}\left(2\left(\frac{19}{4}\right)^\sigma+2\left(\frac{43}{4}\right)^\sigma+\left(\frac{49}{4}\right)^\sigma+2\left(\frac{61}{4}\right)^\sigma\right)\right]^{-1} \tag{26}$$

where $SIR_{SNSC}$ denotes the attained SN's SIR when Sc FrFR technique is deployed in the first configuration.

### 2.1.3 Analysis of SoFR technique

Although Sc FrFR improves the C-H's SIR, the network BW usage is still not used with maximum efficiency. Consequently, Two Level Power Control ($T_{PC}$) strategy with reuse 1 structure is proposed to be the foundation stone of the SoFR technique. This technique divides the entire BW in into three equivalent portions [14]. One portion allotted to the outer area and two parts allocated to inner region as displayed in Fig. 6(a). Furthermore, it is presumed, that each subcarrier has output power $P_o$ in the outer area. Furthermore, each subcarrier has output power $P_{in}$ in the inner region. These powers can be expressed by $P_o = \varepsilon\, P_{in}$ where $\varepsilon$ signifies power control factor ($\varepsilon \geq 1$).
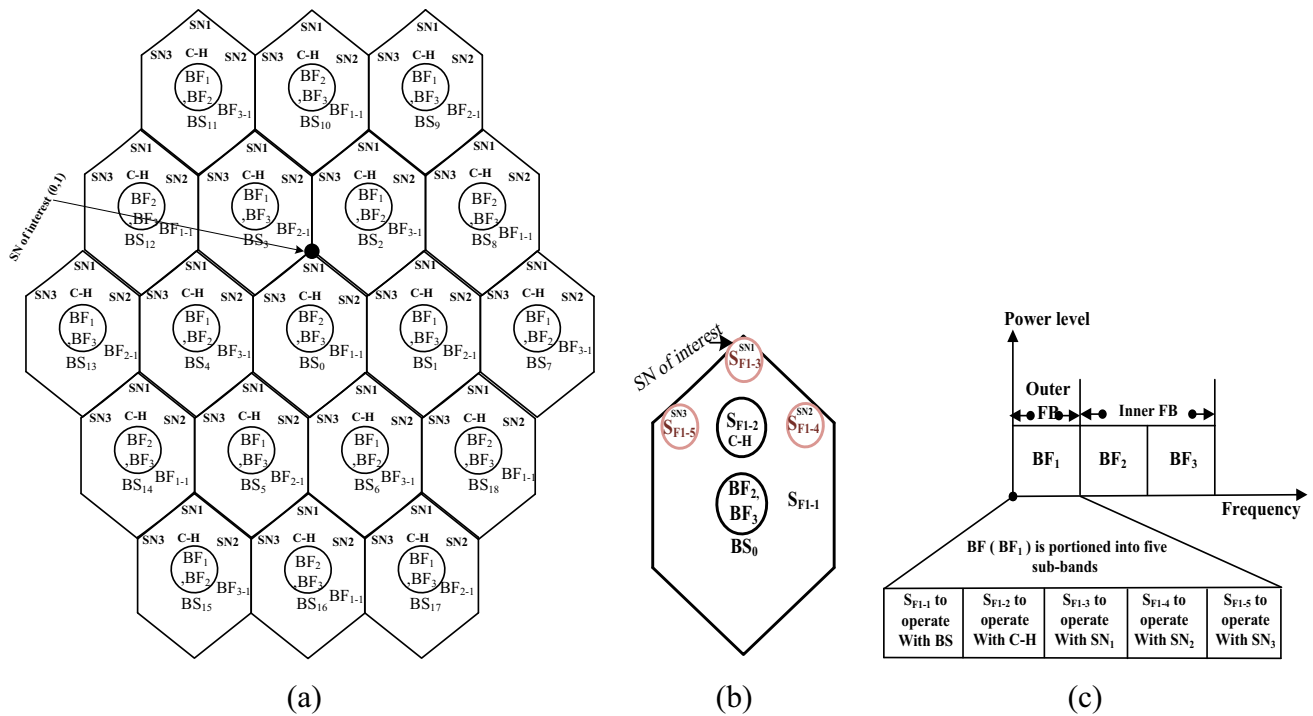
**Fig. 6** SoFR system **a** System design, **b** Cell arrangement, **c** Frequency allocation partition

Each cell allocates the three BW parts ($BF_1$, $BF_2$ and $BF_3$) in different way considering a pseudo-reuse 3 arrangement between outer areas. Consequently, every cell uses the total network BW as depicted in Fig. 6(b). Furthermore, each outer region BF is more portioned into two dissimilar parts of $S_F$s. One part denotes $S_{F1-1}$ which is assigned to BS. Besides, the other portion symbolizes $S_{F1-2}$ which is allotted to C-H as portrayed in Fig. 6(c). In this system, there are 18 interfering cells affecting C-H (6 BSs in outer area and 12 BSs in inner area) which deploys $BF_1$ as depicted in Fig. 6(a). The C-H's SIR expression of the SoFR network is formulated due to $T_{LPC}$ utilization [15] as follows

$$SIR_{SFR} = \frac{E_0 J_{0u}}{\left[ E_{in} \sum_k J_{ku} \right] + \left[ E_0 \sum_g J_{ju} \right]} \tag{27}$$

where $J_{ku}$ denotes channel PPG between C-H and its interfering $BS_k$ in the inner area and $J_{ju}$ represents channel PPG between C-H and its interfering $BS_j$ in the outer area. Also, the parameter $J_{ku}$ is defined as $J_{ku} = J_k s_k^{-\eta}$. Additionally, the factor $J_{ju}$ can be represented by $J_{ju} = J_g s_g^{-\eta}$. Consequently, Eq. (27) is updated as follows

$$SIR_{SFR} = \frac{\varepsilon J_0 s^{-\eta}}{\sum_k J_k s_k^{-\eta} + \varepsilon \sum_j J_g s_g^{-\eta}} \tag{28}$$

In addition, the parameters $J_k$, $J_g$, and $J_o$ use the same centre frequency value during their calculations. Accordingly, they have equivalent rates. Thus, Eq. (28) can be rewritten as follows

$$SIR_{SFR} = \frac{\varepsilon s^{-\eta}}{\sum_k s_k^{-\eta} + \varepsilon \sum_g s_g^{-\eta}} \tag{29}$$

Accordingly, Eq. (29) is updated to definite the C-H's SIR in normalized coordinates as follows

$$SIR_{SFR}(x,y) = \frac{\varepsilon (x^2 + y^2)^\sigma}{T_{iF}(x,y) + \varepsilon T_{oF}(x,y)} \tag{30}$$

where $T_{oF}$ and $T_{iF}$ indicate the outer and inner interference factors in OFDMA network, respectively. The CoCI sources in the outer area resulted from BSs (8, 10, 12, 14, 16 and 18). Additionally, CoCI sources in the inner area originated from BSs (1, 4, 5, 2, 6, 13, 3, 7, 15, 11, 17 and 9). Consequently, the parameter $T_{iF}$ using Table 3 is expressed as follows

$$T_{iF}(x,y) = \begin{bmatrix} \left[ (x \pm 2\sqrt{3})^2 + y^2 \right]^\sigma + \left[ \left( x + \frac{\sqrt{3}}{2} \right)^2 + \left( y \pm \frac{3}{2} \right)^2 \right]^\sigma + \left[ (x \pm \sqrt{3})^2 + (y \mp 3)^2 \right]^\sigma \\ + \left[ (x \pm \sqrt{3})^2 + y^2 \right]^\sigma + \left[ (x \pm \sqrt{3})^2 + (y \pm 3)^2 \right]^\sigma + \left[ \left( x - \frac{\sqrt{3}}{2} \right)^2 + \left( y \pm \frac{3}{2} \right)^2 \right]^\sigma \end{bmatrix} \tag{31}$$

Accordingly, final expression of $T_{iF}$ for a C-H sited at $x = 0$ and $y = 0.5$ is expressed as follows

$$T_{iF}=2\left(\frac{7}{4}\right)^{\sigma}+2\left(\frac{13}{4}\right)^{\sigma}+2\left(\frac{19}{4}\right)^{\sigma}+2\left(\frac{37}{4}\right)^{\sigma}+2\left(\frac{49}{4}\right)^{\sigma}+2\left(\frac{61}{4}\right)^{\sigma} \tag{32}$$

Moreover, the parameter $T_{oF}$ can be computed as follows

$$T_{oF}(x,y)=\left[\left(x\pm\frac{3}{2}\sqrt{3}\right)^{2}+(y-1.5)^{2}\right]^{\sigma}+\left[x^{2}+(y\pm3)^{2}\right]^{\sigma}$$
$$+\left[\left(x\pm\frac{3\sqrt{3}}{2}\right)^{2}+(y+1.5)^{2}\right]^{\sigma} \tag{33}$$

Accordingly, $T_{oF}$ final form for the same C-H can be evaluated as follows

$$T_{oF}=\left(\frac{25}{4}\right)^{\sigma}+2\left(\frac{31}{4}\right)^{\sigma}+2\left(\frac{43}{4}\right)^{\sigma}+\left(\frac{49}{4}\right)^{\sigma} \tag{34}$$

Subsequently, by replacing the values of Eqs. (32) and (34) into Eq. (30), C-H's SIR can be characterized as follows

$$SIR_{SFR}=\left[\left(\frac{1}{4}\right)^{-\sigma}\left(2\left(\left(\frac{7}{4}\right)^{\sigma}+\left(\frac{13}{4}\right)^{\sigma}+\left(\frac{19}{4}\right)^{\sigma}\right.\right.\right.$$
$$+\left(\frac{31}{4}\right)^{\sigma}+\left(\frac{37}{4}\right)^{\sigma}+\left(\frac{43}{4}\right)^{\sigma}+\left(\frac{61}{4}\right)^{\sigma}\right)$$
$$+3\left(\frac{49}{4}\right)^{\sigma}+\left(\frac{25}{4}\right)^{\sigma}\right)\Bigg]^{-1} \tag{35}$$

where $SIR_{SFR}$ characterizes C-H's SIR of SoFR technique when first configuration is used. The above equation represents C-H's SIR CFT for $\varepsilon=1$. The other CFTs for dissimilar $\varepsilon$ values are executed, but not involved in this section. In the ensuing link, when C-H communicates with the SN located at coordinates (0, 1), Eq. (30) can be modified to characterize the cell edge SN's SIR term as follows

$$SIR_{SNSFR}(x,y)=\frac{\varepsilon\left(x^{2}+(y-0.5)^{2}\right)^{\sigma}}{T_{iSN}(x,y)+\varepsilon T_{oSN}(x,y)} \tag{36}$$

where $T_{oSN}$ and $T_{iSN}$ indicate the outer and inner interference factors in WSN, respectively. The CoCI sources in the outer area resulted from BSs (8, 10, 12, 14, 16 and 18). Additionally, CoCI sources in the inner area originated from BSs (1, 4, 5, 2, 6, 13, 3, 7, 15, 11, 17 and 9). Thus, the final expression of $T_{iSN}$ using Table 5 for the SN is expressed as follows

$$I_{iF}=\frac{2}{5}(4)^{\sigma}+\frac{4}{5}(7)^{\sigma}+\frac{2}{5}(13)^{\sigma}+\frac{2}{5}(19)^{\sigma}+\frac{2}{5} \tag{37}$$

Moreover, the final expression of $T_{oSN}$ can be formulated as follows

$$I_{oF}=\left(\frac{25}{4}\right)^{\sigma}+2\left(\frac{31}{4}\right)^{\sigma}+2\left(\frac{43}{4}\right)^{\sigma}+\left(\frac{49}{4}\right)^{\sigma} \tag{38}$$

Hence, by replacing the values of Eqs. (37) and (38) into Eq. (36), SN's SIR can be characterized as follows

$$SIR_{SNSFR}=\left[\left(\frac{1}{4}\right)^{-\sigma}\left(\frac{2}{5}4^{\sigma}+\frac{4}{5}7^{\sigma}+\frac{2}{5}13^{\sigma}+\frac{2}{5}19^{\sigma}\right.\right.$$
$$+\left(\frac{25}{4}\right)^{\sigma}+2\left(\frac{31}{4}\right)^{\sigma}+2\left(\frac{43}{4}\right)^{\sigma}+\left(\frac{49}{4}\right)^{\sigma}+\frac{2}{5}\right)\Bigg]^{-1} \tag{39}$$

where $SIR_{SNSFR}$ denotes the attained SN's SIR using SoFR technique when first configuration is deployed.

## 2.2 Analysis of R-S OFDMA network with classical WSN

The second configuration considers a classical WSN realized with R-S OFDMA network. This configuration like classical COFDMA-WSN but with deploying relaying approach in the prim link to advance the reliability and performance of the linkage. Hence, the analysis is done into two main phases. The first phase represents R-S OFDMA network analysis to get the C-H's SIR in the prim link. Furthermore, the second step signifies the analysis of classical WSN to compute the SN's SIR in the ensuing link as shown in Fig. 7.

### 2.2.1 Analysis of R-S OFDMA network

In this network, every cell has a centralized BS, a definite number of SNs set in a regular arrangement, and relay station (RS) located at distance equal to $R_d$ (m) in OFDMA network ($R_d = 0.25$ of $R_a$) from the BS. Furthermore, full duplex (FD) amplify and forward (AF) RSs are considered in this system because of their efficiency in employing spectrum resources [16]. Hence, the communication is carried out through two time slots (TSs) as shown in Fig. 8. In first TS, RS is inactive, while BS transmits the signal to both C-H and RS through prime and relay link, respectively. In second TS, RS transmits the formerly received signal to the C-H through access link after amplifying it whereas the BS is lazy. Consequently, Maximum Ratio Combined (MRC) procedure is used at C-H to combine the achieved two SIRs. Thus, the C-H's MRC formula can be stated as follows [17]

$$MRC_{SIR}=1^{st}T.S._{SIR}+2^{sc}T.S._{SIR} \tag{40}$$

where $MRC_{SIR}$ denotes the MRC of the two TSs' SIRs, $1^{st}$ T.S.$_{SIR}$ represents obtained C-H's SIR from the first TS and $2^{sc}$ T.S.$_{SIR}$ indicates achieved C-H's SIR from the second TS. Hence, two TSs analysis is conducted in the next subsections for MRC CFT computation using different FrFR techniques.
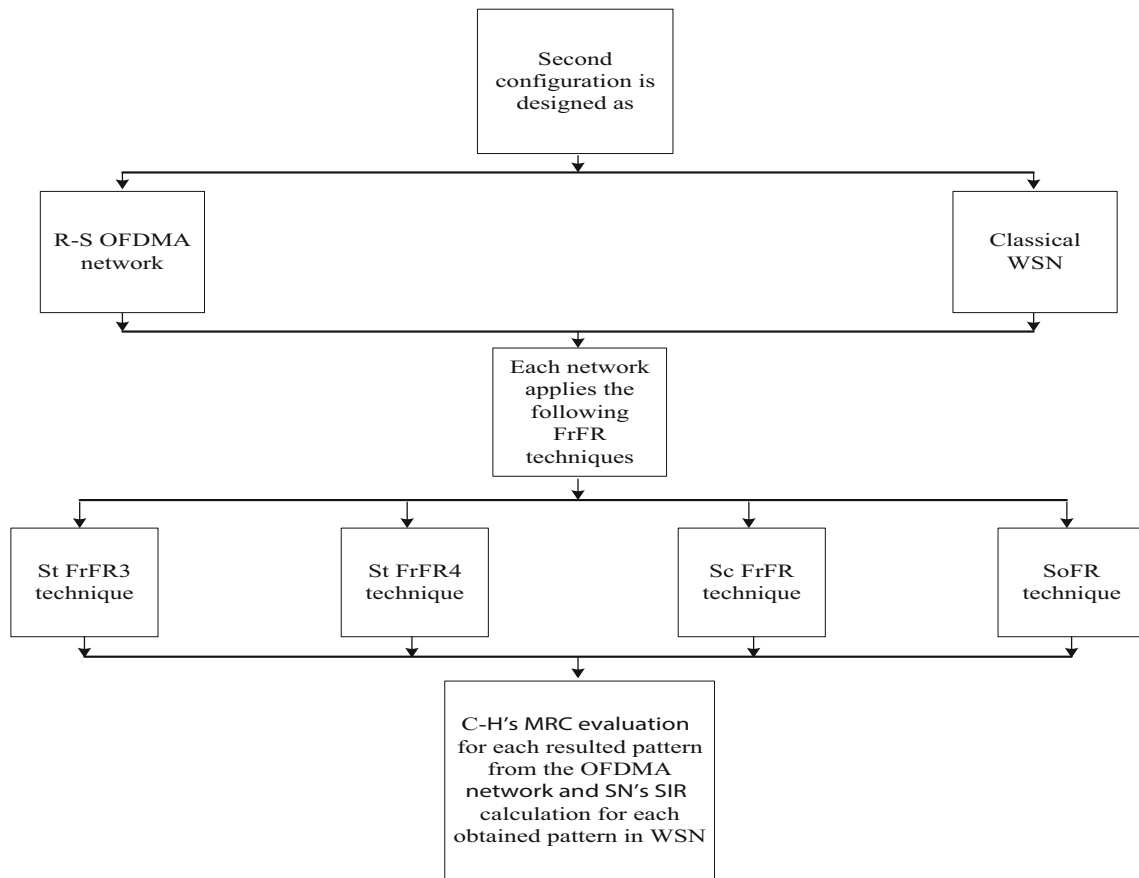
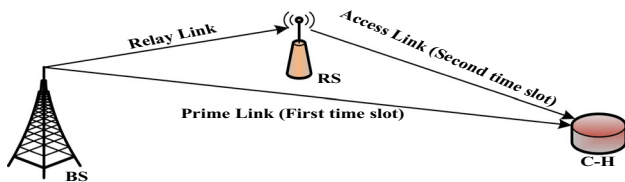**Fig. 7** Conception diagram of second configuration in COFDMA-WSN for energy consumption lessening



**Fig. 8** Conception declaration of MRC technique in R-S OFDMA network

**2.2.1.1 Analysis of R-S St FrFR system** Two-tier St FrFR system based R-S OFDMA network is considered as presented in Fig. 9(a, c). Accordingly, every outer area BF is additional separated in three unlike combinations of $S_F$s to drop the interference impact between the RSs, SNs and BSs as portrayed in Fig. 9(b). The first part represents $S_{F1-1}$ that is allocated to BS. In addition, the second set signifies $S_{F1-2}$, $S_{F1-3}$, $S_{F1-4}$, and $S_{F1-5}$ that are allocated to the SNs. Furthermore, the third portion denotes $S_{F1-6}$ that is apportioned to RS as revealed in Fig. 9(d).

*Analysis of first time slot*: In this TS, the signal is transmitted by BS to both C-H and RS whereas RS keeps inactive. Thus, all neighbouring BSs that usage a BF similar to that of serving BS, represent an interfering sources. Consequently, 6 BSs in the outer section interfering with C-H when St FrFR3 technique is employed. These BSs represent cells number (8, 10, 12, 14, 16 and 18) that use $S_{F1-1}$ as $BS_0$. Furthermore, when St FrFR4 technique is deployed, there are 6 BSs in cells number (7, 9, 11, 13, 15 and 17) interfering with C-H. Therefore, the analysis of this TS is similar to classical St FrFR analysis because the BS in this TS does the communication completely. Thus, achieved C-H's SIR CFTs due to employing St FrFR3 technique and St FrFR4 technique can be evaluated from Eq. (8) and Eq. (11), respectively.

*Analysis of second time slot*: In this TS, C-H receives the amplified signal of RS whereas BSs are inactive. Consequently, C-H's SIR can be framed as follows

$$SIR_R(x,y) = \frac{\left(x^2 + (y - 0.25)^2\right)^\sigma}{T_{RF}(x,y)} \qquad (41)$$

where $T_{RF}$ indicates the interference factor originated form co-channel RSs in surrounding cells. It is assumed, that RS covers C-H through $S_{F1-6}$ in the centre cell. Therefore, 6 RSs in cells with numbers (8, 10, 12, 14, 16 and 18) affecting the C-H when St FrFR3 technique is deployed as revealed in Fig. 9(a). Moreover, there are 6 RSs in cell
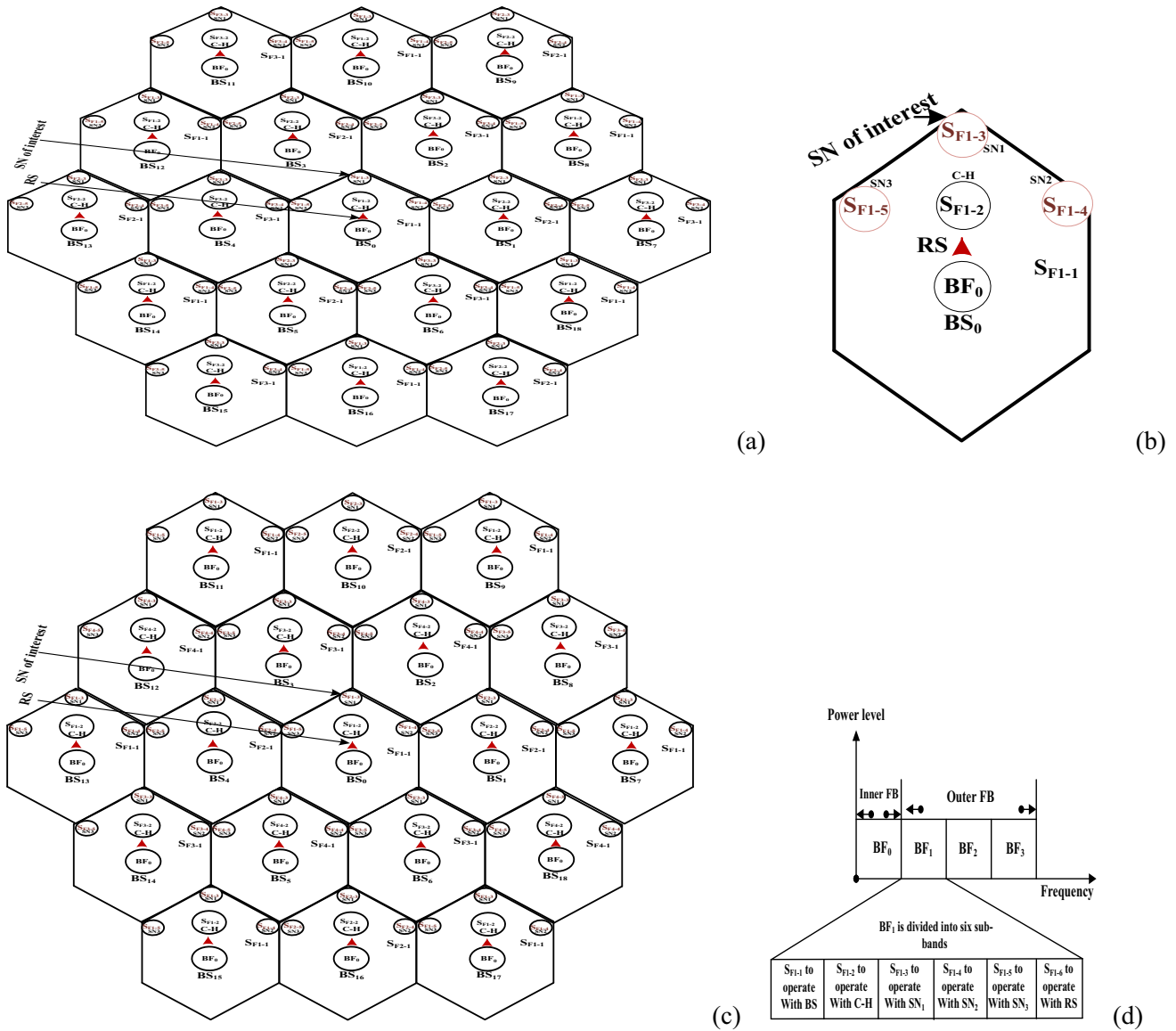
**Fig. 9** Two-tier St FrFR based R-S OFDMA system **a** St FrFR3 system design, **b** Cell arrangement, **c** St FrFR4 system layout, **d** Allocated frequency partition

number (7, 9, 11, 13, 15 and 17) that affecting C-H when St FrFR4 system is used as presented in Fig. 9(c). Furthermore, these RSs' coordinates are declared in Table 6. Consequently, the factor $T_{RF}$ for St FrFR3 system is formulated as follows

$$T_{RF3}(x,y) = \sum_{j_{RS}=1}^{j_{RS}=6} \left[ \left( x + x_{j_{RS}} \right)^2 + \left( y + y_{j_{RS}} \right)^2 \right]^{\sigma} \quad (42)$$

where $j_{RS}$ signifies interfering RSs group in the outer region that use $S_{F1-2}$. Thus, the parameter $T_{RF3}$ is valued as follows

$$T_{RF3}(x,y) = \left[ x^2 + (y+2.75)^2 \right]^{\sigma} + \left[ \left( x \pm \frac{3\sqrt{3}}{2} \right)^2 + (y-1.75)^2 \right]^{\sigma}$$

$$+ \left[ x^2 + (y-3.25)^2 \right]^{\sigma} + \left[ \left( x \pm \frac{3\sqrt{3}}{2} \right)^2 + (y+1.25)^2 \right]^{\sigma}$$

$$(43)$$

Hence, via replacing the worth of Eq. (43) into Eq. (41), C-H's SIR can be obtained as follows

**Table 6** Interfering RSs' Coordinates for St FrFR based R-S OFDMA network

| R-S St FrFR3 network | | | R-S St FrFR4 network | | |
|---|---|---|---|---|---|
| Interfering RS coordinates in cell no | X | Y | Interfering RS coordinates in cell no | X | Y |
| 8 | $3\sqrt{3}/2$ | 1.75 | 7 | $2\sqrt{3}$ | 1/4 |
| 10 | 0 | 3.25 | 9 | $\sqrt{3}$ | 3.25 |
| 12 | $-3\sqrt{3}/2$ | 1.75 | 11 | $-\sqrt{3}$ | 3.25 |
| 14 | $-3\sqrt{3}/2$ | $-1.25$ | 13 | $-2\sqrt{3}$ | 1/4 |
| 16 | 0 | $-2.75$ | 15 | $-\sqrt{3}$ | $-2.75$ |
| 18 | $3\sqrt{3}/2$ | $-1.25$ | 17 | $\sqrt{3}$ | $-2.75$ |

$$SIR_{C-HR3}=\left[\left(\frac{1}{16}\right)^{-\sigma}\left(\left(\frac{121}{16}\right)^{\sigma}+2\left(\frac{133}{16}\right)^{\sigma}+2\left(\frac{157}{16}\right)^{\sigma}+\left(\frac{169}{16}\right)^{\sigma}\right)\right]^{-1} \tag{44}$$

where $SIR_{C-HR3}$ denotes C-H's SIR attained through second TS when St FrFR3 technique is deployed. Consequently, by replacing the worth of Eq. (8) and Eq. (44) into Eq. (40), the CFT of C-H's MRC using St FrFR3 system is formulated as follows

$$MRC_{C-HR3}=\left[\left(\frac{1}{16}\right)^{-\sigma}\left(2\left(\left(\frac{133}{16}\right)^{\sigma}+\left(\frac{157}{16}\right)^{\sigma}\right)+\left(\frac{121}{16}\right)^{\sigma}+\left(\frac{169}{16}\right)^{\sigma}\right)\right]^{-1}$$
$$+\left[\left(\frac{1}{4}\right)^{-\sigma}\left(2\left(\left(\frac{31}{4}\right)^{\sigma}+\left(\frac{43}{4}\right)^{\sigma}\right)+\left(\frac{25}{4}\right)^{\sigma}+\left(\frac{49}{4}\right)^{\sigma}\right)\right]^{-1} \tag{45}$$

where $MRC_{C-HR3}$ represents the obtained C-H's MRC when St FrFR3 system is deployed in the second configuration. On the other hand, the parameter $T_{RF}$ for St FrFR4 system is modelled as follows

$$T_{RF4}(x,y)=\sum_{j_{RS}=1}^{j_{RS}=6}\left[(x+x_{j_{RS}})^{2}+(y+y_{j_{RS}})^{2}\right]^{\sigma} \tag{46}$$

Consequently, the factor $T_{RF4}$ due to CoCI of surrounding RSs is expressed as follows

$$T_{FR4}(x,y)=\left[\left(x\pm\sqrt{3}\right)^{2}+(y+2.75)^{2}\right]^{\sigma}$$
$$+\left[\left(x\pm\sqrt{3}\right)^{2}+(y-3.25)^{2}\right]^{\sigma} \tag{47}$$
$$+\left[\left(x\pm2\sqrt{3}\right)^{2}+\left(y-\frac{1}{4}\right)^{2}\right]^{\sigma}$$

Hence, by replacing the worth of Eq. (47) into Eq. (41), C-H's SIR is symbolized by the following relative

$$SIR_{C-HR4}=\left[\left(\frac{1}{16}\right)^{-\sigma}\left(\left(\frac{73}{16}\right)^{\sigma}+\left(\frac{121}{16}\right)^{\sigma}+\left(\frac{169}{16}\right)^{\sigma}\right.\right.$$
$$\left.\left.+\left(\frac{-191}{16}\right)^{\sigma}+\left(\frac{193}{16}\right)^{\sigma}+\left(\frac{217}{16}\right)^{\sigma}\right)\right]^{-1} \tag{48}$$

where $SIR_{C-HR4}$ denotes achieved C-H's SIR from the second TS when St FrFR4 technique is employed.

Therefore, by replacing the values of Eq. (11) and Eq. (48) in Eq. (40), C-H's MRC using St FrFR4 system can be expressed as follows

$$MRC_{C-HR4}=\left[\left(\frac{1}{16}\right)^{-\sigma}\left(\left(\frac{73}{16}\right)^{\sigma}+\left(\frac{121}{16}\right)^{\sigma}+\left(\frac{169}{16}\right)^{\sigma}\right.\right.$$
$$\left.\left.+\left(\frac{-191}{16}\right)^{\sigma}+\left(\frac{193}{16}\right)^{\sigma}+\left(\frac{217}{16}\right)^{\sigma}\right)\right]^{-1}$$
$$+\left[\left(\frac{1}{4}\right)^{-\sigma}\left(2\left(\left(\frac{37}{4}\right)^{\sigma}+\left(\frac{61}{4}\right)^{\sigma}+\left(\frac{49}{4}\right)^{\sigma}\right)\right)\right]^{-1} \tag{49}$$

where $MRC_{C-HR4}$ represents the achieved C-H's MRC when St FrFR4 system is used in the second configuration.

**2.2.1.2 Analysis of R-S Sc FrFR system** Two tier Sc FFR system based R-S OFDMA network is assumed as presented in Fig. 10(a). Furthermore, each outer BF of each sector is further divided in three unlike $S_F$s groups for interference influence reduction between the SNs, RSs and BSs as displayed in Fig. 10(b). The first portion represents $S_{F1-1}$ which is assigned to BSs. In addition, the second group indicates $S_{F1-2}$, $S_{F1-3}$, $S_{F1-4}$ and $S_{F1-5}$ which are allotted to SNs. Furthermore, the third part signifies $S_{F1-6}$ which is allocated to RS as illustrated in Fig. 10(c).

*Analysis of first time slot*: In this TS, there are 7 BSs which deploy $S_{F1-1}$ and affecting the C-H. These BSs located in cells number (5, 6, 14, 15, 16, 17, and 18). Therefore, the analysis of this TS is similar to classical Sc FrFR analysis because BS in this TS does the communication totally. Therefore, C-H's SIR CFT can be calculated from Eq. (22).

*Analysis of second time slot*: In this TS, every RS transmits the amplified signal to C-H whilst BSs are inactive. Hence, C-H's SIR is valued as follows
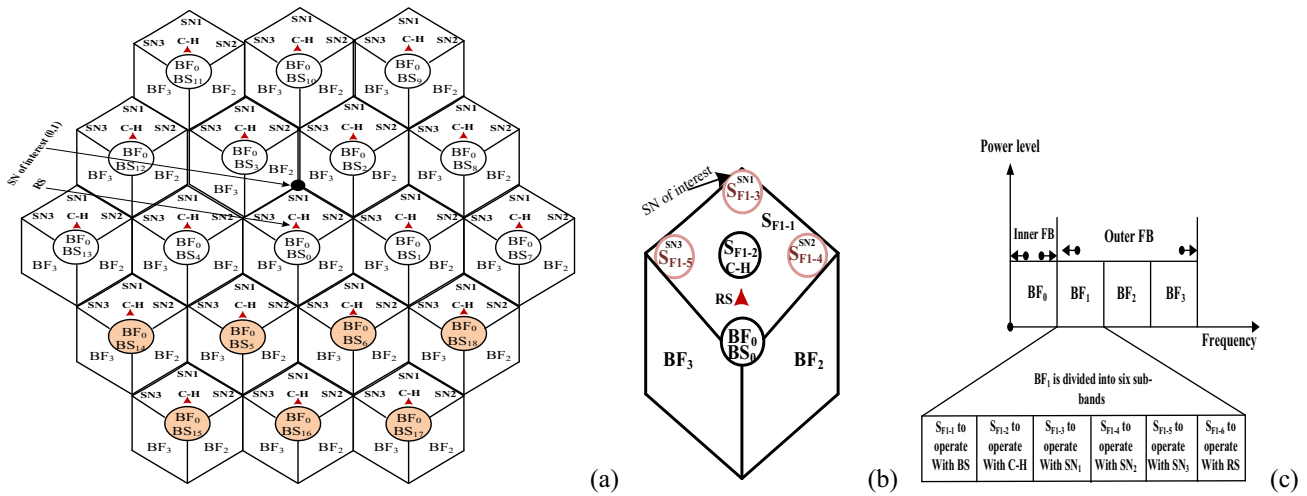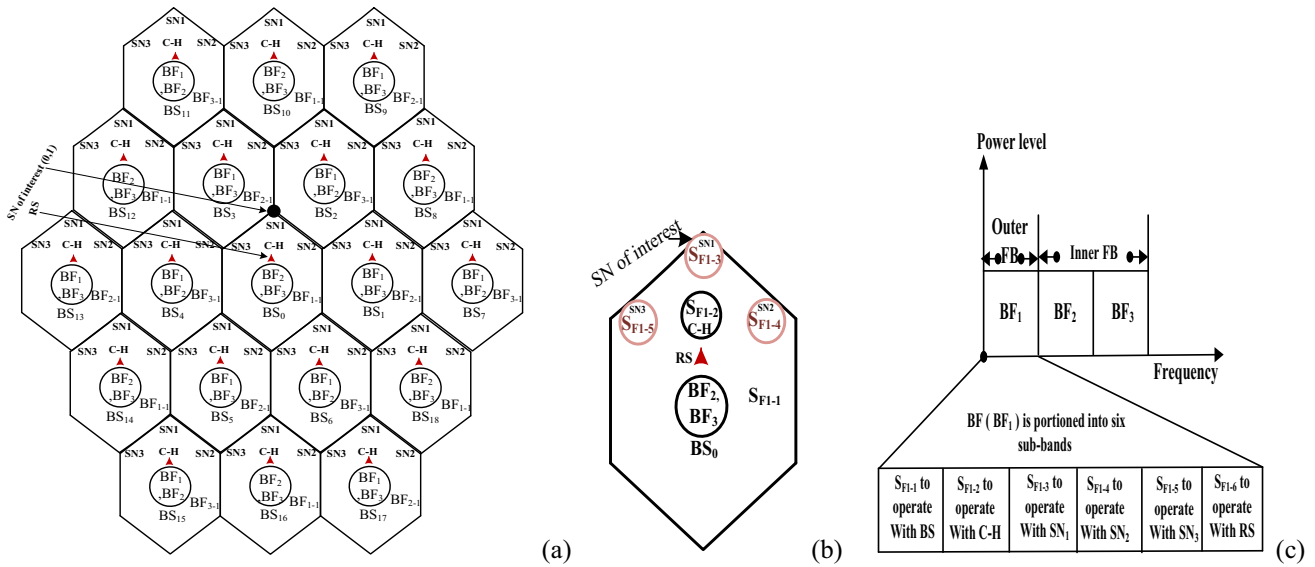
Fig. 10 Two-tier Sc FrFR based R-S OFDMA structure a System design, b Cell arrangement, c Allotted frequency partition

Table 7 Interfering RSs' Coordinates for Sc FrFR and SoFR based R-S OFDMA network

| R-S sectored FrFR system | | | R-S SoFR system | | |
|---|---|---|---|---|---|
| Interfering RS coordinates in cell no | X | Y | Interfering RS coordinates in cell no | X | Y |
| 5 | $-\sqrt{3}/2$ | $-1.25$ | 8 | $3\sqrt{3}/2$ | 1.75 |
| 6 | $\sqrt{3}/2$ | $-1.25$ | 10 | 0 | 3.25 |
| 14 | $-3\sqrt{3}/2$ | $-1.25$ | 12 | $-3\sqrt{3}/2$ | 1.75 |
| 15 | $-\sqrt{3}$ | $-2.75$ | 14 | $-3\sqrt{3}/2$ | $-1.25$ |
| 16 | 0 | $-2.75$ | 16 | 0 | $-2.75$ |
| 17 | $\sqrt{3}$ | $-2.75$ | 18 | $3\sqrt{3}/2$ | $-1.25$ |
| 18 | $3\sqrt{3}/2$ | $-1.25$ | | | |

$$SIR_{R\sec}(x,y) = \frac{\left(x^2 + (y - 0.25)^2\right)^\sigma}{T_{R\sec}(x,y)} \qquad (50)$$

where $T_{R\sec}$ is the interference parameter because of co-channel RSs that deploy $S_{F1-6}$ in surrounding cells as revealed in Fig. 10(a). The coordinates of these RSs that located in cells number (5, 6, 14, 15, 16, 17 and 18) are presented in Table 7. Hence, the factor $T_{R\sec}$ is framed as follows

$$T_{R\sec}(x,y) = \sum_{j_R=1}^{j_R=7} \left[ (x + x_{j_R})^2 + (y + y_{j_R})^2 \right]^\sigma \qquad (51)$$

where $j_R$ denotes the interfering RSs group. Hence, the interference parameter can be evaluated using Table 7 as follows

$$T_{R\sec}(x,y) = \left[ \left(x \pm \frac{\sqrt{3}}{2}\right)^2 + (y + 1.25)^2 \right]^\sigma$$
$$+ \left[ \left(x \pm \sqrt{3}\right)^2 + (y + 2.75)^2 \right]^\sigma$$
$$+ \left[ (x)^2 + (y + 2.75)^2 \right]^\sigma$$
$$+ \left[ \left(x \pm \frac{3\sqrt{3}}{2}\right)^2 + (y + 1.25)^2 \right]^\sigma \qquad (52)$$

Consequently, by replacing the values of Eq. (52) into Eq. (50), SIR of C-H located at coordinates (0, 0.5) is formulated as follows

**Fig. 11** Two-tier SoFR based R-S OFDMA structure **a** System design, **b** Cell arrangement, **c** Allotted frequency partition

$$SIR_{Rsec} = \left[ \left( \frac{1}{16} \right)^{-\sigma} \left( 2 \left( \left( \frac{61}{16} \right)^{\sigma} + \left( \frac{157}{16} \right)^{\sigma} + \left( \frac{217}{16} \right)^{\sigma} \right) + \left( \frac{169}{16} \right)^{\sigma} \right) \right]^{-1}$$

(53)

where $SIR_{Rsec}$ signifies C-H's SIR of the second TS using Sc FrFR system in second configuration. So, by replacing the values of Eq. (22) and Eq. (53) into Eq. (40), MRC CFT for Sc FrFR can be computed as follows

$$MRC_{Sec} = \left[ \left( \frac{1}{4} \right)^{-\sigma} \left( 2 \left( \left( \frac{19}{4} \right)^{\sigma} + \left( \frac{43}{4} \right)^{\sigma} + \left( \frac{61}{4} \right)^{\sigma} \right) + \left( \frac{49}{4} \right)^{\sigma} \right) \right]^{-1}$$
$$+ \left[ \left( \frac{1}{16} \right)^{-\sigma} \left( 2 \left( \left( \frac{61}{16} \right)^{\sigma} + \left( \frac{157}{16} \right)^{\sigma} + \left( \frac{217}{16} \right)^{\sigma} \right) + \left( \frac{169}{16} \right)^{\sigma} \right) \right]^{-1}$$

(54)

where $MRC_{Sec}$ represents the obtained C-H's MRC when Sc FrFR system is deployed in the second configuration.

**2.2.1.3 Analysis of SoFR networks** Two tier SoFR system based R-S OFDMA network is assumed as revealed in Fig. 11(a). Consequently, each outer BF is additional portioned in three different parts of $S_F$s for interference reduction between the SNs, RSs and BSs as shown in Fig. 11(b). One part represents $S_{F1-1}$ which is allocated to BSs. In addition, the second part indicates $S_{F1-2}$, $S_{F1-3}$, $S_{F1-4}$ and $S_{F1-5}$ which are assigned to SNs. Furthermore, the third part denotes $S_{F1-6}$ which is allotted to RS as portrayed in Fig. 11(c).

*Analysis of first time slot*: In this TS, there are18 interfering cells that use $S_{F1-1}$ and affecting C-H. Therefore, the analysis of this TS is similar to the classical SoFR analysis because BS does the communication totally in this TS. Accordingly, C-H's SIR CFT can be evaluated from Eq. (35).

*Analysis of second time slot*: In this TS, the communication is done between the RS and C-H through the access

link. Thus, Eq. (30) can be rewritten to evaluate C-H's SIR in this TS as follows

$$SIR_{SFR-R}(x,y) = \frac{\varepsilon \left( x^2 + (y - 0.25)^2 \right)^{\sigma}}{T_{iR}(x,y) + \varepsilon T_{oR}(x,y)}$$

(55)

where $T_{oR}$ and $T_{iR}$ signify the outer and inner interference parameters, respectively. The interfering BSs' normalized coordinates that deploy $BF_1$ in the inner region are illustrated by Table 3. Accordingly, the factor $T_{iR}$ is stated as follows

$$T_{iR}(x,y) = \frac{1}{6} \left[ \begin{array}{l} \left[ \left( x \pm 2\sqrt{3} \right)^2 + y^2 \right]^{\sigma} + \left[ \left( x + \frac{\sqrt{3}}{2} \right)^2 + \left( y \pm \frac{3}{2} \right)^2 \right]^{\sigma} + \left[ \left( x \pm \sqrt{3} \right)^2 + (y \mp 3)^2 \right]^{\sigma} \\ + \left[ \left( x \pm \sqrt{3} \right)^2 + y^2 \right]^{\sigma} + \left[ \left( x \pm \sqrt{3} \right)^2 + (y \pm 3)^2 \right]^{\sigma} + \left[ \left( x - \frac{\sqrt{3}}{2} \right)^2 + \left( y \pm \frac{3}{2} \right)^2 \right]^{\sigma} \end{array} \right]$$

(56)

Therefore, inner interference parameter expression for C-H located at x = 0 and y = 0.5 is finalized as follows

$$T_{iR} = 3 \left( \frac{7}{4} \right)^{\sigma} + 3 \left( \frac{13}{4} \right)^{\sigma} + 3 \left( \frac{19}{4} \right)^{\sigma} + 3 \left( \frac{37}{4} \right)^{\sigma} + 3 \left( \frac{49}{4} \right)^{\sigma} + 3 \left( \frac{61}{4} \right)^{\sigma}$$

(57)

Furthermore, there are 6 RSs that use $S_{F1-6}$ and interfering with C-H. These RSs' coordinates are presented in Table 7. Subsequently, the factor $T_{oR}$ is valued as follows

$$T_{oR}(x,y) = \left[ x^2 + (y - 3.25)^2 \right]^{\sigma} + \left[ \left( x \pm \frac{3\sqrt{3}}{2} \right)^2 + (y - 1.75)^2 \right]^{\sigma}$$
$$+ \left[ \left( x \pm \frac{3\sqrt{3}}{2} \right)^2 + (y + 1.25)^2 \right]^{\sigma} + \left[ x^2 + (y + 2.75)^2 \right]^{\sigma}$$

(58)

Thus, the outer interference factor formula for the C-H is finalized as follows

$$T_{oR} = \left(\frac{121}{16}\right)^{\sigma} + 2\left(\frac{133}{16}\right)^{\sigma} + 2\left(\frac{157}{16}\right)^{\sigma} + \left(\frac{169}{16}\right)^{\sigma} \qquad (59)$$

Accordingly, by replacing the values of Eqs. (57) and (59) into Eq. (55), C-H's SIR of the SoFR technique can be characterized as follows

$$SIR_{SRC-H} = \left[\left(\frac{1}{16}\right)^{-\sigma}\left(\begin{array}{l} 3\left(\left(\frac{7}{4}\right)^{\sigma} + \left(\frac{13}{4}\right)^{\sigma} + \left(\frac{19}{4}\right)^{\sigma} + \left(\frac{37}{4}\right)^{\sigma} + \left(\frac{49}{4}\right)^{\sigma} + \left(\frac{61}{4}\right)^{\sigma}\right) \\ + \left(\frac{121}{16}\right)^{\sigma} + 2\left(\left(\frac{133}{16}\right)^{\sigma} + \left(\frac{157}{16}\right)^{\sigma}\right) + \left(\frac{169}{16}\right)^{\sigma} \end{array}\right)\right]^{-1} \qquad (60)$$

where $SIR_{SRC-H}$ characterizes C-H's SIR of SoFR technique in the second configuration. Consequently, by substituting the worth of Eqs. (35) and (60) into Eq. (40), the CFT of MRC for the C-H with $\varepsilon = 1$ is calculated as follows

$$\begin{aligned} MRC_{SRC-H} = &\left[\left(\frac{1}{4}\right)^{-\sigma}\left(2\left(\left(\frac{7}{4}\right)^{\sigma} + \left(\frac{13}{4}\right)^{\sigma} + \left(\frac{19}{4}\right)^{\sigma}\right.\right.\right. \\ &\left.+ \left(\frac{31}{4}\right)^{\sigma} + \left(\frac{37}{4}\right)^{\sigma} + \left(\frac{43}{4}\right)^{\sigma} + \left(\frac{61}{4}\right)^{\sigma}\right)]^{-1} \\ &\left.+ 3\left(\frac{49}{4}\right)^{\sigma} + \left(\frac{25}{4}\right)^{\sigma}\right) \\ &+ \left[\left(\frac{1}{16}\right)^{-\sigma}\left(3\left(\left(\frac{7}{4}\right)^{\sigma} + \left(\frac{13}{4}\right)^{\sigma} + \left(\frac{19}{4}\right)^{\sigma} + \left(\frac{37}{4}\right)^{\sigma}\right.\right.\right. \\ &\left.+ \left(\frac{49}{4}\right)^{\sigma} + \left(\frac{61}{4}\right)^{\sigma}\right) + \left(\frac{121}{16}\right)^{\sigma} \\ &\left.\left.+ 2\left(\left(\frac{133}{16}\right)^{\sigma} + \left(\frac{157}{16}\right)^{\sigma}\right) + \left(\frac{169}{16}\right)^{\sigma}\right)\right]^{-1} \end{aligned} \qquad (61)$$

where $MRC_{SRC-H}$ symbolizes C-H's MRC when SoFR technique is used in the second configuration.

### 2.2.2 Analysis of classical WSN

The analysis of this network is identical with that in the first configuration. Consequently, Eqs. (15) and (18) can be used to represent SN's SIR CFTs when St FrFR3 and St FrFR4 techniques are applied, respectively. Furthermore, Eqs. (26) and (39) can be utilized to indicate SN's SIR CFTs when Sc FrFR and SoFR techniques are deployed, respectively. Additionally, the analysis of third configuration (classical OFDMA network with R-S WSN) and fourth configuration (R-S COFDMA-WSN) are proposed and investigated in Appendix A and B, respectively. The comparison of WSN behaviour in different COFDMA-WSN configurations is revealed in Table 8. Furthermore, three different metrics are used to compare different configurations. These metrics represent complexity, achieved SIR and cell cost. Additionally, it is observed, that achieving high SIR requires high complexity and cost. Therefore, the outcomes of this work, in some cases,

provide high network performance with low complexity and cost.

## 3 Metrics for performance estimation of different patterns

In this section, different metrics for performance estimation are valued to contrast all configurations and patterns. These metrics involve the data rate, Energy Efficiency (EE), successful decoding probability, link throughput, packet transmission rate, maximum number of bits per symbols and outage probability deeming the dissimilar channel characteristics in wireless communication.

### 3.1 Outage probability

The probability of outage is a vital measure for cellular networks' performance. It is definite as the probability which the reachable rate can't reach a specified rate of transmission $\delta$ [18]. The significance of this probability acts when an outage happens, the decoding process is more likely to fail. Thus, it represents a typical error. Therefore, different channel propagation influences are considered when calculating the outage probability using the attained SIR expression for each pattern. These influences represent (1) collective influence of shadowing and PLo, (2) joint impact of shadowing, FaF and PLo and (3) combined effect of FaF and PLo.

#### 3.1.1 The collective influence of the shadowing and PLo

For C-H positioned at a distance d (m) from its working BS, the probability of outage by deeming collective shadowing and PLo effect can be valued from the succeeding formula [19]

$$P(SIR_C \prec \delta) = Q\left[\frac{10\log_{10}\left(\frac{1}{\delta}\right) - X_m}{X_s}\right] \qquad (62)$$

where Q denotes the error function which is expressed as $Q(u) = 0.5 erfc(1.414u)$ and $SIR_C$ characterizes the calculated $SIR_C$ in each pattern. Additionally, $X_m$ and $X_s$ factors denote the mean and standard deviation of $G_F$ factor which is expressed as $G_F = (SIR_C)^{-1}$, respectively. Furthermore, mean and standard deviation can be formulated as follows

$$X_m = \frac{1}{\tau}\ln\left(G_f(d,\eta)H(d,Q_{sd})\right) \qquad (63)$$

$$X_s^2 = 2\left(Q_{sd}^2 - \frac{1}{\tau^2}\ln H(d,Q_{sd})\right) \qquad (64)$$

**Table 8** Practical evaluation of WSN behaviour in different COFDMA-WSN configurations

| Different COFDMA-WSN configurations | Evaluation metric | | |
|---|---|---|---|
| | Complexity | Achieved SIR | Cell cost |
| First configuration | Each cell contains BS and four SNs | 26% over that attained in [11] | Ranges from $ (10,000–15000) depending on BS type with an average cost of $104 per sensor |
| Second configuration | Each cell contains BS cooperative with relaying technique and four SNs | Same value as first configuration | Ranges from $ (12,000–20000) depending on the type of both BS and RS with an average cost of $104 per sensor |
| Third configuration | Each cell contains BS and C-H cooperative with relaying technique and three SNs | 14% over second configuration | Ranges from $ (10,000–15000) depending on BS type with an average cost of $2600 for C-H and RS and $104 as an average cost per sensor |
| Fourth configuration | Each cell contains BS and C-H cooperative with relaying technique and three SNs | Same value as third configuration | Ranges from $ (12,000–20000) depending on the type of both BS and RS with an average cost of $2600 for C-H and RS and $104 as an average cost per sensor |

where

$$H(d, Q_{sd}) = e^{\tau^2 Q_{sd}^2/2} \left( A(d,\eta) \left( e^{\tau^2 Q_{sd}^2} - 1 \right) + 1 \right)^{\frac{-1}{2}}$$

$, A(d,\eta) = \dfrac{\sum_j d_j^{-2\eta}}{\left( \sum_j d_j^{-\eta} \right)^2}, G_f(d,\eta) = \dfrac{\sum_j d_j^{-\eta}}{d^{-\eta}}, \tau = \dfrac{\ln(10)}{10}$ and $Q_{sd}$

represents mean received signal logarithmic standard deviation under shadowing effect ($0 \le Q_{sd} \le 8$ dB).

### 3.1.2 Joint shadowing, FaF and PLo impact

Outage probability tacking in to account the joint effect of PLo, shadowing and FaF is considered. Consequently, all configurations and patterns can be contrasted under worst case propagation situation.

Additionally, the succeeding formula can express outage probability in this case as follows [20]

$$P(SIR_C \prec \delta) = \int_0^\infty Q\left[ \frac{10\log_{10}\left(\frac{x}{\delta}\right) - X_m}{X_s} \right] e^{-x} dx \quad (65)$$

### 3.1.3 The combined PLo and FaF effect

The probability of outage under combined PLo and FaF effect due to positioning C-H at a parting point dc (m) from the serving BS, can be formulated as in the next expression [21]

$$P(SIR_C \prec \delta) = 1 - \frac{1}{\left( \frac{\lambda}{dc^{-\eta}} \delta + 1 \right)^v} \quad (66)$$

where

$$v = \left( \sum_{j=1}^N dc_j^{-\eta} \right)^2 \Bigg/ \sum_{j=1}^N dc_j^{-2\eta}$$

and

$$\lambda = \sum_{j=1}^N dc_j^{-2\eta} \Bigg/ \sum_{j=1}^N dc_j^{-\eta}.$$

### 3.2 Successful transmission probability

Successful transmission probability (STP) refers to the probability of achieving a positively decoded message [22]. Accordingly, the STP expression can be formulated as follows

$$P_{SC} = 1 - P_{otg}^{1+L} \quad (67)$$

where $P_{SC}$ represents STP of the message, $P_{otg}$ signifies the outage probability for each transmission attempt and L denotes number of retransmission attempts.

### 3.3 Link throughput valuation

The end-to-end network throughput is a crucial performance metric in cellular networks. It measures the number of packets per second received at the destination. Furthermore, this metric is evaluated from the following formula [22].

$$T_L = \frac{\log(1+\delta)}{1 + L_{avg}} \left( 1 - P_{otg}^{1+L} \right) \quad \text{(bit/sec)} \quad (68)$$

where $T_L$ represents the link throughput and $1 + L_{avg}$ is the average number of transmissions for a successful transmission.

### 3.4 Maximum bits number per symbol

Maximum bits number per symbol that a subcarrier can transmit per unit time at a specific TS can be represented as a function of $\delta$ and maximum bit error rate (BER) [23] as below

$$B_{Sy} = \left[ \log_2 \left( 1 + \frac{-1.5}{\ln(5B_{ER})} \delta \right) \right] \quad \text{(bit/symbol)} \tag{69}$$

### 3.5 Data rate evaluation

Data Rate indicates the transmitted data amount through an identified time period over a network. It can be considered to represent the rapidity at which data is moved from transmitter to the receiver [22]. Accordingly, Eq. (68) can be modified to evaluate the data rate as follows

$$\log(1 + \delta) = \frac{T_L \left( 1 + L_{avg} \right)}{\left( 1 - P_{otg}^{1+L} \right)} \quad \text{(bit/sec)} \tag{70}$$

### 3.6 Assessment of energy efficiency for cellular networks

Energy efficiency represents the compatibility process between the total energy consumption per bit ($P_T$) in a network and the throughput [22]. Accordingly, EE can be represented by the following formula

$$EE = \frac{\left( 1 - P_{otg}^{1+L} \right) \log(1 + \delta)}{\left( 1 + L_{avg} \right) \left( \frac{\delta}{\beta} + P_T \right)} \tag{71}$$

where $P_T$ represents the total energy consumption per bit. Hence, this parameter can be evaluated from the following formula

$$P_T = \sum_{A=1}^{L+1} \frac{P_p + P_{TX} + P_{RX}}{\log(1 + \delta)} \text{(mW)} \tag{72}$$

where $P_{TX}$ is the transmission power consumption, $P_{RX}$ is the consumed power during reception, and $P_P$ is the power consumed by the power amplifier in an one-hop communication network. This consumed power is itself a function of the drain efficiency parameter of the amplifier ($\beta$). So, the power consumed by the power amplifier can be represented by the following formula

$$P_p = \frac{\delta}{\beta} \text{(mW)} \tag{73}$$

### 3.7 Packet transmission rate

Packet transmission rate is an efficient way to handle transmissions on a connectionless network. Therefore, if channel has $B_{BW}$ bandwidth and $N_{sc}$ subcarriers, then each subcarrier has a bandwidth of $\Delta f = B_{BW} / N_{sc}$. If the length of a TS is $L_{TS}$, having $B_{Sy}$ bit rate from Eq. (69) with a packet of length $P_L$ bits, then packet transmission rate $P_{TR}$ per TS for this Node and subcarrier [23] is,

$$P_{TR} = \frac{L_{TS}.B_{Sy}.\Delta f}{P_L} \quad \text{(packet/sec)} \tag{74}$$

### 3.8 Average number of retransmissions

An outage event occurs if a communicated message is not positively decoded at the receiver side. So, the retransmission is a very effective method for reducing the link error rate and outage probability [22]. Hence, Eq. (68) can be reformulated to compute the average number of retransmissions as follows

$$1 + L_{avg} = \frac{\log(1 + \delta)}{T_L} P_{SC} \tag{75}$$

## 4 Outcomes and discussion

This study presents an analytical conduct to reduce energy consumption in OFDMA-WSNs through different interference mitigation systems. This treatment yielded CFTs of the C-H's SIR and worst-case SN's SIR. The obtained CFTs are deployed to value several performance metrics. Consequently, different patterns are compared in this section. This comparison is arranged into two main phases. The first phase compares the effect of using different interference techniques on the behaviour of the C-H through the prim link. So, the attained values of C-H's SIR form first, second, and forth configurations are considered in this stage. Furthermore, it is noticed, that the achieved C-H's SIR of St FrFR3, St FrFR4 and Sc FrFR techniques in second configuration and forth configuration are equal. So, second configuration is considered to represent these two configurations in the comparison from the mentioned techniques perspective. Moreover, the second phase studies the effect of interference reduction techniques on SNs through the ensuing link. Consequently, the attained values
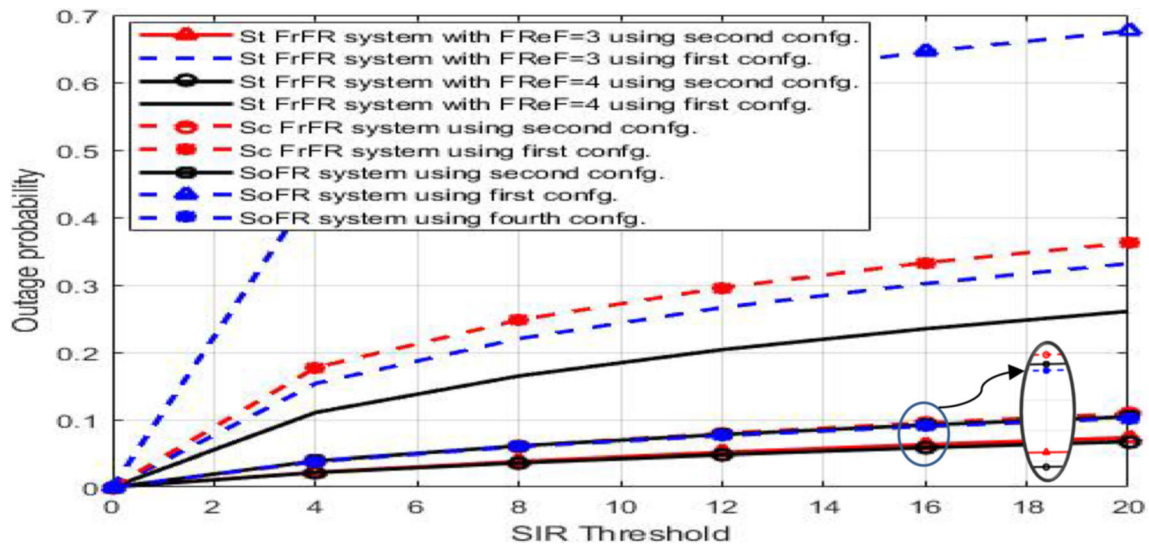
**Fig. 12** Outage probability of different configurations against SIR threshold in the prime link with Ra = 1000 m, BW = 10 MHz, σ = 4 and Qsd = 8 dB

of SN's SIR form first, third, and forth configurations are deliberated in this phase. Additionally, it is observed, that the realized SN's SIR of St FrFR3, St FrFR4 and Sc FrFR techniques in third configuration and forth configuration are identical. Therefore, third configuration is deliberated to characterize these two configurations in the comparison from the declared techniques viewpoint. Accordingly, the consequences of this work introduce an obvious concept about the behaviour of cooperative OFDMA-WSN systems. Consequently, this work contribute to improving the link throughput, STP, and EE of these networks.

The outage probability variant with SIR threshold is shown in Figs. 12, 13. From these figures, it is noted, that probability of coverage surges as the obtained SIR value surpasses the SIR threshold worth. Consequently, rising SIR threshold worth cause, a decreasing in the probability at which network can cover C-H and SNs. Accordingly, probability of outage increases. Additionally, the outage probability valuation deeming different propagation conditions is done. The attained outcomes definite, that the collective influence of the PLo, shadowing and FaF has the poorest influence on achieved SIR worth. Therefore, the following consequences are attained considering this circumstance. In addition, the outcomes under joint influence of (PLo and shadowing) and combined effect of (PLo and FaF) situations are investigated but not involved in this section. Also, it is observed, that in general, the first configuration applies dissimilar FrFR methods attains the lowest performance in the prime link compared to the second and fourth configurations as revealed in Fig. 12. The cause of this consequence can be ascribed, to the presence of RSs that significantly improve the signal strength in the second and fourth configurations. Moreover, the performance significant drop of first

configuration using SoFR can be accredited, to the high interference rates caused by deployment of $T_{PC}$ scheme. Additionally, it is noted, that the performance of second configuration employs St FrFR4 is superior to other patterns. The cause of this outcome, thanks to the decrement of frequency reuse process due to FReF increment. Consequently, the interference sources reduces. Accordingly, the strength of interfering signals decreases. Therefore, this pattern achieves the highest value of the SIR. On the other hand, it is noticed, that the first configuration comes late in terms of performance in the ensuing link compared to the third and fourth configurations as revealed in Fig. 13.

The cause for this consequence can be ascribed, to the strong interference effect, which greatly disturbs the SIR in the first configuration. Consequently, the probability of outage increases. Furthermore, it is noticed, compared to Fig. 12, the performance of St FrFR3 system deployed in the second configuration was retracted, and the SoFR technique using fourth configuration took its place as the second best pattern gives coverage probability for the SNs as revealed in Fig. 13. The cause of this outcome, thanks to the MRC increment in the two TSs due to RSs deployment.The change of EE value with PLoE is represented in Figs. 14, 15. From these figures, it is noted that, PLo gain surges due to PLoE rise which leads to the compensation of the signal attenuation. Accordingly, the obtained SIR from the two TSs increases. Therefore, the gotten MRC increases. Consequently, coverage probability of C-H and SNs increases. Accordingly, the retransmission attempts for reducing the link error rate reduces. Therefore, value of EE increases. Furthermore, it is noticed, that fourth configuration applies SoFR system exhibits better performance than pattern of second configuration deploys St FrFR3 in a
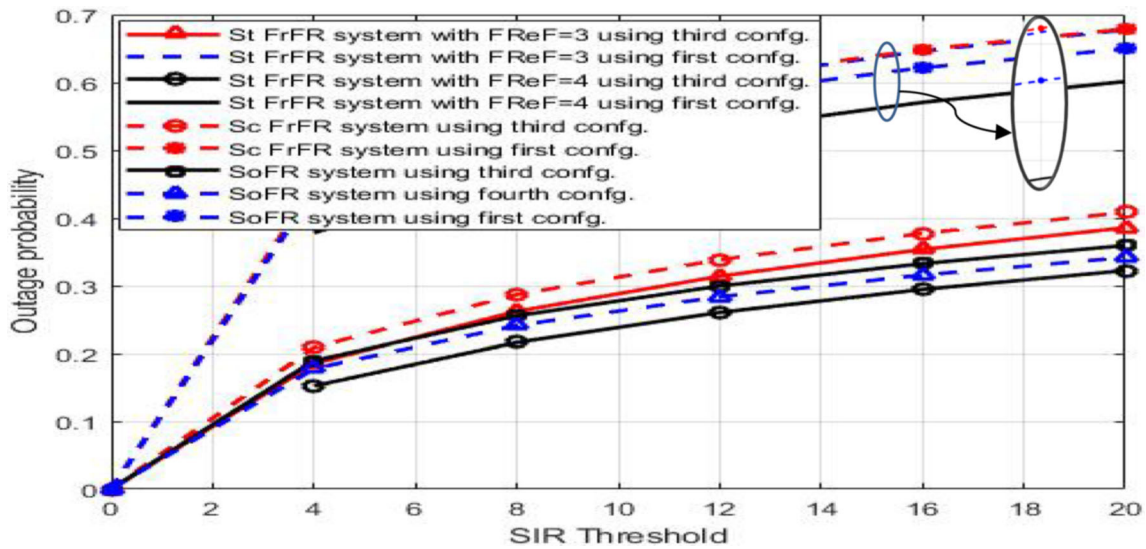
**Fig. 13** Outage probability of different configurations against SIR threshold in the ensuing link with Ra = 1000 m, BW = 10 MHz, σ = 4 and Qsd = 8 dB
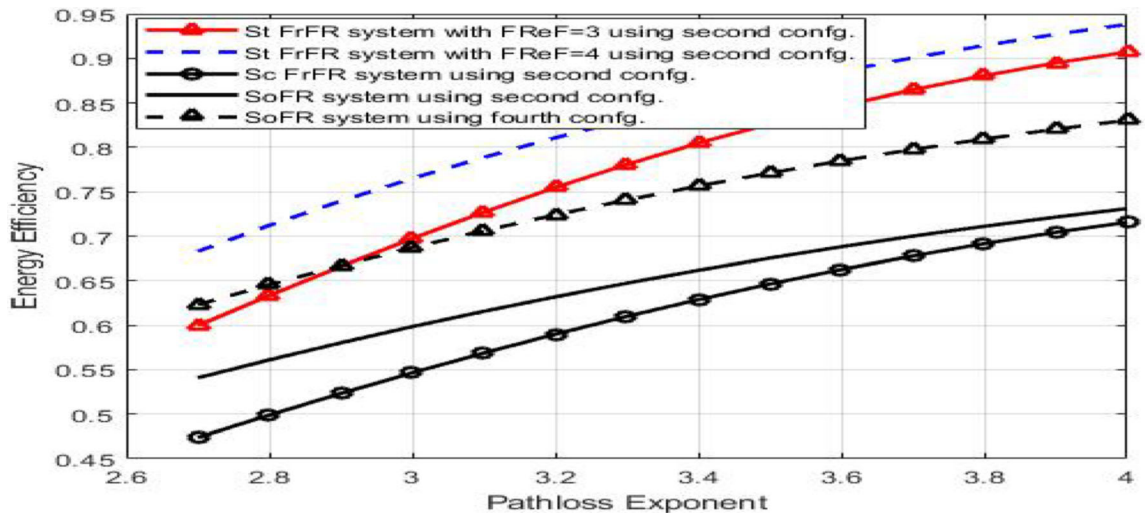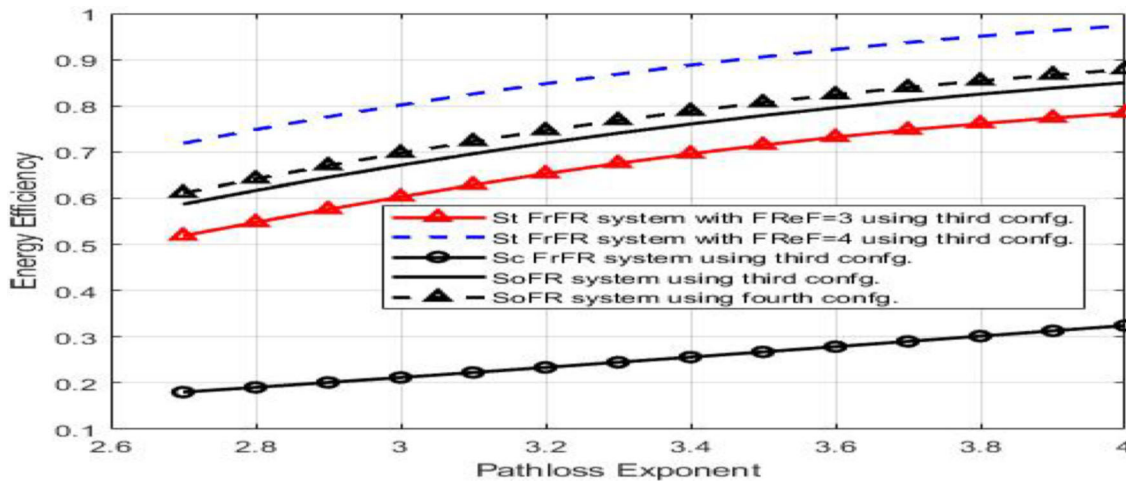


**Fig. 14** Energy efficiency of different configurations against PLoE through prime link with $R_a$ = 1000 m, BW = 10 MHz, $P_{TX}$ = 97.9 mW, $P_{RX}$ = 112.2 mW and β = 0.35

low PLoE range as revealed in Fig. 14. Moreover, SoFR technique lost its supremacy in high PLoE worth and second configuration uses St FrFR3 attains the highest values of EE. The cause of this outcome can be attributed, to the increment rate of SIR worth with PLoE in the second TS of second configuration uses St FrFR3 is much higher than that in fourth configuration applies SoFR. So, St FrFR3 in second configuration resulted in better achieved MRC. Consequently, it realizes much higher EE values than those of SoFR system in fourth configuration under high PLoE values condition. Additionally, it is observed, that Sc FrFR technique performs worse than other techniques when deployed in prim or ensuing link as revealed in Figs. 14, 15. The cause of this outcome can be ascribed,

to Sc FrFR technique inability to reach low the outage probability value. Therefore, STP decreases. This leads to more energy consumption. Accordingly, EE value decreases. Furthermore, it is noticed, that the performance of SoFR technique in third configuration is close to that in fourth configuration as revealed in Fig. 15.

Accordingly, applying SoFR technique with third configuration has the periority of usage from the network cost point of view. The cause of this outcome, thanks to the ability of third configuration employs SoFR pattern to provide nearly the same EE values as using SoFR in fourth configuration with lower cost. These outcomes are suitable in defining the deployment significance level of dissimilar interference mitigation techniques after making a

**Fig. 15** Energy efficiency of different configurations against PLoE through ensuing link with $R_a$ = 1000 m, BW = 10 MHz, $P_{TX}$ = 97.9 mW, $P_{RX}$ = 112.2 mW and $\beta$ = 0.35
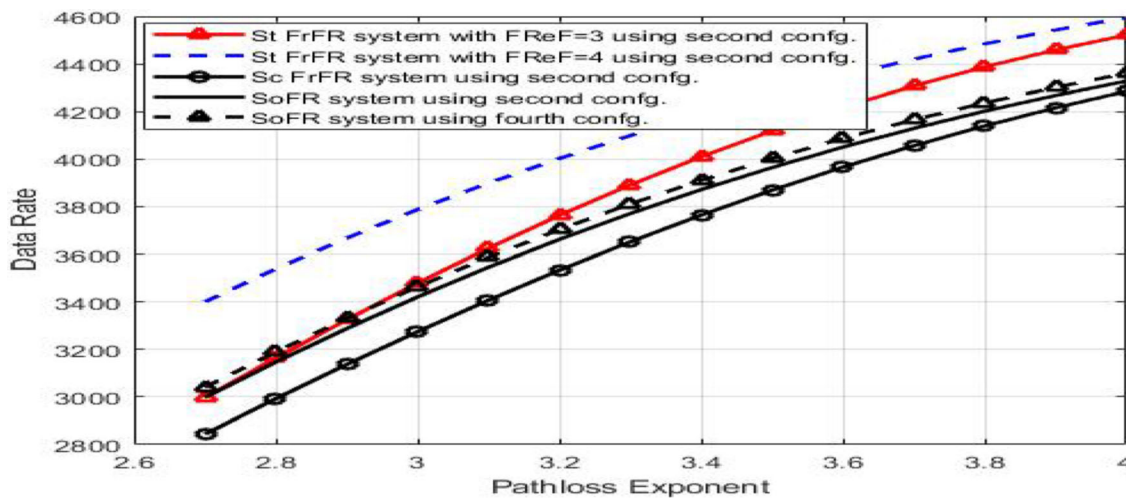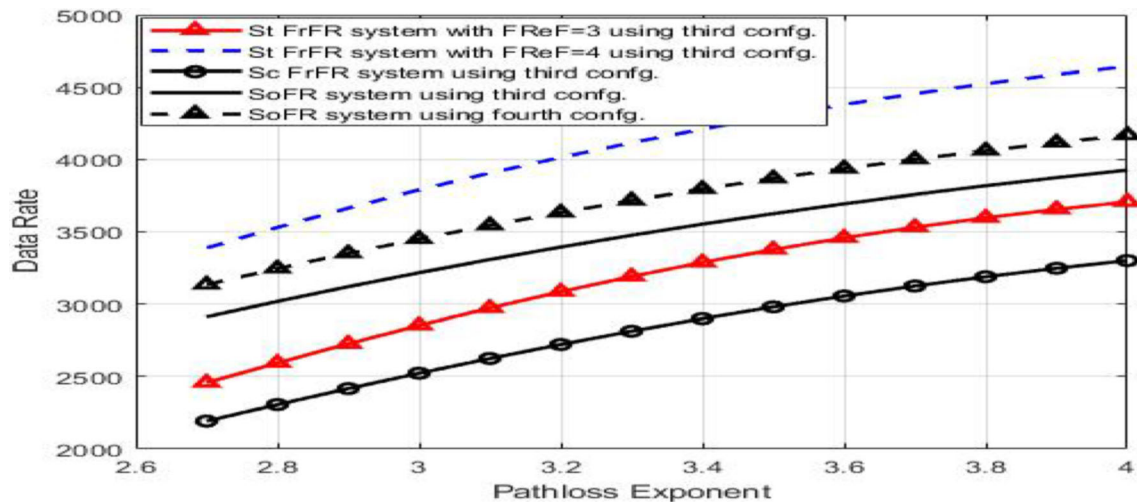


**Fig. 16** Data rate of different configurations through prime link against PLoE with $R_a$ = 1000 m, BW = 10 MHz, $1 + L_{avg}$ = 5, $T_L$ = 5000 bit/sec and $Q_{sd}$ = 8 dB

trade-off between desirable performance and network cost. The alteration of data rate with PLoE is depicted in Figs. 16, 17. From these figures, it is noticed, that transmitted data rate over the system BW increases with SIR increase. Consequently, data rate increase with PLoE increase. Furthermore, it is observed, that negative interference effect decreases as the FReF increases. Accordingly, St FrFR4 attains highest SIR values in the two TSs.

Hence, St FrFR4 technique outperforms the techniques in achieving high MRC values. As a result, patterns of using St FrFR4 with second and third configurations outdoes other patterns. Also, it is noticed, that the adjoining in distance between interfering sources and C-H in the second TS reasons the deploying of SoFR system with fourth configuration has preference in use than using St FrFR3 technique with second configuration under low PLoE

values as revealed in Fig. 16. However, the pattern of deploying St FrFR3 technique in the second configuration has the superiority in a high PLoE range. This result can be accredited, to the high interference impact caused by $T_{PC}$ employment which negatively affects the data transfer rate. Furthermore, it is observed, that applying SoFR technique with third configuration has the usage priority than using it with fourth configuration. The cause of this consequence can be accredited, to the aptitude of SoFR technique in third configuration to achieve closely similar data rate as in fourth configuration as shown in Fig. 17 with lower power consumption and network budget.

Furthermore, the variation of link throughput with PLoE is portrayed in Figs. 18, 19. From these figures, it is observed, that SIR increases with PLoE increase due to the signal lessening compensation.

**Fig. 17** Data rate of different configurations through ensuing link against PLoE with $R_a$ = 1000 m, BW = 10 MHz, $1 + L_{avg}$ = 5, $T_L$ = 5000 bit/sec and $Q_{sd}$ = 8 dB
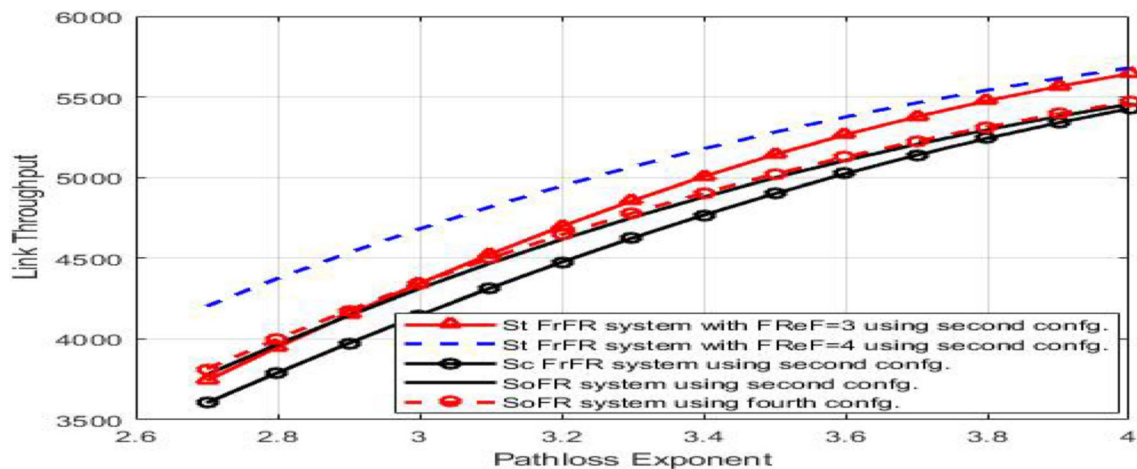


**Fig. 18** Link throughput of different configurations against PLoE through prim link with $R_a$ = 1000 m, BW = 10 MHz, $1 + L_{avg}$ = 5, log $(1 + \delta)$ = 4000 bit/sec and $Q_{sd}$ = 8 dB

Therefore, the number of packets per second received at the destination upsurge. Hence, the throughput rises with PLoE surge. It is noticed, that patterns of second configuration employs FrFR3 and fourth configuration deploys SoFR have approximately the same performance in low PLoE range as revealed in Fig. 18. However, the superiority of the second configuration employs St FrFR3 technique is evident in the high PLoE range. The reason of this outcome can be attributed, to the SIR worth rise rate with PLoE in the second TS of second configuration uses St FrFR3 is much higher than it in fourth configuration deploys SoFR. Therefore, it excels in terms of achieving a high C-H's throughput. However, it was noticed, that the use of St FrFR3 technique with the third configuration in ensuing link led to a decline in the level of performance for the link throughput, to the fourth place in the low PLoE values and the third place in the high PLoE values as

depicted in Fig. 19. Therefore, it is not preferable to use the St FrFR3 technique when high throughput values are required in the ensuing link.

The change of average number of retransmission attempts with SIR threshold is shown in Figs. 20, 21. From these figures, it is observed, that probability of outage surges, as the obtained SIR worth cannot exceed the SIR threshold worth. So, the transmitted message failing probability to reach the receiver increases. Hence, the number of retransmission attempts increase to overcome the outage probability impact. Consequently, the number of retransmission attempts increase as SIR threshold increase. Additionally, the performance difference of the patterns in terms of deliver the message capability is obvious in the high SIR threshold values. Moreover, it is noticed, applying St FrFR4 technique in second and third configurations outperforms the other patterns. The cause of
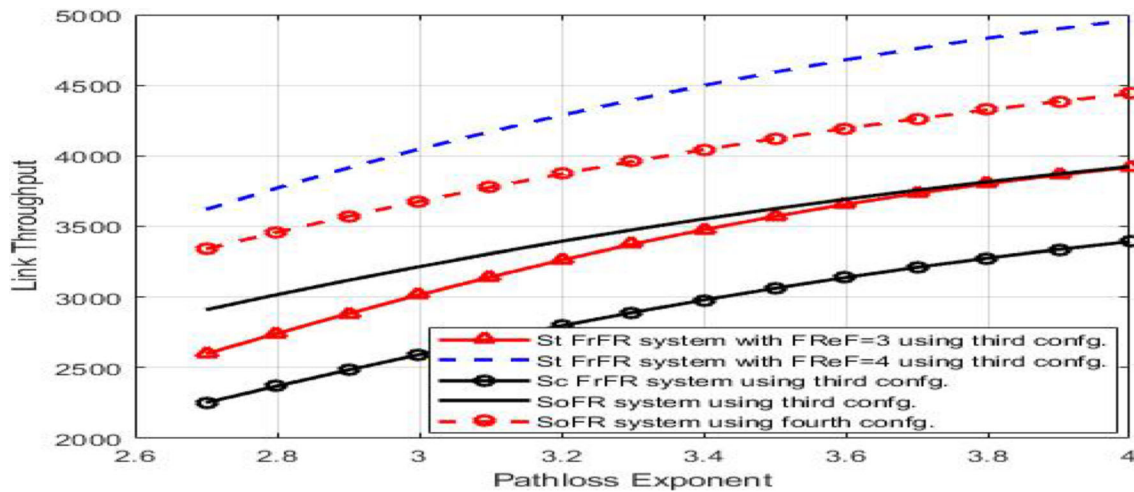
**Fig. 19** Link throughput of different configurations against PLoE through ensuing link with $R_a$ = 1000 m, BW = 10 MHz, $1 + L_{avg}$ = 5, log $(1 + \delta)$ = 4000 bit/sec and $Q_{sd}$ = 8 dB
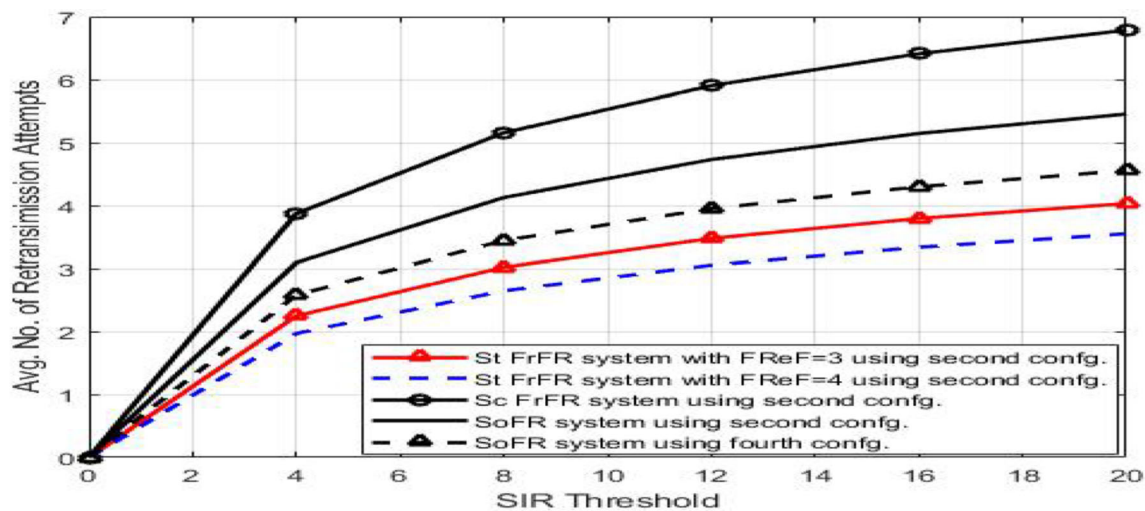


**Fig. 20** Average number of retransmission attempts of different configurations against PLoE through prim link with $R_a$ = 1000 m, BW = 10 MHz, log $(1 + \delta)$ = 4000 bit/sec, $T_L$ = 5000 bit/sec and $Q_{sd}$ = 8 dB

this outcome can be ascribed, to high-attained MRC due to SIR increase. Thus, the coverage probability increases. Therefore, these two patterns attain highest data consistent transfer. Accordingly, retransmission attempts decreases. In addition, it is noted, that deploying SoFR in fourth configuration is superlative than using it in other configurations as portrayed in Figs. 20, 21. This outcome can be credited, to the improved desired signal power due to using relaying technique in both prime and ensuing links. Therefore, employing SoFR technique in fourth configuration is superior to its peers in other configurations. However, this pattern loss its preference in the low SIR threshold range and it is preferable to use the pattern of second and third configurations applying SoFR sysetm. The reason of this consequence can be ascribed, to the

aptitude of these two patterns to do approximately equal performance with reduced cost.

Moreover, it is noted, that applying Sc FrFR in the second, third and fourth configurations leads to an increase in the number of retransmissions. Therefore, the average time taken between a packet initially sent by the source, and the time for successfully receiving the message at the destination increases. Consequently, the network delay increases. However, the SoFR technique achieves the highest network delay when the traditional configuration is used in the prim link. On the other hand, the Sc FrFR technique maintains the performance of the latecomer in terms of achieving the highest network delay when used with the traditional configuration in the ensuing link. Moreover, it is noted, that deploying St FrFR4 technique with all configuration achieves the lowest network delay.
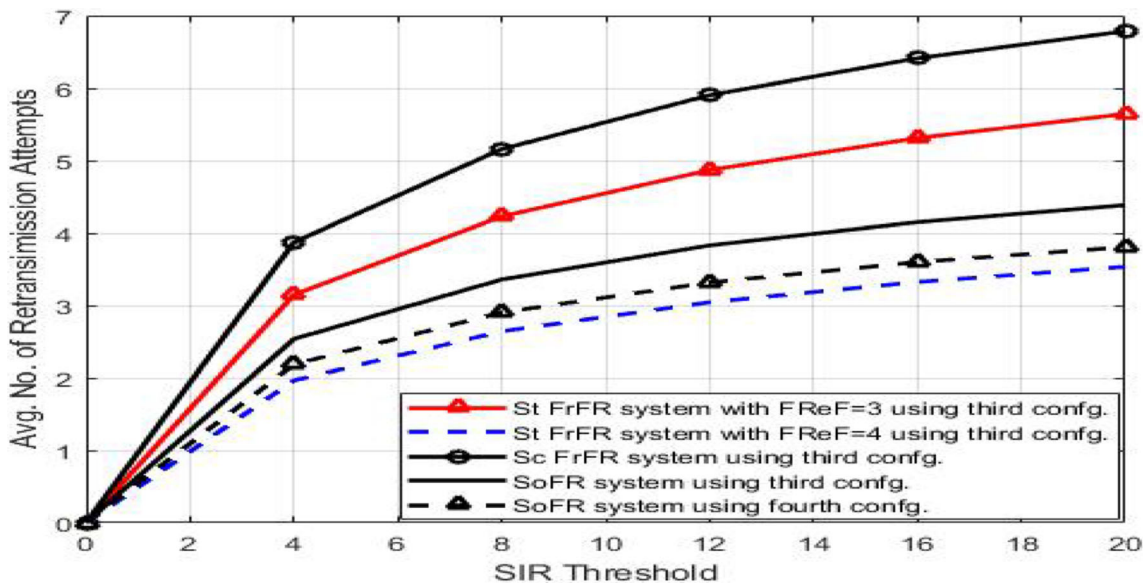
**Fig. 21** Average number of retransmission attempts of different configurations against PLoE through ensuing link with $R_a = 1000$ m, BW = 10 MHz, log $(1 + \delta) = 4000$ bit/sec, $T_L = 5000$ bit/sec and $Q_{sd} = 8$ dB
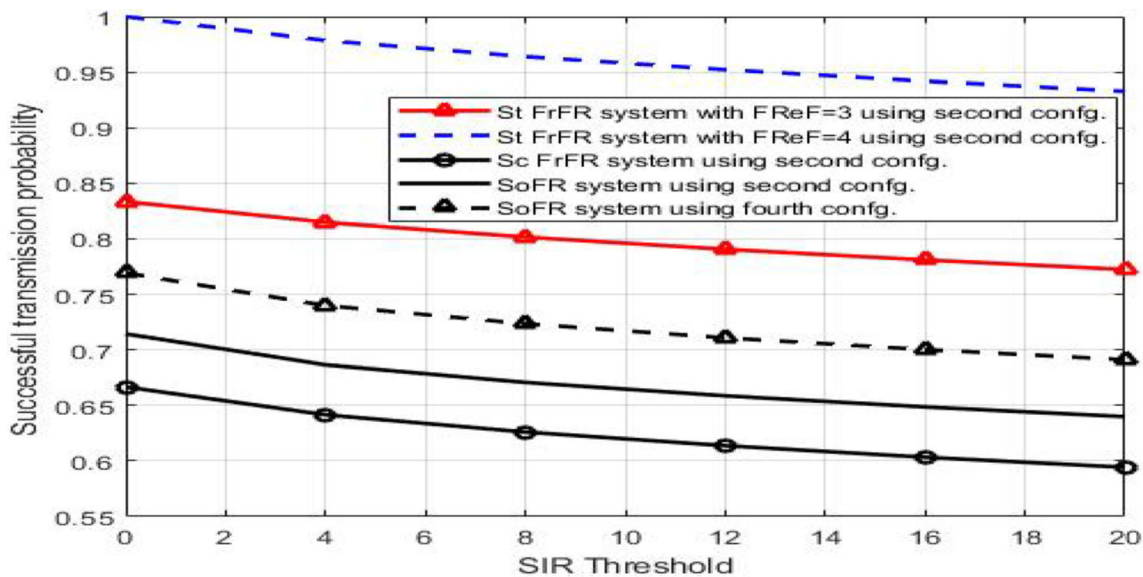


**Fig. 22** STP of different configurations against SIR threshold through prime link with $R_a = 1000$ m, BW = 10 MHz, $\sigma = 4$ and $Q_{sd} = 8$ dB

Moreover, applying St FrFR3 technique in the second configuration achieves the second place in terms of speed of successful message delivery in the prime link as shown in Fig. 20. However, the second priority in the ensuing link is attained by fourth configuration deploys SoFR technique as revealed in Fig. 21. Additionally, it is observed, that the variance rate between dissimilar configurations in low PLoE part is fewer than it in high PLoE part. The cause of this effect can be ascribed, to the decreasing of signal lessening influences in high PLoE worth because of the rise in PLo gain worth.

The successful transmission probability change with SIR threshold is depicted in Figs. 22, 23. From these figures, it is noted, that outage probability increases as the SIR threshold worth increase. Thus, the probability of achieving successful decoded message at the receiver decreases. Therefore, successful transmission probability decreases. Furthermore, it is noticed, that using SoFR in the prime link with the second configuration provides deprived behavior, but this performance improves with the use of the fourth configuration as revealed in Fig. 22. The origin of this effect can be accredited, to the increased SIR caused
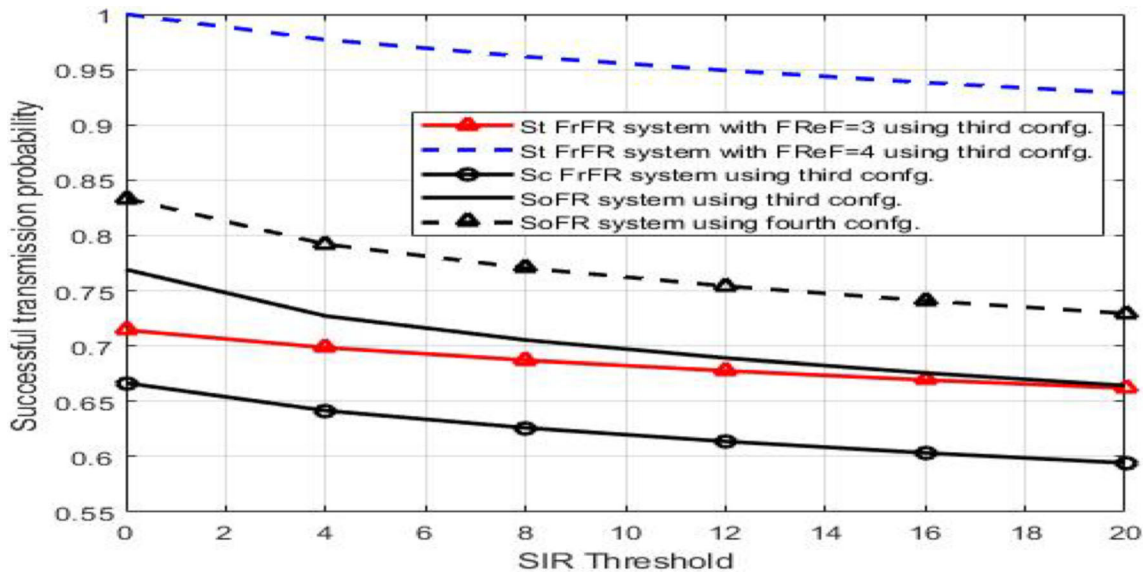
**Fig. 23** STP of different configurations against SIR threshold through ensuing link with $R_a = 1000$ m, BW = 10 MHz, $\sigma = 4$ and $Q_{sd} = 8$ dB
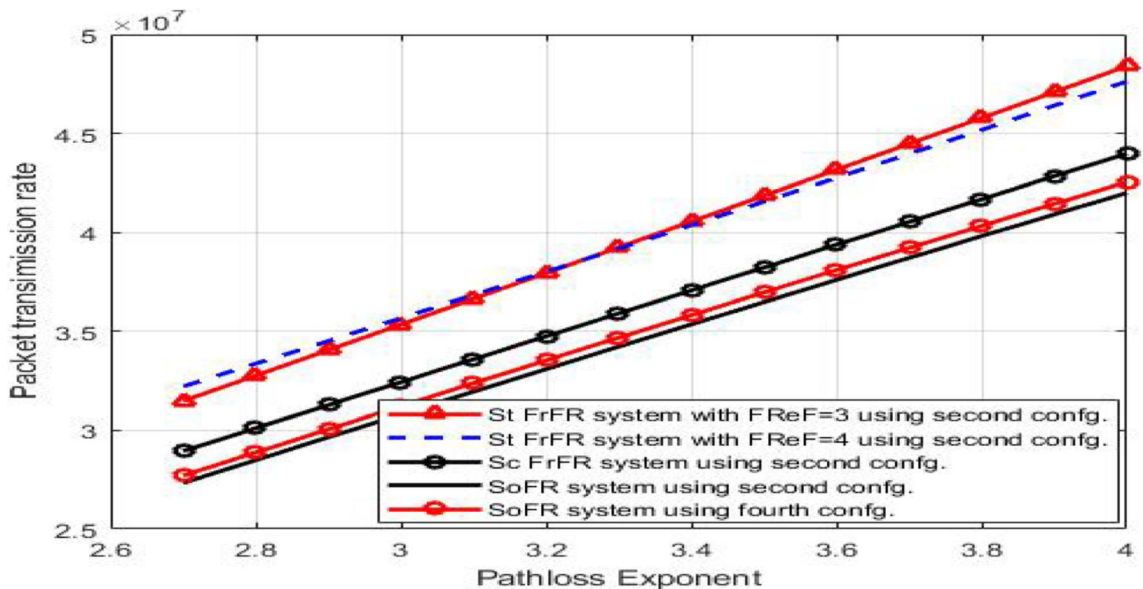


**Fig. 24** Packet transmission rate variation in prime link against PLoE for different network configurations with $R_a = 1000$ m, $P_L = 500$ bytes, $\Delta f = 120$ kHz and $L_{TS} = 10$ ms

by employing relaying technique in both links. Accordingly, STP increases. Additionally, it is noted, that pattern of third configuration deploying Sc FrFR achieves the highest outage probability as shown in Fig. 23. Accordingly, it cannot cover the SNs in an efficient way. Consequently, it achieves the lowest probability of having a successfully decoded message at SN. Additionally, it is noticed, that all patterns that employ St FrFR4 technique are superior to other patterns. The cause of this consequence can be ascribed, to the reduced interference influence due to high FReF. Therefore, obtained SIR in the two

TSs rises. Consequently, the achieved MRC exceeds greatly the attained MRC from other techniques. Accordingly, St FrFR4 technique has the priority to use when high STP is desirable.

The variation of packet transmission rate with PLoE is shown in Figs. 24, 25. From these figures, it is observed, that effect of signal attenuation decreases with PLoE increase. Hence, the data quantity moved positively from one point to another in a specified time period increases. Accordingly, the packet transmission rate increases. Furthermore, it is noted that pattern of second configuration
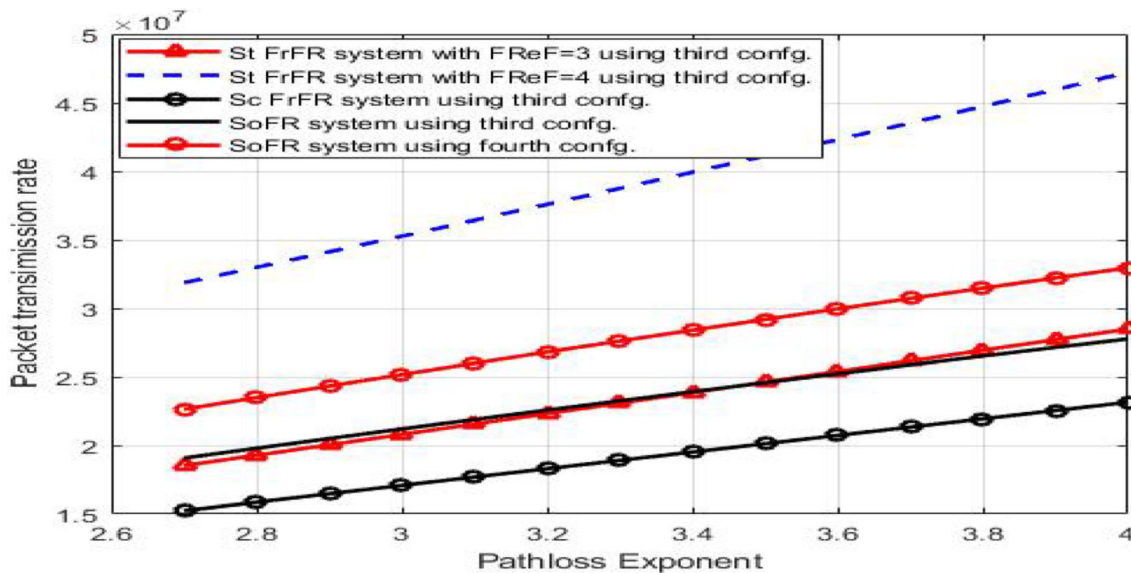
**Fig. 25** Packet transmission rate variation in ensuing link against PLoE for different network configurations with $R_a$ = 1000 m, $P_L$ = 500 bytes, $\Delta f$ = 120 kHz and $L_{TS}$ = 10 ms

uses St FrRF3 technique has preference in usage than other techniques in high PLoE values as shown in Fig. 24. This consequence may be ascribed, to the improved C-H's SIR in the second TS. Accordingly, this technique attains the highest value of MRC, which allow it from realizing the maximum $P_{TR}$ rates.

Additionally, it is noticed, that the near in distance between interfering sources and C-H in the second TS reasons the pattern of second configuration uses St FrRF4 has preference in usage in low PLoE value only. Moreover, it is noticed, that pattern of third configuration uses St FrRF4 technique is superior to other techniques as shown in Fig. 25. This outcome may be accredited, to its aptitude to achieve the highest SN's MRC. Consequently, this pattern attains the maximum $P_{TR}$ values. Moreover, it is noted, that the preference for using St FrRF3 technique has fallen to the third position in the high PLoE range and to the fourth position in low PLoE part. Furthermore, a comparison with existing techniques in terms of several key performance parameters is executed. Specifically, in terms of the SIR, the proposed methodology achieves an increment of 29% in prime link and 26% rise in ensuing link compared to the current state-of-the-art approaches [11]. This increment indicates a higher accuracy and precision in receiving the desired signal. Furthermore, the proposed methodology exhibits an increase in link throughput by 17% in prime link and by 13% in ensuing link compared to [11]. This increase signifies a better overall consistency and reliability in the data transfer. Additionally, the proposed methodology outperforms existing techniques in terms of energy efficiency, increasing the energy efficiency by 25% in prime link and by 15%

in ensuing link compared to [11]. This improvement allows for lower energy consumption, which is crucial in WSN life time. Table 9 shows the performance analysis of the proposed COFDMA-WSN methodology compared to [11]. Overall, the analysis of the proposed methodology highlights its superiority in terms of increased SIR, link throughput and improved energy efficiency compared to existing techniques [11]. These advancements contribute to enhanced energy saving and so maximizing network life time making the proposed methodology a promising and valuable approach for the targeted area.

## 5 Conclusion

In this paper, the WSN performance enhancements by decreasing energy consumption is deliberated. These enhancements are studied through considering two different COFDMA-WSN schemes. These schemes represent classical COFDMA-WSN and R-S COFDMA-WSN. Additionally, there are different pondered configurations due to these schemes. These configurations denote classical OFDMA network with classical WSN, R-S OFDMA network with classical WSN, classical OFDMA network with R-S WSN, and R-S OFDMA network with R-S WSN. Moreover, each configuration is applied with four different FrFR techniques. These techniques represent St FrFR4 technique, St FrFR3 technique, Sc FrFR technique and SoFR technique. Consequently, there are sixteen different patterns of COFDMA-WSN are studied. A comparison of all patterns is presented to improve the network QoS. Analytical dealings are realized. These treatments yielded

**Table 9** Performance analysis of the Proposed COFDMA-WSN methodology compared to [11] applying St FrFR3 technique with $\sigma = 3.2$

| Metric | Proposed first configuration | State-of-the-art approaches [11] | Improvement percentage |
|---|---|---|---|
| Achieved SIR through prime link | 48 | 37 | 29 |
| Achieved SIR via ensuing link | 48 | 38 | 26 |
| Achieved throughput over prime link | $6.7 \times 10^7$ bit/sec | $5.7 \times 10^7$ bit/sec | 17 |
| Achieved throughput via ensuing link | $6.7 \times 10^7$ bit/sec | $5.9 \times 10^7$ bit/sec | 13 |
| Achieved energy efficiency by prime link | 0.44 | 0.35 | 25 |
| Achieved energy efficiency over ensuing link | 0.74 | 0.64 | 15 |

CFTs for C-H's SIR and SN's SIR. Additionally, dissimilar metrics of performance valuation are applied to contrast the performance of altered patterns. The consequences show, that as unpredicted in prime link, SoFR using fourth configuration outperforms St FrFR3 deploying second configuration in low PLoE part only. Furthermore, this technique lost its superiority in high PLoE part and St FrFR3 using second configuration is preferable in use from EE perspectives. Furthermore, it is noticed, that SoFR using third configuration in ensuing link shows performance close to SoFR using fourth configuration from EE viewpoint. Therefore, applying SoFR in third configuration is preferable with respect to the energy preserve and network budget in ensuing link. Moreover, it is noted, that deploying St FrFR4 technique with all configuration attains the lowest average number of retransmission attempts. Consequently, St FrFR4 technique achieves the lowest network delay. Furthermore, it is noticed, that variance worth between dissimilar techniques in low PLoE part is less than it in high PLoE part from average number of retransmission attempts standpoint. The cause of this outcome can be credited, to the decreasing of signal attenuation impacts in high PLoE value due to the increase in PLo gain value. Furthermore, it is noted, that St FrFR4 technique outdoes the other techniques when high STP is needed. This outcome can be accredited, to its capability to attain lower outage probability. Furthermore, it is noted, that pattern of second configuration uses St FrRF3 technique has the first priority in use in high PLoE range from $P_{TR}$ viewpoint in prim link. This outcome may be credited, to the improved C-H's SIR in the second TS. Accordingly, this technique attains the highest values of MRC, which permits it from realizing the maximum $P_{TR}$ values. Additionally, it is noted, that the close in distance between interfering sources and C-H in the second TS reasons the pattern of second configuration uses St FrRF4 has preference in use in low PLoE range only. Additionally, it is noticed, that pattern of third configuration uses St FrRF4 technique is superior to other techniques in ensuing link. This consequence may be credited, to its aptitude to

achieve the highest SN's MRC. Consequently, this pattern attains the maximum $P_{TR}$ values. Moreover, it is observed, that the preference of using St FrRF3 technique has fallen to the third position in the low PLoE range and to the fourth position in low PLoE part in ensuing link. So, there is a necessity to do a trade-off between all different patterns to attain the best network performance. These consequences introduce much higher SIR improvements. Hence, the system will experience to lower outage probability. Therefore, successful transmission probability is enhanced. So, packet loss is minimized. Thus, average number of retransmissions is reduced. Therefore, packet transmission rate is maximized. Accordingly, link throughput and data rate are improved. Also, the value of EE is enhanced. Consequently, the networks lifetime is maximized. The future work will give a special care to more complex developments for further energy consumption reduction in WSNs. These developments represent COFDMA-WSNs with directional antennas apply different beamforming techniques.

# A: Analysis of classical OFDMA network with R-S WSN

The third configuration considers R-S WSN executed with a classical OFDMA network. This configuration is the same as COFDMA-WSN but with using FD AF RSs in the ensuing connection. Consequently, the analysis of this configuration is completed via two key steps. The first stage represents the analysis of a classical OFDMA network to compute the C-H's SIR. Furthermore, the second step signifies the analysis of R-S WSN for the SN's MRC calculation as revealed in Fig. 26.

## Analysis of classical OFDMA network

The analysis of this network is similar to that in the first configuration. Consequently, Eqs. (8), and (11) can be used to represent C-H's SIR CFTs for St FrFR3 and St FrFR4
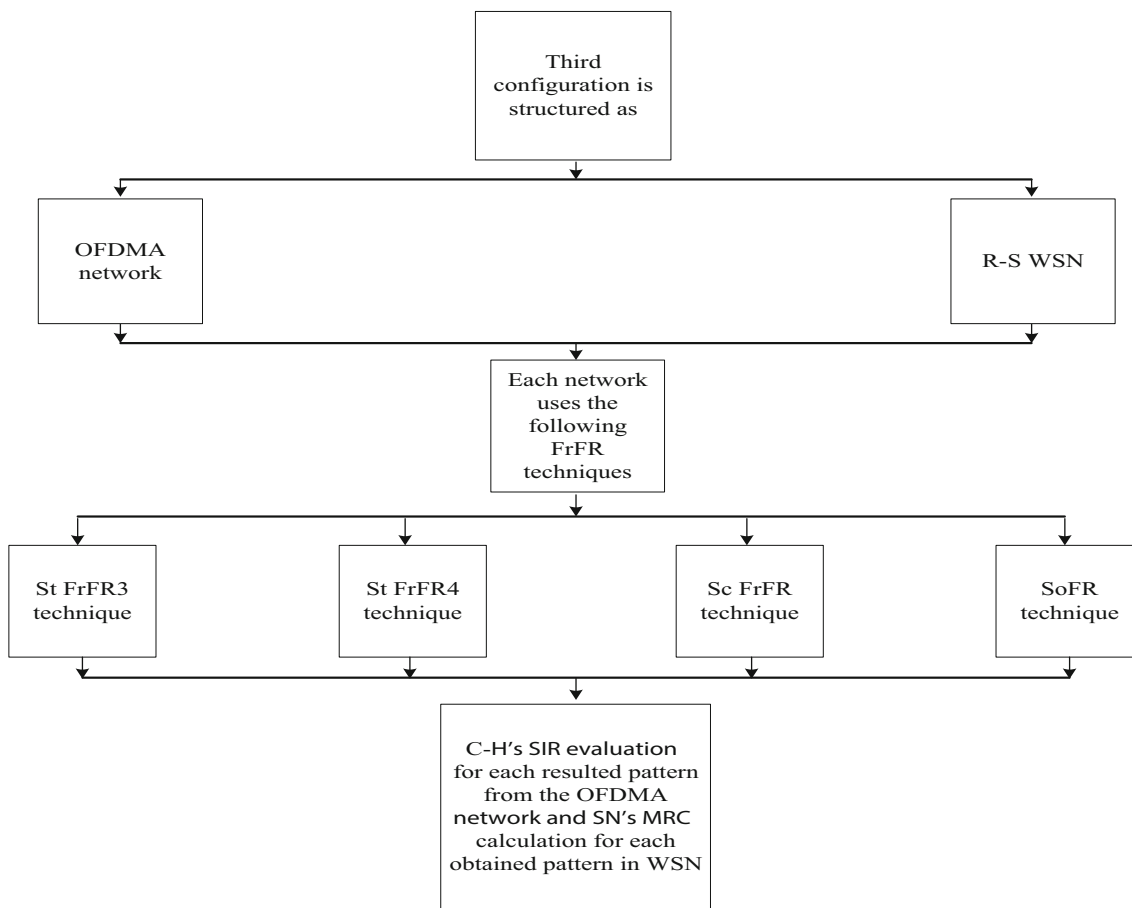
Fig. 26 Conception diagram of third configuration in COFDMA-WSN for energy consumption dropping

techniques, respectively. Furthermore, Eqs. (22), and (35) can be utilized to designate C-H's SIR CFTs when Sc FrFR and SoFR techniques are deployed, respectively.

## Analysis of R-S WSN

In this network, every cell has a centralized BS, a specified numeral of SNs planned in a regular pattern, and a FD AF RS located at distance equal to $R_{dR}$ (m) ($R_{dR} = 0.75$ of $R_{Cell}$) from the BS. Hence, the communication is accomplished in two TSs as shown in Fig. 27. In first TS, RS is inactive, while C-H transmits the signal to both RS and SN through relay and ensuing link, respectively. In second TS, RS transmits the formerly received signal to the SN through access link after amplification process whereas the C-H keeps lazy. Accordingly, SN combines these two TSs' SIRs by MRC technique as displayed in Fig. 27. Consequently, Eq. (40) can be modified to symbolize the SN's MRC calculation as follows

$$MRC_{SN\_SIR} = SIR_1 + SIR_2 \tag{76}$$

where $MRC_{SN\_SIR}$ denotes the MRC of the two TSs' SIRs, $SIR_1$ characterizes reached SN's SIR from the first TS and
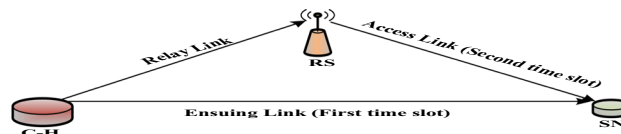


Fig. 27 Idea clarification of MRC technique in R-S WSN

$SIR_2$ designates obtained SN's SIR from the second TS. Consequently, the analysis of two TSs is done in the succeeding subsections to compute MRC CFT using different FrFR techniques.

### Analysis of St FrFR technique

Two-tier St FrFR system based R-S WSN is considered as displayed in Fig. 28(a, c). Consequently, every outer BF is more distributed in three different parts of $S_Fs$ to reduce the CoCI influence between cell elements as represented in Fig. 28(b). The first section symbolizes $S_{F1-1}$ which is allotted to BS. Besides, the next group signifies $S_{F1-2}$, $S_{F1-3}$, $S_{F1-4}$ and $S_{F1-5}$ which are apportioned to SNs. Furthermore, the third sector indicates $S_{F1-6}$ which is allocated to RS as portrayed in Fig. 28(d).
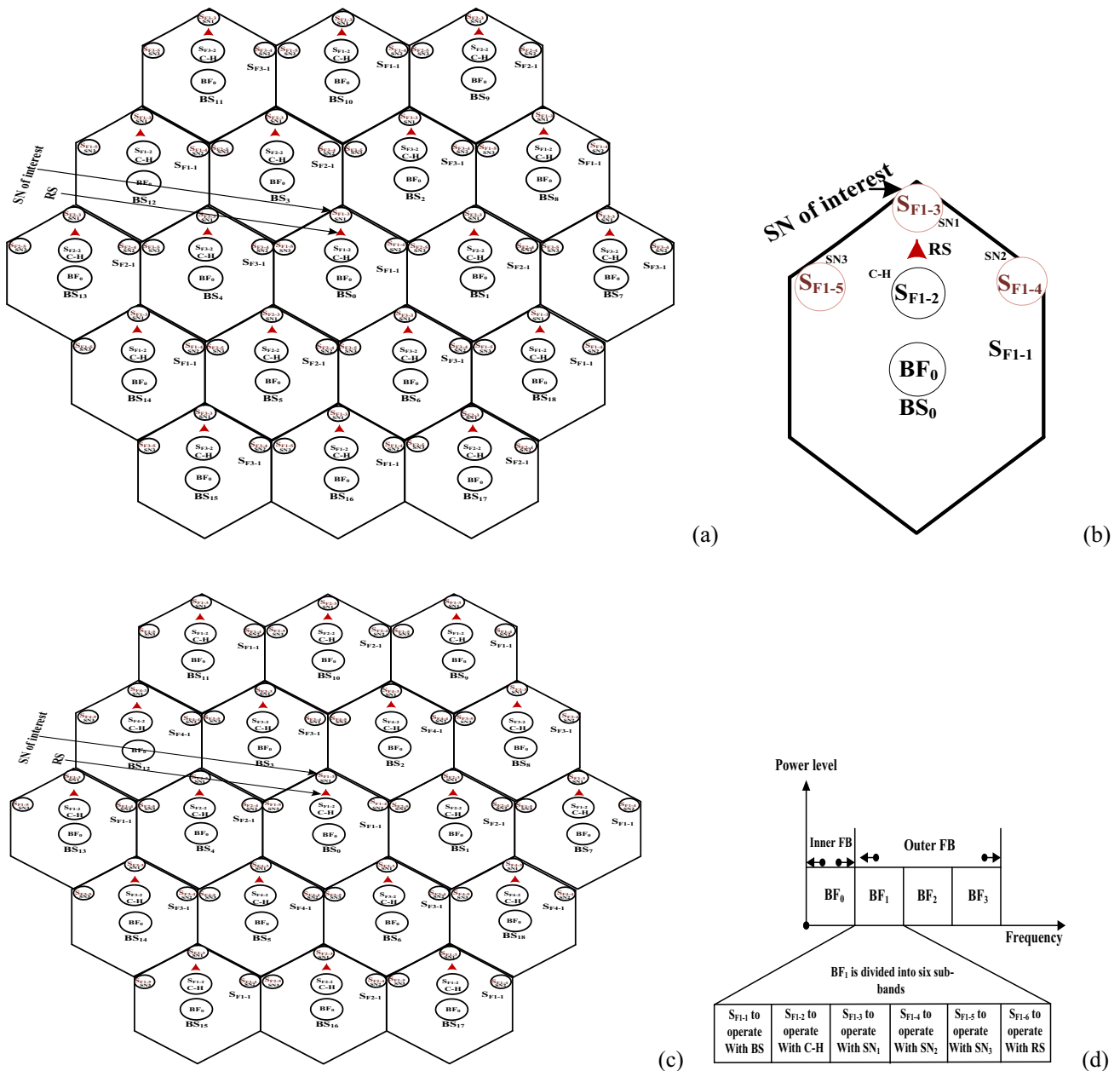
**Fig. 28** Two-tier St FrFR based R-S WSN system **a** St FrFR3 system design, **b** Cell arrangement, **c** St FrFR4 system layout, **d** Assigned frequency division

**Analysis of first time slot** In this TS, C-H transfers the signal to both RS and SN whilst RS preserves inactive. Accordingly, wholly neighboring C-Hs that employ $S_{F1-3}$ as the serving C-H represent an interfering sources. Hence, SN of interest hurts from 6 C-Hs in cells number (8, 10, 12, 14, 16 and 18). These C-Hs usage $S_{F1-3}$ as serving C-H in the outer section when St FrFR3 technique is employed. Furthermore, when St FrFR4 technique is deployed, the SN of interest suffers from 6 interfering C-Hs that characterize cells number (7, 9, 11, 13, 15 and 17). Therefore, the

analysis of this TS is similar to the classical St FrFR analysis because in this TS the C-H does the communication completely. Therefore, SN's SIR CFTs for St FrFR3 technique and St FrFR4 technique can be valued from Eq. (15) and Eq. (18), respectively.

**Analysis of second time slot** In this TS, every RS transmits its signal to SN whereas serving C-H is lazy. Hence, SN's SIR in this TS is assessed as follows

**Table 10** Interfering RSs' Coordinates for St FrFR3 technique and St FrFR4 technique based R-S WSN

| R-S St FrFR3 technique | | | R-S St FrFR4 technique | | |
|---|---|---|---|---|---|
| Interfering RSs' coordinates in cell no | Sub-band frequency $f_{1-1}$ | | Interfering RSs' coordinates in cell no | Sub-band frequency $f_{1-1}$ | |
| | X | Y | | X | Y |
| 8 | $3\sqrt{3}/2$ | 2.25 | 7 | $2\sqrt{3}$ | 3/4 |
| 10 | 0 | 3.75 | 9 | $\sqrt{3}$ | 3.75 |
| 12 | $-3\sqrt{3}/2$ | 2.25 | 11 | $-\sqrt{3}$ | 3.75 |
| 14 | $-3\sqrt{3}/2$ | −0.75 | 13 | $-2\sqrt{3}$ | 3/4 |
| 16 | 0 | −2.25 | 15 | $-\sqrt{3}$ | −2.25 |
| 18 | $3\sqrt{3}/2$ | −0.75 | 17 | $\sqrt{3}$ | −2.25 |

$$SIR_R(x,y) = \frac{\left(x^2 + (y - 0.75)^2\right)^\sigma}{T_{RW}(x,y)} \tag{77}$$

where $T_{RW}$ stands the interference parameter due to CoCI from co-channel RSs that use $S_{F1-6}$ as the serving RS. Therefore, when St FrFR3 system is used, there are 6 RSs in cell number (8, 10, 12, 14, 16 and 18) affecting SN of interest as revealed in Fig. 28(a). Furthermore, when St FrFR4 system is used, there are 6 RSs in cell number (7, 9, 11, 13, 15 and 17) affecting SN of interest as presented in Fig. 28(c). The interfering RSs' coordinates are revealed in Table 10. Accordingly, the factor $T_{RW}$ for St FrFR3 system is valued as follows

$$T_{RW3}(x,y) = \sum_{j_{RW}=1}^{j_{RW}=6} \left[\left(x + x_{j_{RW}}\right)^2 + \left(y + y_{j_{RW}}\right)^2\right]^\sigma \tag{78}$$

where $j_{RW}$ signifies interfering RSs group. Accordingly, this interference factor can be expressed as follows

$$\begin{aligned} T_{RW3}(x,y) = &\left[\left(x \pm \frac{3\sqrt{3}}{2}\right)^2 + (y - 2.25)^2\right]^\sigma \\ &+ \left[\left(x \pm \frac{3\sqrt{3}}{2}\right)^2 + (y + 0.75)^2\right]^\sigma \\ &+ \left[x^2 + (y - 3.75)^2\right]^\sigma + \left[x^2 + (y + 2.5)^2\right]^\sigma \end{aligned} \tag{79}$$

Therefore, by replacing the account of Eq. (79) into Eq. (77) with x = 0 and y = 1, SN's SIR of St FrFR3 system can be obtained as follows

$$SIR_{RW3} = \left[\left(\frac{1}{16}\right)^{-\sigma}\left(\left(\frac{121}{16}\right)^\sigma + 2\left(\frac{133}{16}\right)^\sigma + 2\left(\frac{157}{16}\right)^\sigma + \left(\frac{169}{16}\right)^\sigma\right)\right]^{-1} \tag{80}$$

where $SIR_{RW3}$ denotes SN's SIR achieved by using St FrFR3 technique in the third configuration. Accordingly, by replacing the values of Eq. (15) and Eq. (80) into

Eq. (76), the SN's MRC CFT for St FrFR3 system is expressed as follows

$$\begin{aligned} MRC_{W3} = &\left[\left(\frac{1}{4}\right)^{-\sigma}\left(\left(\frac{25}{4}\right)^\sigma + 2\left(\frac{31}{4}\right)^\sigma + 2\left(\frac{43}{4}\right)^\sigma + \left(\frac{49}{4}\right)^\sigma\right)\right]^{-1} \\ &+ \left[\left(\frac{1}{16}\right)^{-\sigma}\left(\left(\frac{121}{16}\right)^\sigma + 2\left(\frac{133}{16}\right)^\sigma + 2\left(\frac{157}{16}\right)^\sigma + \left(\frac{169}{16}\right)^\sigma\right)\right]^{-1} \end{aligned} \tag{81}$$

where $MRC_{W3}$ signifies SN's MRC attained by using St FrFR3 technique in the third configuration. Additionally, the factor $T_{RW}$ for St FrFR4 technique is definite as follows

$$T_{RW4}(x,y) = \sum_{j_{RS}=1}^{j_{RS}=6} \left[\left(x + x_{j_{RS}}\right)^2 + \left(y + y_{j_{RS}}\right)^2\right]^\sigma \tag{82}$$

Consequently, by using interfering RSs' coordinates that are revealed in Table 10, this interference parameter can be evaluated as follows

$$\begin{aligned} T_{RW4}(x,y) = &\left[\left(x \pm 2\sqrt{3}\right)^2 + \left(y - \frac{3}{4}\right)^2\right]^\sigma \\ &+ \left[\left(x \pm \sqrt{3}\right)^2 + (y + 2.25)^2\right]^\sigma \\ &+ \left[\left(x \pm \sqrt{3}\right)^2 + (y - 3.75)^2\right]^\sigma \end{aligned} \tag{83}$$

Thus, by replacing the rate of Eq. (83) into Eq. (77), SN's SIR of St FrFR4 technique is expressed as follows

$$\begin{aligned} SIR_{RW4} = &\left[\left(\frac{1}{16}\right)^{-\sigma}\left(\left(\frac{73}{16}\right)^\sigma + \left(\frac{121}{16}\right)^\sigma + \left(\frac{169}{16}\right)^\sigma\right.\right. \\ &\left.\left. + \left(\frac{-191}{16}\right)^\sigma + \left(\frac{193}{16}\right)^\sigma + \left(\frac{217}{16}\right)^\sigma\right)\right]^{-1} \end{aligned} \tag{84}$$

where $SIR_{RW4}$ denotes attained SN's SIR by using St FrFR4 technique in the third configuration. Therefore, by replacing the worth of Eq. (18) and Eq. (84) in Eq. (76), the CFT of the SN's MRC for St FrFR4 system is computed as follows

$$MRC_{W4} = \left[ \left(\frac{1}{4}\right)^{-\sigma} \left( 2\left(\frac{37}{4}\right)^{\sigma} + \left(\frac{13}{4}\right)^{\sigma} + \left(\frac{-47}{4}\right)^{\sigma} \right.\right.$$
$$\left. + \left(\frac{49}{4}\right)^{\sigma} + \left(\frac{61}{4}\right)^{\sigma} \right) \right]^{-1}$$
$$+ \left[ \left(\frac{1}{16}\right)^{-\sigma} \left( \left(\frac{73}{16}\right)^{\sigma} + \left(\frac{121}{16}\right)^{\sigma} + \left(\frac{169}{16}\right)^{\sigma} \right.\right.$$
$$\left.\left. + \left(\frac{-191}{16}\right)^{\sigma} + \left(\frac{193}{16}\right)^{\sigma} + \left(\frac{217}{16}\right)^{\sigma} \right) \right]^{-1}$$

$$(85)$$

where $MRC_{W4}$ indicates SN's MRC reached by using St FrFR4 technique in the third configuration.

### Analysis of Sc FrFR technique

Two tier Sc FrFR system based R-S WSN is assumed as shown in Fig. 29(a). Additionally, each outer sector's BF is scattered in three unlike $S_F$s groups for the purpose of reducing CoCI as shown in Fig. 29(b). The first set characterizes $S_{F1\text{-}1}$, which is allocated to BSs. In addition, the second set symbolizes $S_{F1\text{-}2}$, $S_{F1\text{-}3}$, $S_{F1\text{-}4}$, and $S_{F1\text{-}5}$, which are allotted to RSs. Furthermore, the third set denotes $S_{F1\text{-}6}$ which is allocated to RS as showed in Fig. 29(c).

**Analysis of first time slot** In this TS, SN of interest hurts from 7 interfering C-Hs that usage the $S_{F1\text{-}3}$ in cells number

(5, 6, 14, 15, 16, 17, and 18). Therefore, the analysis of this TS is similar to that in classical Sc FrFR because in this TS the communication is completed totally by the serving C-H. So, SN's SIR CFT can be evaluated from Eq. (26).

**Analysis of second time slot** In this TS, every RS transfers its signal to SN of interest while C-Hs are still. Hence, SN's SIR can be assessed as follows

$$SIR_{RW\,\sec}(x,y) = \frac{\left(x^2 + (y - 0.75)^2\right)^{\sigma}}{T_{RW\sec}(x,y)} \qquad (86)$$

where $T_{RWsec}$ is the interference parameter because of all co-channel RSs that use $S_{F1\text{-}2}$ similar to the aiding RS. Therefore, there are 7 RSs in cells number (5, 6, 14, 15, 16, 17 and 18) cause CoCI as demonstrated in Fig. 29(a). The coordinates of these 7 RSs that affecting SN of interest are presented in Table 11. Consequently, the factor $T_{RWsec}$ is valued as follows

$$T_{RW\sec}(x,y) = \sum_{j_{RWS}=1}^{j_{RWS}=7} \left[ \left(x + x_{j_{RWS}}\right)^2 + \left(y + y_{j_{RWS}}\right)^2 \right]^{\sigma} \qquad (87)$$

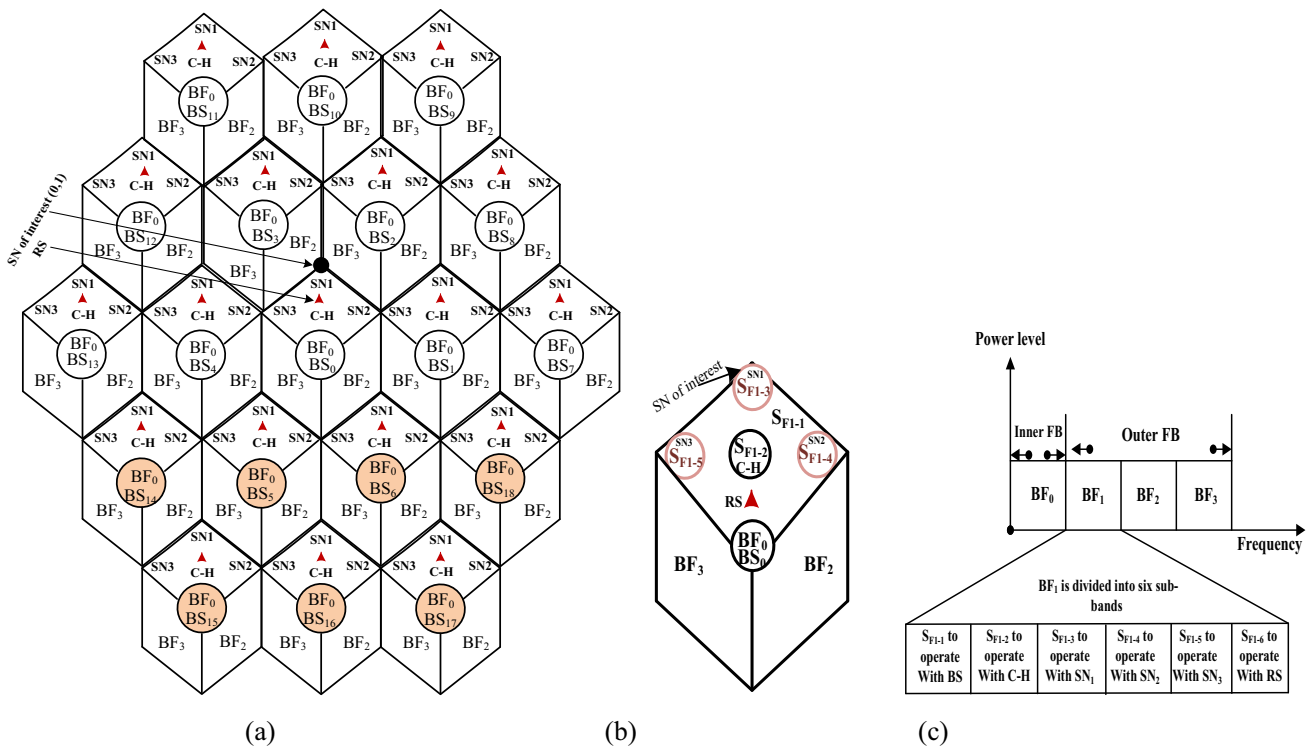where $j_{RWS}$ denotes the group of interfering RSs. Hence, this interference factor can be calculated as follows



Fig. 29 Two-tier Sc FrFR based R-S WSN structure a System design, b Cell arrangement, c Allotted frequency partition

**Table 11** Interfering RSs' Coordinates for Sc FrFR and SoFR based R-S WSNs

| Sc FrFR Model based R-S WSN | | | SoFR Model based R-S WSN | | |
|---|---|---|---|---|---|
| Interfering RSs' coordinates in cell no | Sub-band frequency $f_{1-1}$ | | Interfering RSs' coordinates in cell no | Sub−band frequency $f_{1-1}$ | |
| | X | Y | | X | Y |
| 5 | $-\sqrt{3}/2$ | $-3/4$ | 8 | $3\sqrt{3}/2$ | 2.25 |
| 6 | $\sqrt{3}/2$ | $-3/4$ | 10 | 0 | 3.75 |
| 14 | $-3\sqrt{3}/2$ | $-3/4$ | 12 | $-3\sqrt{3}/2$ | 2.25 |
| 15 | $-\sqrt{3}$ | $-2.25$ | 14 | $-3\sqrt{3}/2$ | $-0.75$ |
| 16 | 0 | $-2.25$ | 16 | 0 | $-2.25$ |
| 17 | $\sqrt{3}$ | $-2.25$ | 18 | $3\sqrt{3}/2$ | $-0.75$ |
| 18 | $3\sqrt{3}/2$ | $-3/4$ | | | |

$$T_{RWsec}(x,y) = \left[\left(x\pm\sqrt{3}\right)^2+(y+2.5)^2\right]^\sigma + \left[(x)^2+(y+2.5)^2\right]^\sigma$$
$$+ \left[\left(x\pm\frac{\sqrt{3}}{2}\right)^2+(y+0.75)^2\right]^\sigma + \left[\left(x\pm\frac{3\sqrt{3}}{2}\right)^2+(y+0.75)^2\right]^\sigma \tag{88}$$

Thus, by replacing the rate of Eq. (88) into Eq. (86), the SIR of SN located at x = 0, y = 1 is formulated as follows

$$SIR_{RWsec} = \left[\left(\frac{1}{16}\right)^{-\sigma}\left(2\left(\left(\frac{61}{16}\right)^\sigma+\left(\frac{157}{16}\right)^\sigma+\left(\frac{217}{16}\right)^\sigma\right)+\left(\frac{169}{16}\right)^\sigma\right)\right]^{-1} \tag{89}$$

where $SIR_{RWsec}$ signifies SN's SIR of the second TS for Sc FrFR system applied with the third configuration. Accordingly, by placing the values of Eq. (26) and Eq. (89) into Eq. (76), the CFT of SN's MRC for Sc FrFR system can be computed as follows

$$MRC_{WSec} = \left[\left(\frac{1}{4}\right)^{-\sigma}\left(2\left(\left(\frac{19}{4}\right)^\sigma+\left(\frac{43}{4}\right)^\sigma+\left(\frac{61}{4}\right)^\sigma\right)+\left(\frac{49}{4}\right)^\sigma\right)\right]^{-1}$$
$$+ \left[\left(\frac{1}{16}\right)^{-\sigma}\left(2\left(\left(\frac{61}{16}\right)^\sigma+\left(\frac{157}{16}\right)^\sigma+\left(\frac{217}{16}\right)^\sigma\right)+\left(\frac{169}{16}\right)^\sigma\right)\right]^{-1} \tag{90}$$

where $MRC_{WSec}$ designates SN's MRC gotten by using Sc FrFR technique in the third configuration.

### Analysis of SoFR network

Two tier SoFR system based R-S WSN is assumed as shown in Fig. 30(a). Consequently, the outer BF is additional portioned in three dissimilar groups of $S_{FS}$ for interference reduction purpose as shown in Fig. 30(b). The first portion represents $S_{F1-1}$ which is assigned to BSs. In addition, the second set represents $S_{F1-2}$, $S_{F1-3}$, $S_{F1-4}$ and $S_{F1-5}$ which are allocated to SNs. Furthermore, the third set

signifies $S_{F1-6}$ which is allotted to RS as portrayed in Fig. 30(c).

**Analysis of first time slot** In this TS, there are 18 interfering cells affecting origin BS. These cells can be divided to 12 BSs in inner area and 6 C-Hs in outer area. Therefore, the analysis of this TS is similar to the classical SoFR analysis because the C-H does the communication wholly in this TS. So, SN's SIR CFT can be valued from Eq. (39).

**Analysis of second time slot** In this TS, the communication is completed via the access link, so the RS transmits its amplified signal to SN of interest. Thus, Eq. (36) can be modernized to determine SN's SIR as follows

$$SIR_{SFR-RW}(x,y) = \frac{\varepsilon\left(x^2+(y-0.75)^2\right)^\sigma}{T_{iRW}(x,y)+\varepsilon T_{oRW}(x,y)} \tag{91}$$

where $T_{oRW}$ and $T_{iRW}$ signify the outer and inner interference parameters, respectively. The interfering BSs' normalized coordinates that use $BF_1$ in the inner area are demonstrated by Table 3. Thus, the inner interference parameter expression for SN positioned at coordinates (0,1) is finalized as follows

$$T_{iRW} = \frac{1}{3}4^\sigma + \frac{2}{3}7^\sigma + \frac{1}{3}13^\sigma + \frac{1}{3}19^\sigma + \frac{1}{3} \tag{92}$$

Additionally, the outer interference parameter in final form can be expressed as follows

$$T_{oWR} = \left(\frac{121}{16}\right)^\sigma + 2\left(\frac{133}{16}\right)^\sigma + 2\left(\frac{157}{16}\right)^\sigma + \left(\frac{169}{16}\right)^\sigma \tag{93}$$

Therefore, by replacing the worth of Eqs. (92) and (93) into Eq. (91), the SN's SIR due to applying SoFR technique in the third configuration can be characterized as follows
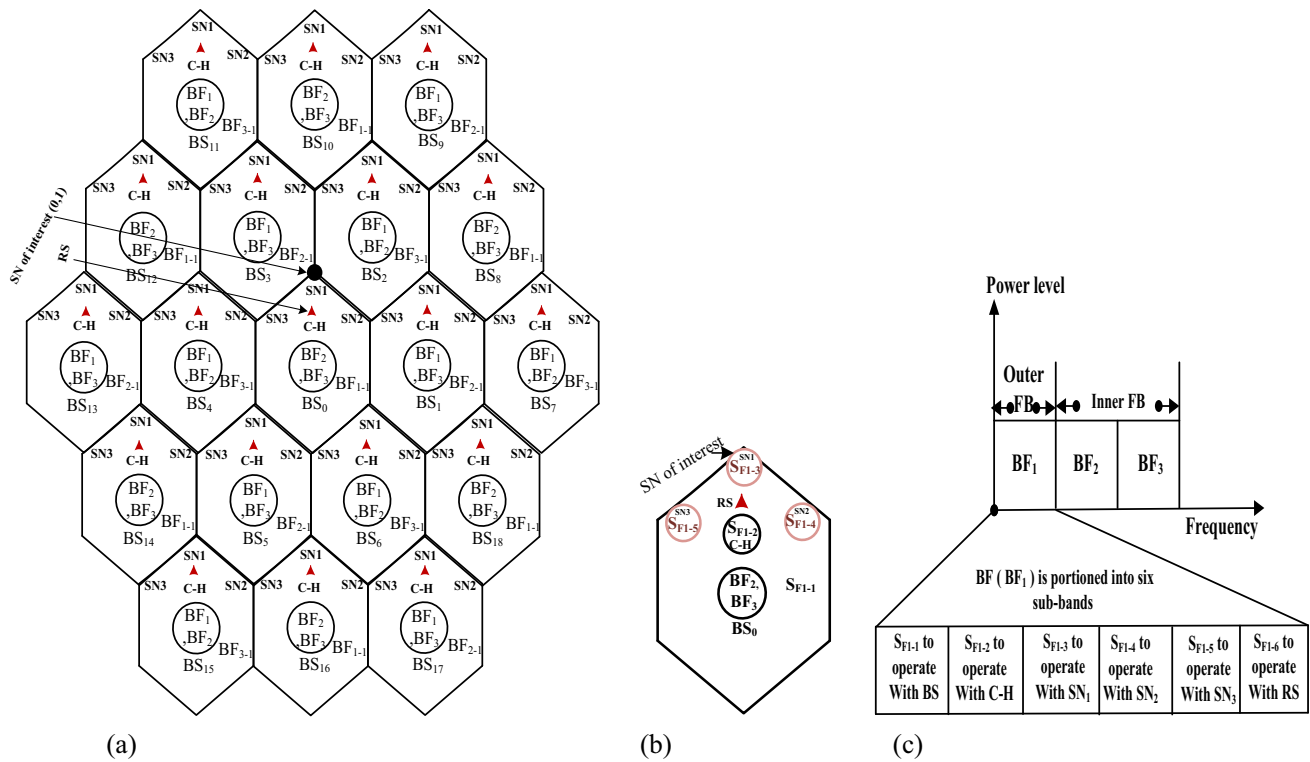
**Fig. 30** Two-tier SoFR based R-S WSN structure **a** System design, **b** Cell arrangement, **c** Allotted frequency partition

$$
SIR_{WSFR} = \left[ \left(\frac{1}{16}\right)^{-\sigma} \left( \begin{array}{l} \frac{1}{3}4^{\sigma} + \frac{2}{3}7^{\sigma} + \frac{1}{3}13^{\sigma} + \frac{1}{3}19^{\sigma} + \left(\frac{121}{16}\right)^{\sigma} \\ + 2\left( \left(\frac{133}{16}\right)^{\sigma} + \left(\frac{157}{16}\right)^{\sigma} \right) + \left(\frac{169}{16}\right)^{\sigma} + \frac{1}{3} \end{array} \right) \right]^{-1}
$$
(94)

where $SIR_{WSFR}$ characterizes SN's SIR of SoFR technique in the third configuration. Consequently, by.

replacing the value of Eqs. (39) and (94) into Eq. (76), the MRC CFT for SN of interest with $\varepsilon = 1$ can be computed as follows

$$
MRC_{WS} = \left[ \left(\frac{1}{4}\right)^{-\sigma} \left(\frac{2}{5}4^{\sigma} + \frac{4}{5}7^{\sigma} + \frac{2}{5}13^{\sigma} + \frac{2}{5}19^{\sigma} + \left(\frac{25}{4}\right)^{\sigma} + 2\left(\frac{31}{4}\right)^{\sigma} + 2\left(\frac{43}{4}\right)^{\sigma} + \left(\frac{49}{4}\right)^{\sigma} + \frac{2}{5} \right) \right]^{-1} + \left[ \left(\frac{1}{16}\right)^{-\sigma} \left(\frac{1}{3}4^{\sigma} + \frac{2}{3}7^{\sigma} + \frac{1}{3}13^{\sigma} + \frac{1}{3}19^{\sigma} + \left(\frac{121}{16}\right)^{\sigma} + 2\left( \left(\frac{133}{16}\right)^{\sigma} + \left(\frac{157}{16}\right)^{\sigma} \right) + \left(\frac{169}{16}\right)^{\sigma} + \frac{1}{3} \right) \right]^{-1}
$$
(95)

where $MRC_{WS}$ denote the attained MRC of SN of interest due to deploying SoFR technique in the third configuration.

## B: Analysis of R-S COFDMA-WSN

The fourth configuration considers R-S WSN employed with R-S OFDMA network. This network uses FD AF RSs in the prime and ensuing links. Thus, in this configuration, each cell has centralized BS, a specific figure of SNs organized in a regular form, and two RSs positioned at distance equal to $R_d$ and $R_{dR}$ from the BS, respectively.

Consequently, R-S OFDMA network and R-S WSN analytical handlings are conducted in the following subsections. These treatments are done through two principal steps. The first stage represents the analysis of R-S OFDMA network to calculate the C-H's MRC in the prim link. Moreover, the second step signifies the analysis of R-S WSN for the SN's MRC calculation in the ensuing link as revealed in Fig. 31.

### Analysis of R-S OFDMA network

Analytical treatments of R-S OFDMA network is presented in this subsection. Accordingly, the analysis of the two TSs is implemented to compute C-H's MRC CFT using different FrFR techniques.

### Analysis of St FrFR technique

Two-tier St FrFR system based R-S OFDMA network is considered as revealed in Fig. 32(a, c). Accordingly, every outer BF is advance portioned in seven $S_Fs$ for interference level controlling between the SNs, RSs and BSs as displayed in Fig. 32(b). These $S_{FS}$ are grouped into three sets. The first set represents $S_{F1-1}$, which is allocated to BS. Moreover, the second set signifies $S_{F1-2}$, $S_{F1-3}$, $S_{F1-4}$, and $S_{F1-5}$ which are assigned to the SNs. Additionally, the third set denotes $S_{F1-6}$, and $S_{F1-7}$, which are assigned to first RS
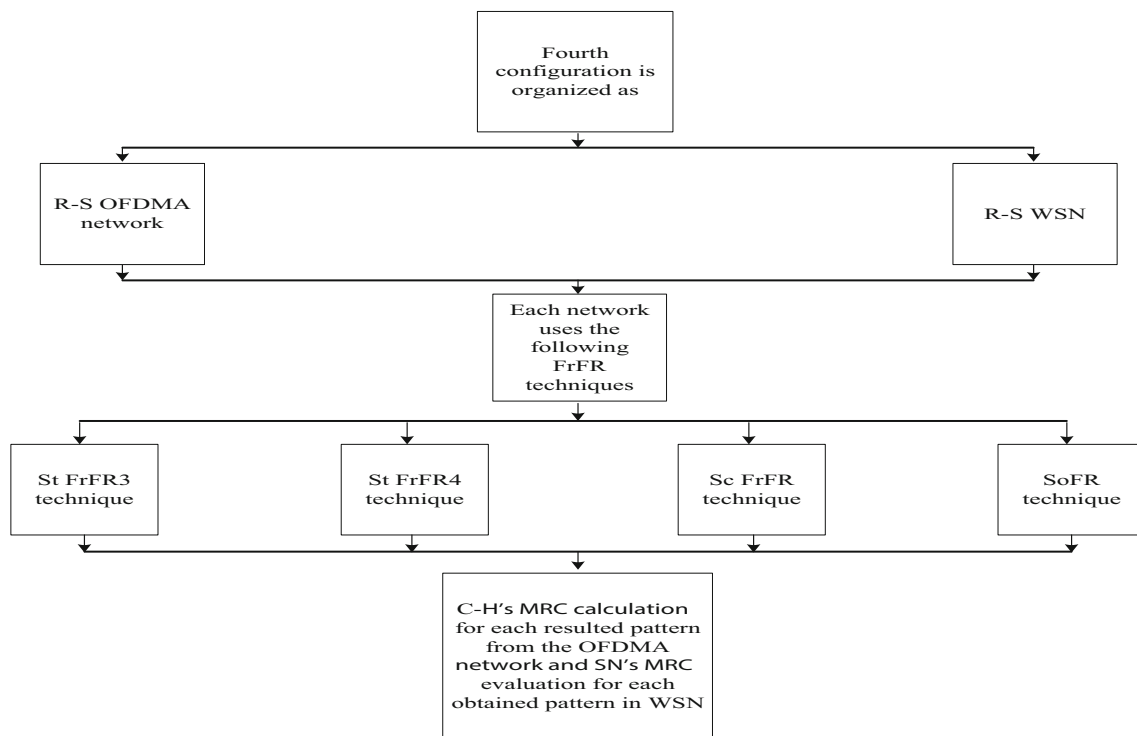
**Fig. 31** Conception diagram of fourth configuration in COFDMA-WSN for energy consumption reducing

(RS$_1$) and second RS (RS$_2$), respectively as depicted in Fig. 32(d).

Furthermore, the CFTs for St FrFR3 and St FrFR4 techniques are derived. It is observed, that current configuration provides equal C-H's SIR in the two TSs as the second configuration. This outcome can be attributed, to presence of the same interference sources that negatively affecting the centralized C-H. Consequently, Eqs. (45), and (49) can be used to represent C-H's MRC CFTs when St FrFR3 and St FrFR4 techniques are applied, respectively.

### Analysis of Sc FrFR system

R-S OFDMA network that applies Sc FrFR system is considered as revealed in Fig. 33(a). Accordingly, every outer BF is further portioned by the same manner as in St FrFR technique as revealed in Fig. 33(b, c). Also, CFTs for Sc FrFR technique are implemented. It is noticed, that Sc FrFR technique attains equal C-H's SIR in the two TSs for the second and fourth configurations. Consequently, Eq. (54) can be used to signify C-H's MRC CFTs when Sc FrFR technique is employed in the fourth configuration.

### Analysis of SoFR technique

R-S OFDMA network that employs SoFR system is considered as depicted in Fig. 34(a). Consequently, each outer BF is more portioned by similar method as in St FrFR

technique as revealed in Fig. 34(b, c). Also, CFTs for SoFR technique are implemented. It is noticed, that this pattern of SoFR achieves C-H's SIR CFTs different from those in the second configuration. This outcome can be ascribed, to the utilization of SoFR power control factor. Hence, the fourth configuration applies SoFR technique analysis is completed through the following subsections.

**Analysis of first time slot**  In this TS, there are 18 cells (6 BSs in outer area and 12 BSs in inner area) which deploy $S_{F1-1}$. So, these 18 cells affecting the centralized BS. Therefore, the analysis of this TS is identical with the classical SoFR analysis because in this TS the communication is done completely by the BS. So, C-H's SIR CFT can be evaluated from Eq. (35).

**Analysis of second time slot**  In this TS, the communication is done via the access link, so RS transmits its amplified signal to the C-H. Hence, Eq. (55) can be updated to evaluate C-H's SIR in this TS as follows

$$SIR_{SFR-R4}(x,y) = \frac{\varepsilon\left(x^2 + (y - 0.25)^2\right)^\sigma}{T_{iR4}(x,y) + \varepsilon T_{oR4}(x,y)} \tag{96}$$

where $T_{oR4}$ and $T_{iR4}$ symbolize the outer and inner interference parameters, respectively. The BSs' normalized coordinates that use BF$_1$ in the inner area are demonstrated
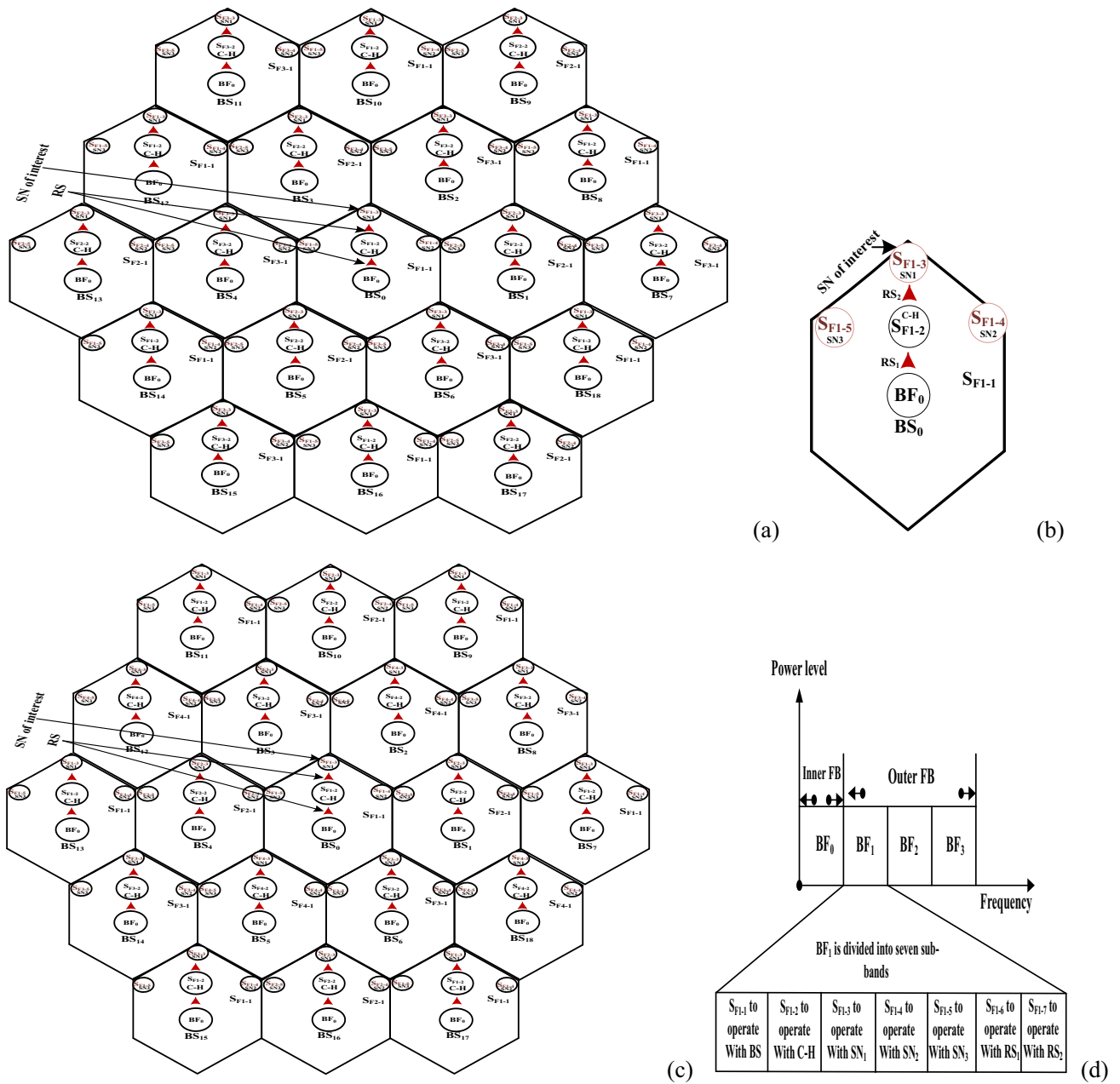
Fig. 32 Two-tier St FrFR based R-S COFDMA-WSN system **a** St FrFR3 system design, **b** Cell arrangement, **c** St FrFR4 system layout, **d** Designated frequency partition

by Table 3. Consequently, the factor $T_{iR4}$ is stated as follows

$$T_{iR}(x,y)=\frac{1}{7}\begin{bmatrix}\left[(x\pm2\sqrt{3})^2+y^2\right]^\sigma\\+\left[\left(x+\frac{\sqrt{3}}{2}\right)^2+\left(y\pm\frac{3}{2}\right)^2\right]^\sigma\\+\left[(x\pm\sqrt{3})^2+(y\mp3)^2\right]^\sigma\\+\left[(x\pm\sqrt{3})^2+y^2\right]^\sigma\\+\left[(x\pm\sqrt{3})^2+(y\pm3)^2\right]^\sigma\\+\left[\left(x-\frac{\sqrt{3}}{2}\right)^2+\left(y\pm\frac{3}{2}\right)^2\right]^\sigma\end{bmatrix}$$

(97)

Thus, the inner interference parameter for C-H sited at (0, 1) point is expressed by the succeeding equation

$$T_{iR4}=\frac{2}{7}\left[\left(\frac{7}{4}\right)^\sigma+\left(\frac{13}{4}\right)^\sigma+\left(\frac{19}{4}\right)^\sigma+\left(\frac{37}{4}\right)^\sigma+\left(\frac{49}{4}\right)^\sigma+\left(\frac{61}{4}\right)^\sigma\right]$$

(98)

Furthermore, there are 6 RSs deploy $S_{F1-6}$ and interfering with serving RS. These RSs' coordinates of are presented in Table 7. Thus, the factor $T_{oR4}$ is calculated as follows
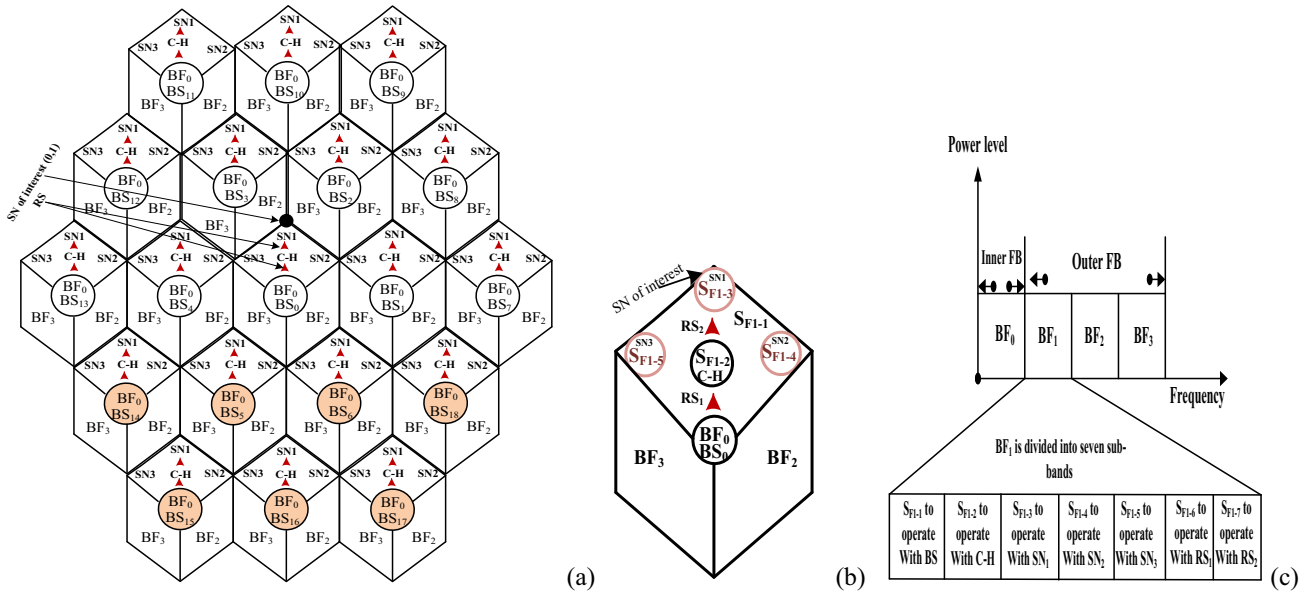
**Fig. 33** Two-tier Sc FrFR based R-S COFDMA-WSN structure **a** System design, **b** Cell arrangement, **c** Assigned frequency partition
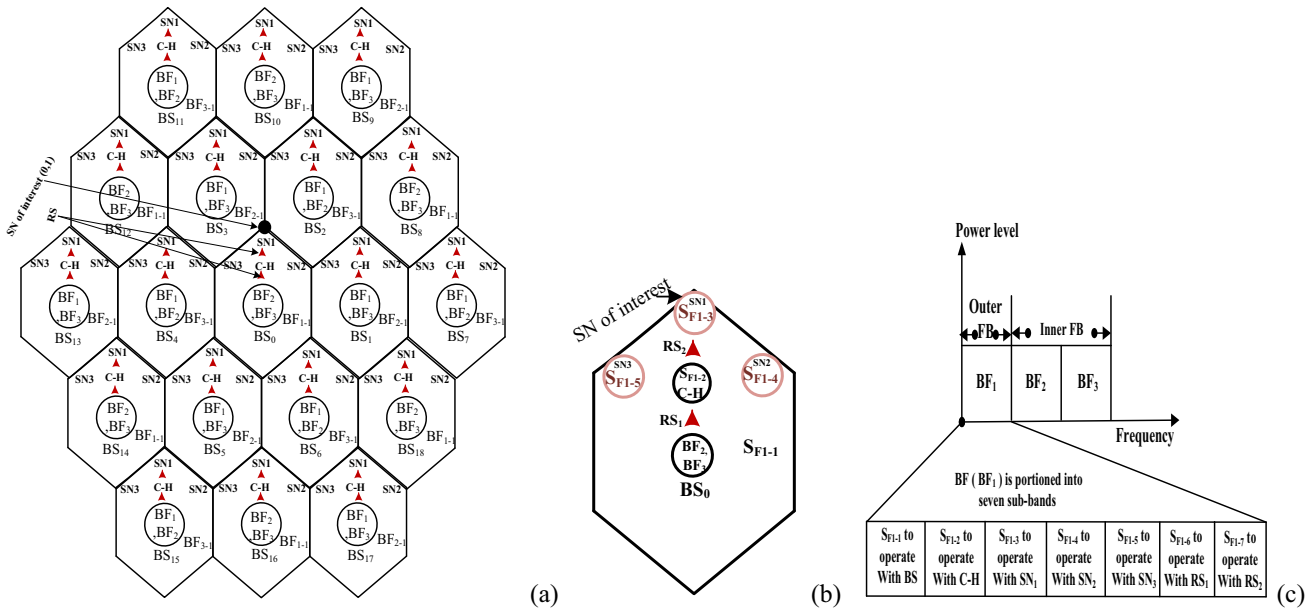


**Fig. 34** Two-tier SoFR based R-S COFDMA-WSN structure **a** System design, **b** Cell arrangement, **c** Allotted frequency division

$$T_{oR4}(x,y) = \left[x^2 + (y-3.25)^2\right]^\sigma + \left[\left(x \pm \frac{3}{2}\sqrt{3}\right)^2 + (y-1.75)^2\right]^\sigma$$
$$+ \left[x^2 + (y+2.75)^2\right]^\sigma + \left[\left(x \pm \frac{3}{2}\sqrt{3}\right)^2 + (y+1.25)^2\right]^\sigma \quad (99)$$

Accordingly, the outer interference factor for the C-H is expressed as follows

$$T_{oR} = \left(\frac{169}{16}\right)^\sigma + 2\left(\frac{133}{16}\right)^\sigma + 2\left(\frac{157}{16}\right)^\sigma + \left(\frac{121}{16}\right)^\sigma \quad (100)$$

Subsequently, by replacing the value of Eqs. (98) and (100) into Eq. (96), C-H's SIR of the SoFR technique can be characterized as follows

$$SIR_{SRC-H4} = \left[\left(\frac{1}{16}\right)^{-\sigma}\left(\begin{array}{l}\frac{2}{7}\left(\left(\frac{7}{4}\right)^\sigma + \left(\frac{13}{4}\right)^\sigma + \left(\frac{19}{4}\right)^\sigma + \left(\frac{37}{4}\right)^\sigma + \left(\frac{49}{4}\right)^\sigma + \left(\frac{61}{4}\right)^\sigma\right) \\ + \left(\frac{121}{16}\right)^\sigma + 2\left(\left(\frac{133}{16}\right)^\sigma + \left(\frac{157}{16}\right)^\sigma\right) + \left(\frac{169}{16}\right)^\sigma\end{array}\right)\right]^{-1} \quad (101)$$

where $SIR_{SRC-H4}$ characterizes C-H's SIR of SoFR technique applied in the fourth configuration. Consequently, by replacing the rates of Eqs. (35) and (101) into Eq. (40), the MRC CFT of the C-H with.

$\varepsilon = 1$ is calculated as follows

$$MRC_{SRC-H4} = \left[ \left(\frac{1}{4}\right)^{-\sigma} \left( \begin{array}{c} 2\left(\left(\frac{7}{4}\right)^{\sigma} + \left(\frac{13}{4}\right)^{\sigma} + \left(\frac{19}{4}\right)^{\sigma} + \left(\frac{31}{4}\right)^{\sigma} + \left(\frac{37}{4}\right)^{\sigma} + \left(\frac{43}{4}\right)^{\sigma} + \left(\frac{61}{4}\right)^{\sigma}\right) \\ + 3\left(\frac{49}{4}\right)^{\sigma} + \left(\frac{25}{4}\right)^{\sigma} \end{array} \right) \right]^{-1}$$
$$+ \left[ \left(\frac{1}{16}\right)^{-\sigma} \left( \begin{array}{c} \frac{2}{7}\left(\left(\frac{7}{4}\right)^{\sigma} + \left(\frac{13}{4}\right)^{\sigma} + \left(\frac{19}{4}\right)^{\sigma} + \left(\frac{37}{4}\right)^{\sigma} + \left(\frac{49}{4}\right)^{\sigma} + \left(\frac{61}{4}\right)^{\sigma}\right) + \left(\frac{121}{16}\right)^{\sigma} \\ + 2\left(\left(\frac{133}{16}\right)^{\sigma} + \left(\frac{157}{16}\right)^{\sigma}\right) + \left(\frac{169}{16}\right)^{\sigma} \end{array} \right) \right]^{-1}$$
$$(102)$$

where $MRC_{SRC-H4}$ denotes C-H's MRC of R-S OFDMA network uses SoFR technique.

## Analysis of R-S WSN

Analytical treatments of R-S WSN is introduced in this subsection. Accordingly, the two TSs are analyzed to evaluate SN's MRC CFT using different FrFR techniques.

### Analysis of St FrFR system

Two-tier St FrFR system based R-S WSN network is considered as shown in Fig. 32(a, c). Furthermore, as mentioned above, different sets of $S_F$s in the outer BF are allocated to BS, RS and SNs as depicted in Fig. 32(d). Furthermore, the CFTs for St FrFR3 and St FrFR4 techniques are derived. It is observed, that current configuration provides equal SN's SIR in the two TSs as the third configuration. This consequence can be attributed, to presence of the same interference sources that negatively affecting the SN of interest. Consequently, Eqs. (81), and (85) can be used to represent SN's MRC CFTs when St FrFR3 and St FrFR4 techniques are applied, respectively.

### Analysis of Sc FrFR technique

R-S WSN that applies Sc FrFR system is considered as shown in Fig. 33(a). Therefore, outer BF is divided as presented in Fig. 33(c) to reduce the interference negative influence between cell elements as revealed in Fig. 33(b). Also, CFTs for Sc FrFR technique are executed. It is noticed, that Sc FrFR technique attains equal SN's SIR in the two TSs for the third and fourth configurations. Consequently, Eq. (90) can be used to indicate SN's MRC CFTs when Sc FrFR technique is employed in the fourth configuration.

## Analysis of SoFR system

R-S WSN that deploys SoFR system is deliberated as depicted in Fig. 34(a). Therefore, BF allocation of outer region is revealed in Fig. 34(c) for cell layout shown in Fig. 34(b). In addition, CFTs for present pattern are carried out. It is noted, that SoFR technique in this configuration achieves SN's SIR CFTs unlike from those in the third configuration. Thus, the analysis of present pattern is completed in the following subsections.

**Analysis of first time slot** In this TS, C-H hurts from 18 interfering cells. These cells contain 12 BSs in inner area and 6 C-Hs in outer area. Therefore, because of communicating by the C-H in this TS, this TS analysis is same as that in the classical WSN deploys SoFR technique. Accordingly, SN's SIR CFT can be computed from Eq. (39).

**Analysis of second time slot** In this TS, RS transfers its signal through the access linkage after amplification process to the SN of interest. Hence, Eq. (91) can be revised to represent SN's SIR in this TS as follows

$$SIR_{SFR-RW4}(x,y) = \frac{\varepsilon\left(x^2 + (y-0.75)^2\right)^{\sigma}}{T_{iRW4}(x,y) + \varepsilon T_{oRW4}(x,y)} \quad (103)$$

where $T_{oRW4}$ and $T_{iRW4}$ indicate the outer and inner interference parameters, respectively. Additionally, Table 3 illustrates the normalized coordinates of the 12 interfering cells that use BF1 in the inner region. Accordingly, the inner interference parameter for SN of interest is valued as follows

$$T_{iRW4} = \frac{2}{7}4^{\sigma} + \frac{4}{7}7^{\sigma} + \frac{2}{7}13^{\sigma} + \frac{2}{7}19^{\sigma} + \frac{2}{7} \quad (104)$$

Additionally, the outer interference parameter can be expressed as follows

$$T_{oWR4} = \left(\frac{121}{16}\right)^{\sigma} + 2\left(\frac{133}{16}\right)^{\sigma} + 2\left(\frac{157}{16}\right)^{\sigma} + \left(\frac{169}{16}\right)^{\sigma} \quad (105)$$

Hence, by replacing the rates of Eqs. (104) and (105) into Eq. (103), SN's SIR of the SoFR technique can be characterized as follows

$$SIR_{WSFR4} = \left[ \left(\frac{1}{16}\right)^{-\sigma} \left( \begin{array}{c} l\frac{2}{7}4^{\sigma} + \frac{4}{7}7^{\sigma} + \frac{2}{7}13^{\sigma} + \frac{2}{7}19^{\sigma} + \left(\frac{121}{16}\right)^{\sigma} \\ + 2\left(\left(\frac{133}{16}\right)^{\sigma} + \left(\frac{157}{16}\right)^{\sigma}\right) + \left(\frac{169}{16}\right)^{\sigma} + \frac{2}{7} \end{array} \right) \right]^{-1}$$
$$(106)$$

where $SIR_{WSFR4}$ characterizes SN's SIR of SoFR technique in the fourth configuration. Consequently, by substituting

the rates of Eqs. (39) and (106) into Eq. (76), the MRC CFT of the SN of interest with $\varepsilon = 1$ is computed as follows

$$MRC_{WS4} = \left[ \left(\frac{1}{4}\right)^{-\sigma} \left( \begin{array}{c} \frac{2}{5}4^\sigma + \frac{4}{5}7^\sigma + \frac{2}{5}13^\sigma + \frac{2}{5}19^\sigma + \left(\frac{25}{4}\right)^\sigma \\ +2\left(\frac{31}{4}\right)^\sigma + 2\left(\frac{43}{4}\right)^\sigma + \left(\frac{49}{4}\right)^\sigma + \frac{2}{5} \end{array} \right) \right]^{-1}$$
$$+ \left[ \left(\frac{1}{16}\right)^{-\sigma} \left( \begin{array}{c} \frac{2}{7}4^\sigma + \frac{4}{7}7^\sigma + \frac{2}{7}13^\sigma + \frac{2}{7}19^\sigma + \left(\frac{121}{16}\right)^\sigma \\ +2\left(\left(\frac{133}{16}\right)^\sigma + \left(\frac{157}{16}\right)^\sigma\right) + \left(\frac{169}{16}\right)^\sigma + \frac{2}{7} \end{array} \right) \right]^{-1} \quad (107)$$

where $MRC_{WS4}$ represents SN's MRC achieved by R-S WSN deploys SoFR technique.

**Author's contribution** OHE conceived the concept, designed the models, analyzed the results, and wrote the manuscript. IIM participated in the conception, supervised on results' analysis and revised the paper.

**Data availability** We also declare that data availability is not applicable in this paper.

## Declarations

**Ethical approval** We also declare that ethics approval is not applicable in this paper.

## References

1. Alazzawi, L., & Elkateeb, A. (2008). Performance evaluation of the WSN routing protocols scalability. *Journal of Computer Systems, Networks, and Communications, 2008*, 1–9. https://doi.org/10.1155/2008/481046

2. Du, Y. (2020). Method for the optimal sensor deployment of WSNs in 3D terrain based on the DPSOVF algorithm. *IEEE Access, 8*, 140806–140821. https://doi.org/10.1109/ACCESS.2020.3013106

3. Arora, V. K., Sharma, V., & Sachdeva, M. (2016). A survey on LEACH and other's routing protocols in wireless sensor network.

*Optik, 127*, 6590–6600. https://doi.org/10.1016/j.ijleo.2016.04.041

4. Gong, Y., Wang, J., & Lai, G. (2022). Energy-efficient query-driven clustering protocol for WSNs on 5G infrastructure. *Energy Reports, 8*, 11446–11455. https://doi.org/10.1016/j.egyr.2022.08.279

5. Elshrkawey, M., Elsherif, S. M., & Wahed, M. E. (2018). An enhancement approach for reducing the energy consumption in wireless sensor networks. *Journal of King Saud University-Computer and Information Sciences, 30*, 259–267. https://doi.org/10.1016/j.jksuci.2017.04.002

6. Tsiropoulou, E. E., Mitsisb, G., & Papavassiliou, S. (2018). Interest-aware energy collection and resource management in machine to machine communications. *Ad Hoc Networks, 68*, 48–57. https://doi.org/10.1016/j.adhoc.2017.09.003

7. Alaerjan, A. (2023). Towards sustainable distributed sensor networks: An approach for addressing power limitation issues in WSNs. *Sensors, 23*, 2–23. https://doi.org/10.3390/s23020975

8. Xia, X., & Liang, Q., (2007). Packets transmission in wireless sensor networks: interference, energy and delay-aware approach. In: IEEE wireless communications and networking conference, pp. 2501–2505. https://doi.org/10.1109/WCNC.2007.466.

9. Ren, J., Yue, S., Zhang, D., Zhang, Y., & Cao, J. (2019). Joint channel assignment and stochastic energy management for RF-powered OFDMA WSNs. *IEEE Transactions on Vehicular Technology, 68*, 1578–1592. https://doi.org/10.1109/TVT.2018.2888635

10. Zhang, H., Xing, H., Cheng, J., Nallanathan, A., & Leung, V. C. M. (2016). Secure resource allocation for OFDMA two-way relay wireless sensor networks without and with cooperative jamming. *IEEE Transactions on Industrial Informatics, 12*, 1714–1725. https://doi.org/10.1109/TII.2015.2489610

11. Jamalabdollahi, M., & Zekavat, S. A. R. (2015). Joint neighbor discovery and time of arrival estimation in wireless sensor networks via OFDMA. *IEEE Sensors Journal, 15*, 5821–5833. https://doi.org/10.1109/JSEN.2015.2449079

12. Wei, L., & Longmei, Z. (2012). A novel multi-channel MAC protocol for cluster based wireless multimedia sensor networks. *Physics Procedia Journal, 25*, 2203–2210. https://doi.org/10.1016/j.phpro.2012.03.371

13. Han, J. S., & Lee, Y. H. (2016). Interference-robust transmission in wireless sensor networks. *Sensors, 16*, 1910–1933. https://doi.org/10.3390/s16111910

14. Kim, J., Kim, T., Noh, J., & Cho, S. (2018). Fractional frequency reuse scheme for device to device communication underlaying cellular on wireless multimedia sensor networks. *Sensors, 18*, 2661–2682. https://doi.org/10.3390/s18082661

15. Mahmoud, I. I., Elgazzar, O. H., Hashima, S., & Konber, H. A. (2018). Analysis and performance evaluation of relay assisted OFDMA cellular systems with different beamforming techniques. *Physical Communication, 31*, 49–61. https://doi.org/10.1016/j.phycom.2018.09.004

16. Mahmoud, I. I., Elgzzar, O. H., Hashima, S., & Konber, H. A. (2020). Analysis and comparison of different cooperative cellular networks. *International Journal of Communication Systems, 33*, 1–22. https://doi.org/10.1002/dac.4378

17. Mora, H. C., Grazon, N. O., & Almeida, C. D. (2018). On the cellular spectral efficiency of MC-CDMA systems with MMSE multiuser detector employing fractional and soft frequency reuse. *AEU - International Journal of Electronics and Communications, 84*, 34–45. https://doi.org/10.1016/j.aeue.2017.11.011

18. Mahmoud, I. I., Elgazzar, O. H., Hashima, S., & Konber, H. A. (2019). Analysis of relay-assisted OFDMA cellular systems with different frequency reuse techniques. *Arabian Journal for Science and Engineering, 44*, 2045–2065. https://doi.org/10.1007/s13369-018-3274-3

19. Khalil, M. I., Berber, S. M., & Sowerby, K. W. (2017). High SNR approximation for performance analysis of two-way multiple relay networks. *Physical Communication, 24*, 62–70. https://doi.org/10.1016/j.phycom.2017.04.007

20. Elgazzar, O. H., Mahmoud, I. I., Hashima, S., & Konber, H. A. (2018). Analytical performance evaluation of relay assisted OFDMA cellular systems with various frequency reuse schemes under different propagation impacts. *International Journal of Circuits, Systems and Signal Processing, 12*, 190–199.

21. Su, X., Liang, C., Choi, D., & Choi, C. (2016). Power allocation scheme for femto-to-macro downlink interference reduction for smart devices in ambient intelligence. *Mobile Information Systems Journal, 2016*, 1–10. https://doi.org/10.1155/2016/7172515

22. Ngo, H. Q., & Larsson, E. G. (2011). Linear multihop amplify-and-forward relay channels: Error exponent and optimal number of hops. *IEEE Transactions on Wireless Communications Journal, 10*, 3834–3842. https://doi.org/10.1109/TWC.2011.092011.102194

23. Kelif, J. M., Coupechoux, M., & Godlewski, P. (2012). On the dimensioning of cellular OFDMA networks. *Physical Communication, 5*, 10–21. https://doi.org/10.1016/j.phycom.2011.09.008

24. Cheikh, D. B., Kelif, J.-M., Coupechoux, M., & Godlewski, P. (2011). SIR distribution analysis in cellular networks considering the joint impact of path-loss, shadowing and fast fading. *EUR-ASIP Journal on Wireless Communications and Networking, 2011*, 1–10. https://doi.org/10.1186/1687-1499-2011-137

25. Ramezanipour, I., Alves, H., Nardelli, P. H. J., & Pouttu, A. (2020). A throughput and energy efficiency scheme for unlicensed massive machine type communications. *Sensors, 20*, 2357–2377. https://doi.org/10.3390/s20082357

26. Ansar, H., & Noor, M. S. (2018). Bandwidth utilization efficiency enhancement for OFDM-based WSN. *International Journal of Communication Systems, 31*, 1–23. https://doi.org/10.1002/dac.3776.

**Osama H. Elgazzar** received the B.Sc. and M.Sc. degrees in the Electronics and Electrical Communications Engineering Department from Faculty of Electronic Engineering, Menoufia University in 2004 and 2014, respectively. Also, he received a Doctater and Engineering degree in Electronics and Electrical Communications Engineering from Al Azhar University, Cairo, Egypt in 2018. He is working as lecturer at the Engineering Department, Nuclear Research Center, Egyptian Atomic Energy Authority, Cairo, Egypt since 2018.

His areas of interest are optical communication systems, advanced optical communication networks, optoelectronic devices, passive optical access communication networks, radio over fiber communication systems, wireless mobile networks, cellular OFDMA networks, LTE-A cellular systems, internet of things, image and signal processing, wireless sensor networks and Fifth-Generation mobile communications system.

**Imbaby I. Mahmoud** received a Dr. Eng degree in ECE from Waseda University, Tokyo, Japan, in March 1994 through a Japanese Government Doctorate Scholarship. In 1983, he was appointed as demonstrator at the Egyptian Atomic Energy Authority (EAEA), Cairo, Egypt. He became a professor at the same authority in February 2006 and served as Head of Eng. Dept. in June 2009, Vice Chair for scientific affairs for Material Division in Oct. 2010 and Chair of the division from 2013.

He served as Chair of the Nuclear Research Center from 2017. He received nuclear engineering young scientist prize from Egyptian Society for Nuclear Sciences and Applications (ESNSA) and Atomic Energy Authority in 1996 and IEEE paper grants for ICIP 2009 and 2010. He was a recipient of ICTP (Trieste, Italy) regular associate award in January 2002. He was a member of IEICE from 1990 to 1994 - Japan, IEEE (Computer society affiliate) -1994 – USA, ESNSA and senior member of URSI. He is a member of National Radio Science Committee – URSI and Energy Research Council (both of Academy of Scientific Research and Technology). He was the coordinator of IAEA TC project EGY/043 titled: Environmental Monitoring Instruments (1999-2002). He was CSI of IAEA CRP 16409: Development of Algorithms and their H/W Implementation for Gamma Radiation Spectrometry (2011-2015). He was CSI of IAEA CRP I31028 RA 18572: Application of Wireless Technologies in Nuclear Power Plant Instrumentation and Control Systems (2014-2018) and PI of ASRT-JINR Project: Development of Wireless Sensor Network for Nuclear Material Detection (2015-2017), IAEA CRP J02014 and IAEA CRP J02017: Enhancing Computer Security for Radiation Detection Systems. His research interests include digital nuclear instruments design, modelling and simulation in devices, circuits and systems, nuclear reactor instrumentation and control, computer networking, computer security, VLSI design and algorithms.